UPPSALA
UNIVERSITET

Digital Comprehensive Summaries of Uppsala Dissertations from the Faculty of Science and Technology 1837

Heterocystous cyanobacteria, Dps proteins and H_2 production

CHRISTOPH HOWE

ACTA
UNIVERSITATIS
UPSALIENSIS
UPPSALA
2019

ISSN 1651-6214
ISBN 978-91-513-0716-9
urn:nbn:se:uu:diva-390471

Dissertation presented at Uppsala University to be publicly examined in Lecture hall 80101, Ångström Laboratory, Lägerhyddsvägen 1, Uppsala, Wednesday, 2 October 2019 at 09:15 for the degree of Doctor of Philosophy. The examination will be conducted in English. Faculty examiner: Nir Keren (Hebrew University of Jerusalem).

Abstract

Howe, C. 2019. Heterocystous cyanobacteria, Dps proteins and H_2 production. *Digital Comprehensive Summaries of Uppsala Dissertations from the Faculty of Science and Technology* 1837. 89 pp. Uppsala: Acta Universitatis Upsaliensis. ISBN 978-91-513-0716-9.

To mitigate climate change, CO_2-emitting technologies have to be exchanged by renewable alternatives such as H_2. H_2 can be produced by cyanobacteria, but major efforts to enhance H_2 production yields by genetic modifications or optimised cultivation conditions resulted in energetic photo-to-H_2 conversion efficiencies of 4.0 %, far from its theoretical maximum. New concepts to enhance photobiological H_2 production are described in two separate thesis chapters.

In photobioreactors, photosynthesis can lead to high O_2 concentrations promoting oxidative stress that decreases the photosynthetic efficiency. Genetic modifications could potentially increase the cellular robustness facing oxidative stress e.g. by the introduction of Dps proteins. This protein class is known to mitigate oxidative stress, but cyanobacterial Dps proteins are fairly unexplored. In the 1st thesis chapter, I searched to identify the function of five Dps proteins from the filamentous and heterocystous cyanobacterium *Nostoc punctiforme*. Since the physiologically active Dps proteins are twelve subunit complexes, various methods were utilised to verify their multimeric state and stability. All five NpDps formed high multimeric complexes that allowed for further enzymatic characterisations. In spectroscopic analyses NpDps1-3 were found to utilise H_2O_2 for Fe^{2+} oxidation, whereas NpDps4 only used O_2. NpDps4 crystal structures revealed an uncommon ferroxidase center (FOC) with a His character. This His-type FOC was found across the cyanobacterial phylum. Based on their O_2 and H_2O_2 consumption, all four NpDps display interesting candidates to enhance the cellular robustness in photobioreactors.

To enhance H_2 production yields, a reallocation of photosynthetic energy from cell growth to H_2 production is required. In the 2nd thesis chapter, *Nostoc* PCC 7120 Δ*hupW* was set under iron starvation to evaluate this cultivation strategy for the purpose of H_2 production. The Fe-limited culture comprised a ~ 5.3 fold lower chlorophyll a and a ~ 4.5 fold higher specific carbohydrate concentration as compared to the control. The Fe-limited cells retained long filaments with high heterocyst frequency of ~ 6 %. The microoxic environment inside heterocysts enables efficient H_2-production from O_2-senstive photo fermentative pathways. Therefore, iron-starvation could display the basis of enhanced H_2 production on the cost of growth. For this purpose a biofilm-containing photobioreactor was designed.

Keywords: H2 production, Cyanobacteria, Dps, ferritin-like proteins, iron, nutrient limitation, oxidative stress, biofilm, photobioreactor, iron homeostasis, H2O2

Christoph Howe, Department of Chemistry - Ångström, Molecular Biomimetics, Box 523, Uppsala University, SE-75120 Uppsala, Sweden.

ISSN 1651-6214
ISBN 978-91-513-0716-9
urn:nbn:se:uu:diva-390471 (http://urn.kb.se/resolve?urn=urn:nbn:se:uu:diva-390471)

Das nachdenkende, betrachtende,
forschende Leben ist eigentlich das höchste.
- Alexander von Humboldt (1769 - 1859)
The reflective, observing,
researching life is actually the highest.

List of Papers

This thesis is based on the following papers, which are referred to in the text by their Roman numerals.

I **Howe, C.**, Ho, F.M., Nenninger, A., Raleiras, P., Stensjö, K. (2018) Differential biochemical properties of three canonical Dps proteins from the cyanobacterium *Nostoc punctiforme* suggest distinct cellular functions. *J. Biol. Chem.,* 293(43):16635–16646.

II **Howe, C.**, Moparthi, V.K., Ho, F., Persson, K., Stensjö, K. (2019) The Dps4 from *Nostoc punctiforme* ATCC 29133 is a member of His-type FOC containing Dps class that can be broadly found among cyanobacteria, *PLoS ONE*, 14(8):e0218300.

III Moparthi, V.K., Moparthi, S.B., **Howe, C.**, Raleiras, P., Wenger, J., Stensjö, K., (2019) Structural diffusion properties of two atypical Dps from *Nostoc punctiforme* disclose interactions with ferredoxins and DNA, *BBA Bioenergetics,* https://doi.org/10.1016/j.bbabio.2019.148063.

IV **Howe, C.**, Becker, D., Steinweg, C., Posten, C., Stensjö, K., Iron limitation as a growth-restricted cultivation strategy in the diazotrophic cyanobacterium *Nostoc* PCC 7120 Δ*hupW* for a new perspective on H_2 production systems, *Manuscript to be submitted to Bioresource Technology*.

Contents

Abbreviations

ADP – adenosine diphosphate
ATP – adenosine triphosphate
Bfr – bacterioferritin
BSA – bovine serum albumin
CAT – catalase
CO_2 – carbon dioxide
DLS – dynamic light scattering
DNA - deoxyribonucleic acid
Dps – DNA-binding protein from starved cells
EMSA – electrophoretic mobility shift assay
Fe – iron
Fe^{2+} – ferrous iron
Fe^{3+} – ferric iron
FOC – ferroxidase center
FRET – fluorescence resonance energy transfer
Ftn – ferritin
GFP – green fluorescent protein
H_2 – hydrogen
H_2ase – hydrogenase
H_2O_2 – Hydrogen peroxide
N_2 – nitrogen
N_2ase – nitrogenase
NH_3 – ammonia
O_2 – oxygen
$^1O_2$ – singlet oxygen
$OH^{\bullet}$ – hydroxyl radical
PAGE – polyacrylamide gel electrophoresis
PCE – energetic photon-to-H_2 conversion efficiency
PS I – photosystem I
PS II – photosystem II
ROS – reactive oxygen species
SOD – superoxide dismutase

Introduction

Motivation

Climate change is a major threat to our globalised society in the current century. With rising global temperatures more extreme weather events such as hurricanes, wildfires and draughts, but also impacts on human society with an increased risk of migration, political unrests and wars are expected (1). The responsibility for climate change has been acknowledged to originate from human activities increasingly burning fossil fuels since the beginning of the industrial revolution dating back 250 years (2). Since then, about 120 ppm of the greenhouse gas carbon dioxide (CO_2) has been introduced into Earth's atmosphere, an addition of about 40 % as compared to pre-industrial levels. The danger of climate change has been recently recognised by many countries ratifying the Paris Agreement under the United Nations Framework Convention on Climate Change. It has been agreed that CO_2 emissions need to be limited to stop rising temperatures (1). While our current global economy is majorly based on fossil fuels, a drastic change in the production of energy is demanded. However, one consequence out of many is certain: petroleum, which fuels the global transport sector, has to be exchanged by a renewable alternative. This displays a great technological challenge on a global scale.

The alternative to petroleum is required to originate from renewable sources as it should not contribute to higher atmospheric levels of CO_2. Electro mobility solutions based on batteries could potentially replace the petroleum-driven transport sector (3). Batteries can be recharged via renewable energy sources based on wind, water and solar power. Additionally to batteries, the so-called 'power-to-gas' technology also displays an alternative to petroleum and is based on electrolysis. In electrolysis hydrogen (H_2) can be produced by the electrochemical splitting of water (H_2O) (4), but requires a renewable energy source to be CO_2 free. In fuel cells, H_2 can then be recombined with oxygen (O_2) to H_2O delivering the energy to move vehicles. Only 5 % of the global H_2 production is currently produced by renewable energy, from which only a small percentage is used for transportation (4). Major H_2 quantities are utilised to produce fertiliser e.g. ammonia (NH_3) and processing oil and coal. Besides electrolysis, there are biological ways to produce H_2 (5). For longer than 30 years, cyanobacteria have been investigated in regards to their

potential of producing a large variety of fuels including the photobiological production of H_2 (5).

Many challenges have been identified that need to be overcome to enhance H_2 production yields from cyanobacteria and to render the photobiological process economically viable (6, 7). In this thesis some of these challenges are addressed in two separate chapters. In chapter one, the biochemical investigation of five members of a Dps protein class is presented. This protein class has been known for its involvement in iron homeostasis and mitigating oxidative stress (8). Dps proteins might be utilised to protect H_2-producing cyanobacteria from elevated and thereby toxic O_2 levels inside closed photobioreactors. In chapter two, a novel concept of cyanobacterial cultivation for the purpose of H_2 production is described. This concept is based on reaching a halted state of cyanobacterial growth to transform more photosynthetic energy into H_2. Non-proliferating cultures can be immobilised in biofilm photobioreactors for potentially cheaper H_2 production. A conceptional design for a novel biofilm photobioreactor is enclosed at the end of this thesis.

H_2 production from cyanobacteria

Cyanobacteria are photosynthetic bacteria that require sunlight, water, CO_2 and a small amount of nutrients for cellular proliferation. Using metabolic engineering cyanobacteria can be turned into H_2 producers using photolysis (5). In the process of photolysis, the sun light energy is used for the natural water splitting reaction at the photosynthetic machinery generating O_2, electrons (e^-) and protons (H^+), from which e^- and H^+ can be enzymatically recombined to H_2 (5). This recombination is catalytically supported by two different enzymes: hydrogenase (H_2ase) and nitrogenase (N_2ase). Hydrogenases can directly catalyse the reaction between electrons and protons into H_2, but usually the reverted reaction is catalysed in so called uptake hydrogenases. However, there are bidirectional hydrogenases, but there function are fairly unexplored (9). The enzyme nitrogenase catalyse the N_2-fixation reaction converting N_2 into NH_3, while H_2 is evolved as a bi-product (10). In the absence of N_2, nitrogenases function similar to hydrogenases, except that ATP is consumed during the reduction of protons.

Two different photolysis processes, direct and indirect photolysis, are known (11). Direct photolysis requires a direct coupling of one of the two H_2-producing enzymes to the photosynthetic apparatus, but is largely unexplored (12) (Fig. 1 A, C). Indirect photolysis is based on the photosynthetic production of temporal intermediate biomolecules, such as carbohydrates via carbon fixation. In a second step these carbohydrates are metabolically converted into H_2, either via the final enzyme hydrogenase or nitrogenase (Fig. 1

B, D). Indirect photolysis has been frequently investigated in N_2-fixing cyanobacteria, which naturally utilise the enzyme nitrogenase. H_2, as a by-product in the N_2-fixation reaction is naturally re-oxidised by an uptake-hydrogenase feeding back the H^+ and e^- into the metabolism. This natural H_2-uptake system can be successfully inactivated (9) in order to free the H_2 from the cells. The energy conversion efficiency of this process, represented by the energetic photon-to-H_2 conversion efficiency (PCE) has not exceeded peak values of ~ 4 % in laboratory experiments (6, 13). In regards to its theoretical maximum of about 27.1 % or 16.3 % for a H_2ase-based or N_2ase-based production, respectively, novel strategies have to be developed to enhance cyanobacterial H_2 production (11). One focus of this study was to find cultivation conditions that could halt cellular proliferation and provide an optimal production platform for H_2 in future studies. The main idea is to reallocate the fixed photosynthetic energy in forms of carbohydrates towards H_2 production, as recently discussed in the field of biofuel research to overcome the frequently reported low biofuel synthesis efficiencies (6, 14). Quantitative analysis on cyanobacterial H_2 production is usually conducted in photobioreactors, which resembles also the production system for any kind of fuel or commodity from cyanobacteria.

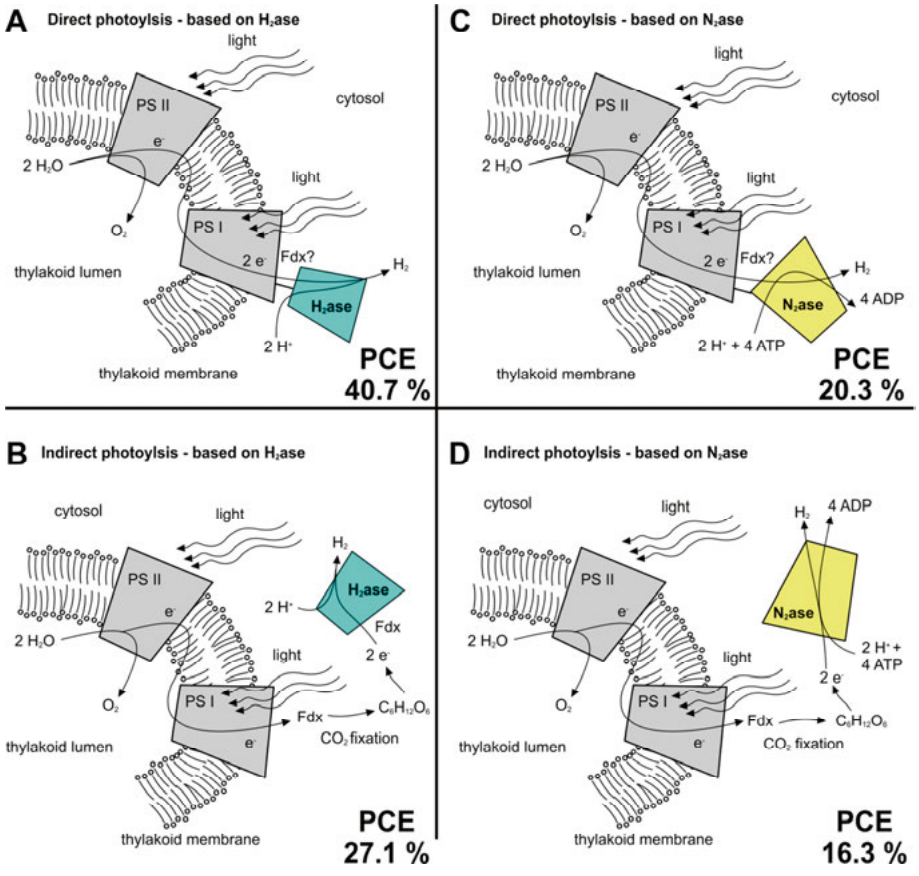

Figure 1 A simplified model of the variety of photolysis processes. A. direct and B. indirect photolysis process utilising the enzyme hydrogenase (H_2ase) to produce H_2. C. direct and D. indirect photolysis using the enzyme nitrogenase (N_2ase) to produce H_2. For each process, the maximal theoretical energetic photon-to-H_2 conversion efficiency (PCE) is given at photons of 680 nm. Key enzymes for photosynthesis, namely photosystem I (PS I) and photosystem II (PS II), embedded in the thylakoid membrane. Electron transport between the donator site of PS I towards CO_2 fixation mediated by a ferredoxin (Fdx). The ultimate H_2 producing enzymes H_2ase and N_2ase highlighted in light blue and yellow colour, respectively. It should be noted that direct photolysis might require the coupling of a photosystem to the H_2-producing enzyme, which may be differently achieved and is fairly unexplored (15). Direct photolysis may also require an electron-transfer protein between the electron donator side of PS I and the H_2 producing enzyme e.g. a Fdx (shown with question mark). N_2-deprived nitrogenase activity shown for optimised H_2 production condition. All shown metabolic processes were simplified (16) and are based on theoretical calculations by Prince and Kheshgi (11).

Photobioreactor systems

Photobioreactors can be open or closed systems, in which phototrophic organisms such as algae or cyanobacteria are cultivated for the production of fuel or other commodities (17–19). In open photobioreactor systems a constant exchange of mass and energy between the reactor and the environment is allowed. Often these systems are constructed as raceway ponds, where paddle wheels deliver agitation to ensure homogeneity of the culture. Due to the missing barrier, these open reactors can lose significant amounts of water due to evaporation (20), and the production culture can suffer from infections caused by harmful organisms entering the system (21). Open raceway ponds have been widely used in large scale production systems for biomass (19) and pigments (22). The advantage of raceway ponds are their considerably low construction costs and long life time (23).

In contrast to open photobioreactors, closed photobioreactors do not allow for mass exchange with their environment due to their construction. Harmful pathogens are hindered to enter the system and closed photobioreactors are a suitable for the production of volatile substances or gasses such as H_2. In open reactor systems these products would simply escape into the atmosphere. The construction costs of closed photobioreactors as compared to open pond systems have been considered to be higher, due to custom made designs and expensive materials (24, 25). However, innovative concepts over the last years have significantly reduced these costs facilitating industrial up-scaling of closed photobioreactor systems (26, 27). Most research on closed photobioreactors has been conducted on tubular and flat panel systems, but also other geometric designs exist (28).

In general, open and closed photobioreactor systems share a common feature, which is the liquid phase that is in contact with the phototrophic cells. Either the culture is homogeneously distributed inside the liquid phase (suspension culture), or as several studies have demonstrated, cells can be immobilised onto a surface creating a biofilm that is submersed in the liquid phase (30, 31). This liquid phase, often called culture medium, provides the necessary water, salinity and nutrients for the phototrophic organisms (29). Studies on cell immobilisation for biofuel production generally reported an increased level of biofuel yields that has been suggested to be linked to the increased biomass retention in the biofilm photobioreactor (30, 31). While these studies mostly were performed on photo fermentative bacteria that require a constant supply of organic nutrients, these systems have been commonly designed to continuously pass through the nutrient-containing liquid medium (32). As for conventional photobioreactors, maintaining a process of a continuous medium circulation has economic drawbacks on the energetic efficiency of the overall process (25). Since H_2 is a low cost prod-

uct, the economic viability of photobioreactor systems has been considered to highly depend on the cultivation process and energy input requirements for it. In this study I aimed to design and manufacture a novel concept for a biofilm photobioreactor, in which cellular proliferation as well as liquid circulation e.g. for nutrient feed were not intended. This biofilm photobioreactor was solely designed for low cost H_2 production. Research on the development of biofilm reactors containing cyanobacteria has been rarely considered in the past and has just begun to emerge in the field of biofuel production

Another common feature of closed and open photobioreactors is that elevated O_2 concentrations can be reached due to the photosynthetic activity of cyanobacteria. Too high concentrations need to be avoided as they can be toxic to cyanobacteria in a cascade of oxidative stress reactions. If not controlled, long-term elevated O_2 levels can negatively affect the production process (33, 34). Energy-intensive gas-exchange mechanisms to extract O_2 from the reactor are standard procedures to protect the producing culture from oxidative stress (35). One aim of the study was to identify the physiological function for members of an enzyme class that are naturally involved in mitigating oxidative stress. These proteins could be potentially utilised in a cyanobacterial H_2 production system to mitigate the effects of oxidative stress and partially replace technical solutions that can require a substantial energy input. According to Acién et al. the extraction of O_2 with air blowers resulted in ~ 21 % of the total power consumption in a pilot production plant for biomass production (25).

Oxidative stress in cyanobacteria

Cyanobacteria are photosynthetic prokaryotes and can be found all around the Earth e.g. in the arctic, deserts, forests and oceans (36). Cyanobacteria comprise different morphologies as there are unicellular, filamentous and filamentous-branching forms (37). They have evolved more than 2.5 billion years ago and affected ecosystems on a global scale, especially due to their oxygenic photosynthesis (38). During the great oxygen event that was caused by cyanobacteria, the atmosphere of planet Earth accumulated substantial amounts of O_2, a potent electron acceptor and the precursor of reactive oxygen species (ROS) that can be cytotoxic (Fig. 2) (39).

If not controlled, ROS can be created by a stepwise reduction of molecular O_2 by a simultaneous oxidation of cellular components such as lipids, proteins and DNA (39, 40). Singlet oxygen ($^1O_2$), superoxide ion radical ($O_2^{\bullet -}$), hydrogen peroxide (H_2O_2) and the highly reactive hydroxyl radical ($OH^{\bullet}$) are the intermediate products of this reaction cascade and display the major ROS

that cells need to regulate. The reactivity of these ROS depends on the molecular properties such as charge, diffusion rate and the biomolecule it is reacting with (40). So is the reactivity of H_2O_2 comparatively low to that of $O_2^{\bullet -}$ or $OH^{\bullet}$ due to the relatively stable O-O bond in H_2O_2. The reaction rate of $OH^{\bullet}$ is limited only by its diffusion, which renders it to be the most toxic ROS. Depending on the level of the oxidative damage caused by ROS, the functions of lipids, proteins or DNA can be lost and vital cellular mechanisms can be in danger. While the oxidation of an enzyme might only lead to its malfunction and degradation, a single oxidation event in the DNA, if not repaired, could eventually lead to cell death (40).

In cyanobacteria, photosynthesis is a continuous source of O_2 produced at the photosystem II (PS II) during daytime (39). Additionally, external O_2 of the atmosphere can permanently enter the cell by molecular diffusion (Fig. 2). There are clear indications that even before cyanobacteria caused the great oxygen event, life on Earth developed regulation mechanisms for ROS. There is an ongoing debate concerning ROS being one of the most early signal molecules (38). Intracellular ROS concentrations need to be regulated to limit their potential damage and cells have developed enzymatic or non-enzymatic protection mechanisms. Singlet oxygen is regulated by e.g. carotenoids and the orange carotenoid protein via quenching (39, 41). $O_2^{\bullet -}$ is controlled by the superoxide dismutase (SOD) (39) and H_2O_2 can be detoxified via catalases (CAT) or peroxidases (PER). Catalases have been demonstrated to be most effective at high levels of H_2O_2 as they catalyse the reaction between two molecules of H_2O_2 resulting in the formation of O_2 and H_2O (42). In contrast to catalases, peroxidases reduce peroxides by a variety of reductants, such as glutathione or cytochrome c, depending on the peroxidase class.

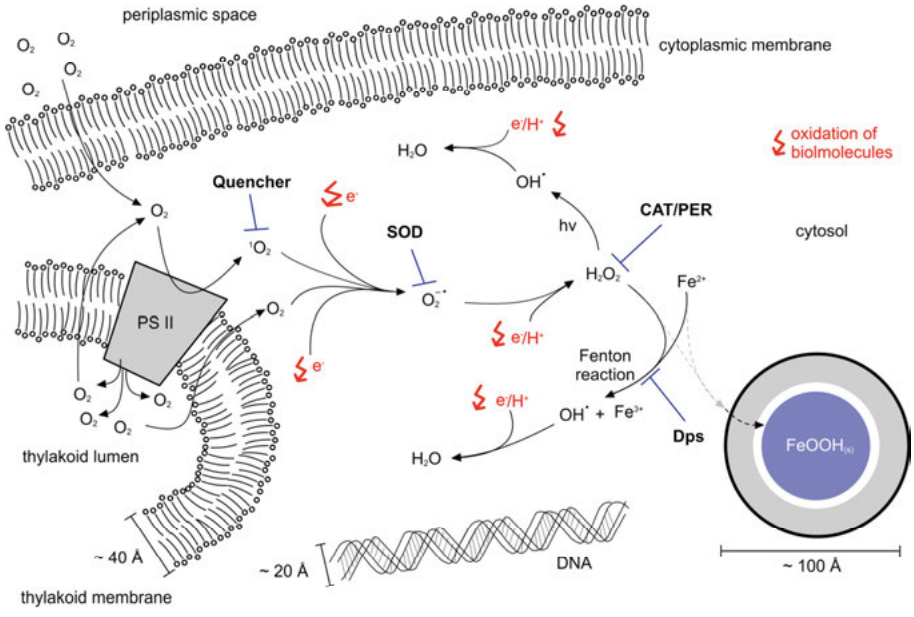

Figure 2 Simplified model of the ROS-protective mechanisms inside a cyanobacterial cell. External and photosynthetically-produced O_2 oxidises biomolecules resulting in the production of super oxide anion radicals ($O_2^{\bullet-}$). By an energy transfer at e.g. the photosystem II (PS II), O_2 is also a source for the production of singlet Oxygen ($^1O_2$). If not detoxified by molecular quenchers e.g. carotenoids or the orange carotenoid protein, the stepwise reduction of $^1O_2$ leads to $O_2^{\bullet-}$ and subsequently to H_2O_2. $O_2^{\bullet-}$ and H_2O_2 can be regulated by super oxide dismutase (SOD) and catalases/peroxidases (CAT/PER), respectively. Not detoxified H_2O_2 can react with Fe^{2+} in the Fenton reaction to produce hydroxyl radicals ($OH^{\bullet}$). In the presence of Dps proteins, the reaction between H_2O_2 and Fe^{2+} results in a Fe^{3+} sequestration process without the release of $OH^{\bullet}$. Spontaneous fission of H_2O_2, which can be enhanced by light photons (hv), results in the direct formation of $OH^{\bullet}$. The reduction of $OH^{\bullet}$ eventually can lead to the formation e.g. of H_2O (or adducts between $OH^{\bullet}$ and the biomolecule). Reduction steps from O_2 to H_2O may comprise the addition of protons (H^+), which are indicated in red colour. A red arrow indicates an oxidation event of a biomolecule with a ROS and the transfer of an e^- to the ROS. Dps proteins, double-strain DNA, cytoplasmic and thylakoid membrane displayed in their relative size. For simplification, only a single Dps protein is shown to representing a Fe-sequestering protein that is involved in H_2O_2 detoxification. Dimensions are given in Å.

In 1992 the discovery of a new protein class, the Dps protein family, introduced a third group of H_2O_2-regulating enzymes besides CAT and PER (Fig. 2) (43). Dps proteins utilise ferrous iron (Fe^{2+}) to reduce H_2O_2 and thereby displaying an important role at the cutting point between iron homeostasis and ROS protection (44). Under physiological conditions, the Fenton reaction between Fe^{2+} and H_2O_2 leads to the production of cytotoxic $OH^{\bullet}$, whereas Dps proteins catalyse this reaction without the release of $OH^{\bullet}$ while ferric iron (Fe^{3+}) is sequestered inside the Dps. Dps proteins belong to the ferritin-

like protein family that also includes ferritins (Ftn) and bacterioferritins (Bfr). Ftn and Bfr are maxiferritins that consist of 24 subunits and can sequester up to 4500 Fe ions using only O_2 as the oxidant (45). Dps on the other hand are miniferritins consisting of twelve subunits and possess an iron storage capacity of about 500 Fe ions (46). Dps proteins have been frequently found to be involved in H_2O_2 detoxification, but all three ferritin-like proteins are linked to bacterial iron homeostasis (39, 45). The regulation of free Fe^{2+} needs to be tightly controlled since it might lead to $OH^{\bullet}$ production, but Fe^{2+} is also an important cofactor in numerous cellular systems. For example, iron is an important part of Fe-S clusters in photosynthesis and N_2 fixation, mediating e^- transport (44, 47–49).

The filamentous and diazotrophic cyanobacterium *Nostoc punctiforme* sp. ATCC 29133 possesses a sophisticated machinery of ROS-protecting enzymes such as three CATs, three SODs and various PERs (42). Additionally, a surprisingly high number of five Dps proteins was discovered, but no further maxiferritin is present in *N. punctiforme* (50). With some exceptions (50, 51), prokaryotes are often described to contain only one or two Dps proteins (8, 52–54), and in contrast to the situation in *N. punctiforme*, maxiferritins, especially Bfr are often found among cyanobacteria (50). It remains largely unknown how the five Dps proteins in *N. punctiforme* are integrated in cellular ROS-protection and iron homeostasis. One focus of this study was to identify their functions.

Iron homeostasis in cyanobacteria

Iron plays a key role in the cyanobacterial metabolism and can be found in iron-rich proteins, which are involved in photosynthesis such as photosystem I (PS I, 12 iron ions per PS I dimer (49)) and proteins in the photosynthetic electron transport chain e.g. cytochrome b_6f lipoprotein (6 iron ions per protein complex (47)). For all diazotrophic cyanobacteria, including *N. punctiforme*, an additional iron demand is caused by the enzyme nitrogenase (19 iron ions per active Mo-Fe nitrogenase protein cluster (48)).

When deprived of iron, which frequently occurs in nature (55), cyanobacteria acclimate by three major processes. One of them is cellular retrenchment that can mean the degradation of phycobilisomes as suggested for the *Synechococcus* sp. PCC 7001 under iron starvation (56). Phycobilisomes are pigment protein complexes that serve as an antenna for light capturing and their biosynthesis has been shown to rely on Fe-containing enzymes (56). Another major effect of iron starvation is that it can result in exchanging iron–demanding enzymes e.g. ferredoxins and SODs with their iron-free variants (56, 57). As a third major adaptation to iron starvation, some cyano-

bacteria enhance their capacity for iron acquisition (44). It should be noted that these adaptations depend on the individual physiological capacity of the cyanobacterial strain and differences can be observed among cyanobacteria (56). In non-diazotrophic cyanobacteria, iron limitation can cause subsequent co-limitations of nitrogen and lead to a chlorotic phenotype (56, 58, 59). In diazotrophic cyanobacteria on the other hand, Fe limitation resulted in slower growth rates and the accumulation of carbon-based storage compartments such as glycogen granules (58–64).

Under iron-replete conditions, cyanobacterial iron homeostasis can be divided into three steps: (i) Initially, iron is imported into the cytosol from an external source, followed by (ii) an intracellular step of iron sequestration inside ferritin-like proteins and (iii) iron is re-mobilised to be distributed to iron-requiring proteins. In cyanobacteria two different ways for the iron uptake, have been identified (Fig. 3).

One of the two known iron-uptake mechanisms is the 'siderophore-mediated Fe uptake', which is thought to be wide-spread among filamentous and heterocystous cyanobacteria and has been mostly explored in *Nostoc* sp. PCC 7120 (65, 66). The siderophore-mediated Fe uptake requires the synthesis of specific iron chelators (in *Nostoc* PCC 7120 e.g. schizokinen). These chelators are capable to bind extracellular Fe and will then be re-imported into the cyanobacterial cell. The second iron-uptake mechanism is to acquire iron by the 'reductive Fe-uptake pathway', mostly explored in the unicellular cyanobacterium *Synechocystis* PCC 6803 (67, 68). It is still under debate whether extracellular Fe^{3+} species might be first reduced to Fe^{2+} or directly taken up by transporter proteins into the periplasmic space. However, from the periplasmic space, Fe^{2+} can be directly transported into the cytoplasm (or undergoes re-oxidation to Fe^{3+} before). It should be noted that both iron-uptake mechanisms can exist in parallel, as shown for *Nostoc* sp. PCC 7120 (65). It has been estimated that 99 % of the Fe^{3+} amount is complexed by organic molecules in aquatic ecosystems and therefore requires effective Fe capture strategies (69, 70). Under physiological conditions Fe^{3+} is highly insoluble in contrast to its reduced form Fe^{2+} (71). Both forms are interconvertible states of iron and under physiological conditions Fe^{3+} displays the main form.

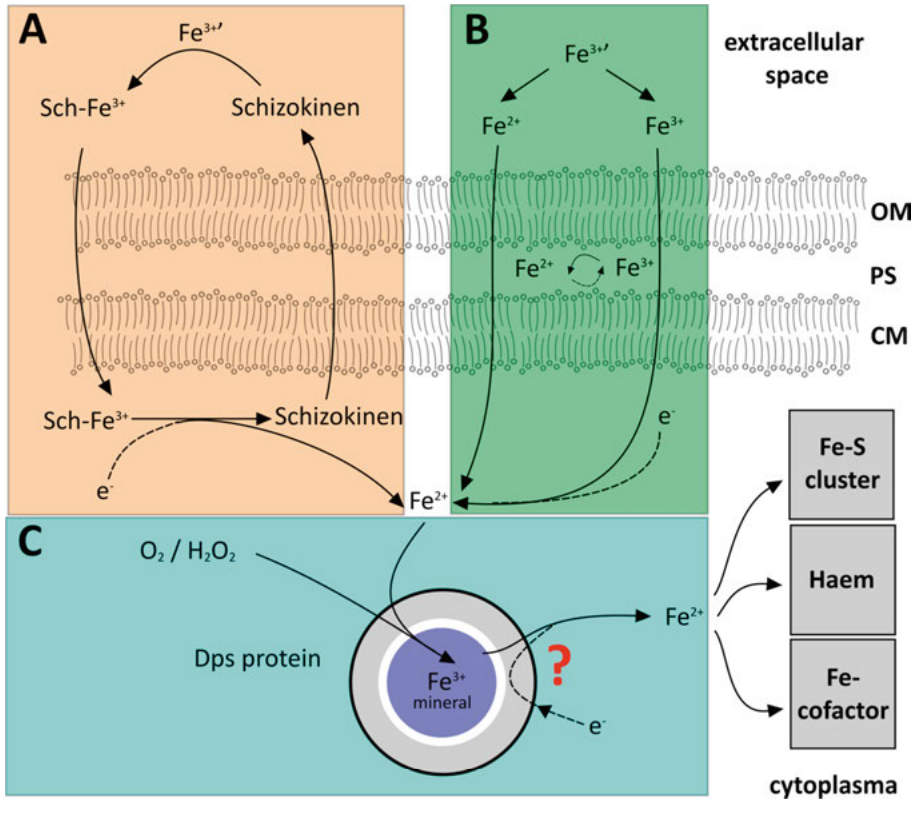

Figure 3 A simplified model of iron homeostasis adapted from the cyanobacteria *Nostoc* sp. PCC 7120 and *Synechocystis* PCC 6803. A. The siderophore-mediated Fe uptake in the schizokinen-secreting cyanobacteria *Nostoc* PCC 7120 (orange box). Export of the siderophore schizokinen into the extracellular space to bind to various external Fe^{3+} species (Fe^{3+}' represents Fe^{3+} complexed by organic molecules) forming a Schizokinen-Fe^{3+} complex (Sch-Fe^{3+}) that is imported via a transporter cascade. B. The reductive iron uptake mechanism in the cyanobacterium *Synechocystis* PCC 6803 (green box). Various Fe^{3+} species (Fe^{3+}') imported the by a TonB transport system (or as a possible alternative by previous external reduction to Fe^{2+}). Import of periplasmic Fe^{2+} or Fe^{3+} into the cytosol by different transport systems. C. The uptake and sequestration of Fe^{2+} mediated by Dps via the reduction of O_2 or/and H_2O_2 (or by a maxiferritin via O_2) (blue box). The unknown Fe^{2+} release mechanism from the Dps core into the cytoplasm is highlighted with a red question mark. Fe^{2+} is incorporated into heme, iron-sulphur clusters (Fe-S) and as single ions to serve as co-factors in metalloproteins. Scheme adapted from a study by Kranzler et al. (44).

After Fe^{2+} has entered the cytoplasm, it needs to be prevented to form an insoluble precipitate inside the cell. Ferritin-like proteins such as Ftn, Bfr and Dps proteins have shown to sequester iron as a Fe^{3+} mineral in their hollow protein cavity (8). O_2 is utilised for the sequestration process in Ftn and Bfr, whereas Dps proteins usually use both O_2 and H_2O_2, while H_2O_2 is the preferred oxidant (8). Dependent on the nature of the ferritin-like protein, different iron release strategies are known. Ftn have been suggested to re-

lease iron upon a ferritin-degradation pathway (72, 73), while Bfr have been shown to release Fe^{2+} by the reduction of the Fe^{3+} mineral by an interacting ferredoxin and a porphyrin, while the latter is integrated inside the Bfr structure (73). The iron release mechanism has not been resolved or even studied in any details for Dps proteins. However, it has been shown that iron release can be triggered by the excess of dithionite or a mixture of NADPH and Flavin mononucleotide (FMN) as shown *in vitro* for *Listeria innocua* Dps (LiDps) (74). Whether NADPH and FMN are utilised *in vivo* to trigger iron release from Dps is unknown. After its release, Fe^{2+} is incorporated into the metabolism. It should be noted that two of the three steps in iron homeostasis, namely iron sequestration and iron release require ferritin-like proteins. Both steps underlie a strong relation between the structure of the Dps protein (or maxiferritin) and its function to incorporate, oxidise and release Fe^{2+}. To initiate a thorough study on the structure of Dps proteins, I chose NpDps4 as a candidate. This Dps is of interest since earlier studies indicated it to be a structurally atypical Dps protein (50). Furthermore, Dps4 may be involved in O_2 reduction as it was suggested for the homolog from *Thermosynechococcus elongatus* BP-1 (51) and therefore displays an interesting candidate to mitigate elevated O_2 concentrations in photobioreactors for the purpose of H_2 production.

Dps proteins

The name 'DNA-binding proteins from starved cells (Dps)' originates from the properties of the first discovered Dps from *Escherichia coli* (EcDps) in 1992 (43). EcDps was found to be highly abundant under starvation conditions in *E. coli* and it formed large Dps-DNA complexes that were shown to be resistant to oxidative damage. The connection of the DNA-binding capability to the name of this new protein family implied a similar function for all Dps members that were subsequently discovered and described.

The DNA-binding motifs have been investigated for the EcDps and Dps1 from *Mycobacterium smegmatis* (MsDps1) that both comprise numerous Lys (and to a lesser extent Arg) at their N- and C-terminal sequences, respectively (75, 76). DNA-binding has been observed to be pH dependent as Lys and Arg remain protonated only in a certain range of pH conditions. Under physiological conditions these amino acids can be positively charged and interact with the negatively charged surface of DNA. Lys/Arg-rich DNA-binding motifs were also found for both Dps from *Lactococcus lactis* (LlDpsA and LlDpsB) as well as for both *Deinococcus radiodurans* (DrDps1 and DrDps2), which stood in well agreement with their DNA-binding capability (54, 77, 78). However, more than half of the studied Dps proteins do not bind to DNA and do not comprise a similar DNA-binding motif as described

for EcDps or MsDps1. Interestingly, *Helicobacter pylori* Dps (HpDps) does not comprise such a motif, but DNA-binding was observed (79). On the other hand there are Dps that exhibit Lys/Arg-rich motifs, but were not shown to interact with DNA e.g. the Dps from *Agrobacterium tumefaciens* (AtDps) or the Dps from *Bacteriods fragilis* (BfDps) (80, 81). Often the DNA-binding properties were thought to be the prerequisite of DNA protection by the Dps. However, the overall conclusion was that the consumption of both, Fe^{2+} and H_2O_2, in the Fe sequestration process, thereby circumventing the Fenton reaction, displays the key function in Dps and protects DNA (8).

For a few Dps proteins it was shown that their DNA-binding property could physically protect the DNA from enzymatic cleavage via DNase I, but the biological relevance remains to be shown (82, 83). Some Dps proteins have been suggested to be involved in bacterial nucleoid formation (84–86) and theoretical models for efficient DNA-Dps condensation in a multi-layered structure has been proposed (87), but lacks *in vivo* proof. One focus of this study was to investigate the DNA-binding potential of the five Dps proteins from *N. punctiforme* to gather further indications on their physiological role.

The Dps protein structure

Dps proteins belong to the ferritin-like protein family and they are evolutionarily related to the iron-storing Ftn and Bfr (88). While Ftn and Bfr are assembled by 24 subunits, Dps proteins consist of twelve subunits forming a protein dodecamer (Fig. 4) (8). Each subunit of a Dps protein consists of a four helix bundle (helix A, B, C and D), in which the helix pairs A-B and C-D are connected by a long loop between helix B and C. In contrast to Ftn and Bfr, Dps proteins comprise a short helix within this loop, the so-called BC helix.

When assembled, Dps proteins consist of a nearly spherical three-dimensional structure with 332 point group symmetry (Fig. 4). The Dps dodecamer forms a hollow sphere (Fig. 4A), which can incorporate up to 500 Fe^{3+} ions in a mineral form (46). The symmetrical 2-fold axis is located perpendicular to each dimeric plane (Fig. 4B). Each of the two 3-fold axes cross the interface of the two distinct trimeric protein regions (Fig. 3 C and D). Each of the two trimeric substructures form a pore structure that allow for the translocation of ions and molecules (8).

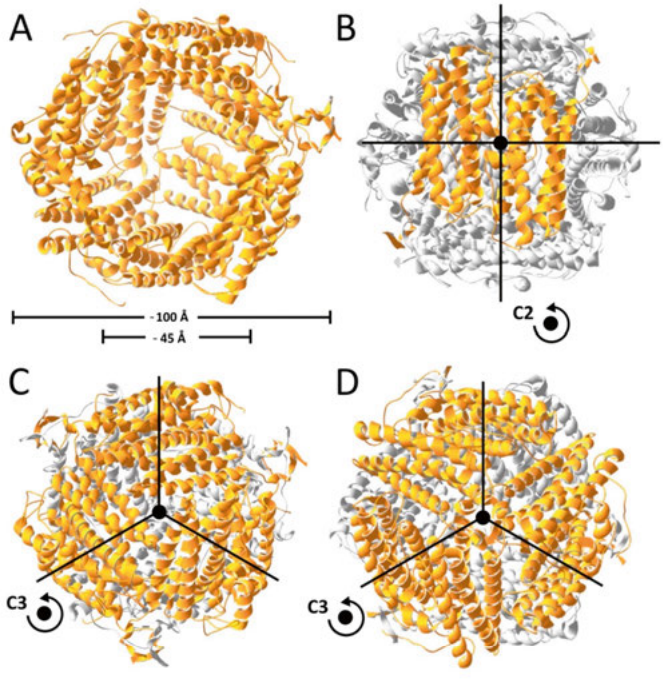

Figure 4 Dps protein structure and symmetry. View on A. the hollow Dps interior, B. the two-fold axis (C2) perpendicular to the dimeric plane, C. the three-fold axis (C3) through the ferritin-like pore and D. the three-fold axis (C3) through the Dps-type pore (8).

To reach the internal cavity, Fe^{2+} ions may travel through these two types of pores. The ferritin-like pore, related to those of Ftn, commonly accommodates negatively charged amino acids such as Asp (74). For the Dps from *Listeria innocua* it has been shown that each subunit of the pore-forming trimer contributes three Asp to line the passage of the pore attracting and guiding Fe^{2+} ions to the twelve FOCs in the internal Dps cavity (Fig. 5).

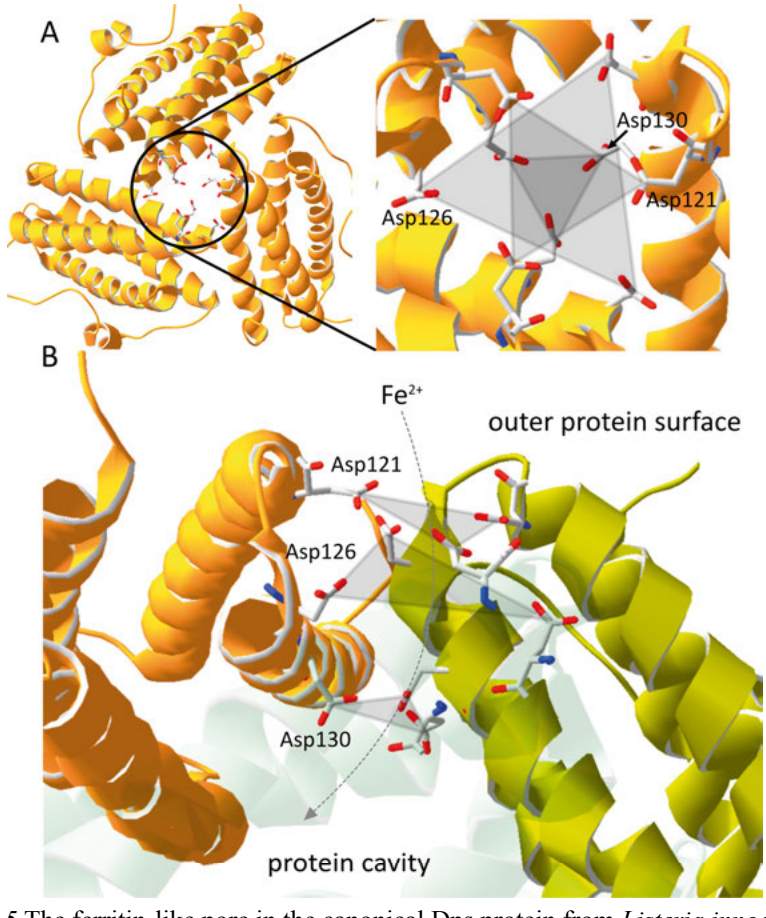

Figure 5 The ferritin-like pore in the canonical Dps protein from *Listeria innocua* (PDB: 6HV1). A. Top view on the ferritin-like pore showing its aspartate arrangement (Asp121, Asp126 and Asp 130) by the trimer and B. side view on the ferritin-like pore. All three symmetrical Asp indicated with transparent triangular planes. The three Dps subunits are displayed in yellow, green and transparent cyan. Fe^{2+} import direction indicated by a grey dashed-lined arrow (74).

The other pore type, which is unique to the Dps protein family, is the so-called Dps-type pore (8). Due to its rather hydrophobic chemical character, ionic attraction and Fe translocation was commonly ruled out from its otherwise unknown function (89).

When inside the Dps cavity, Fe^{2+} binds to the FOC, which is located at the inner dimeric interface. The FOC of a Dps usually contains two His and one Asp/Glu/Gln from one subunit, and one Glu and one Asp from the other subunit (8), which can be summarised as the following FOC motif: His-[11]-His-[3]-Asp/Glu/Gln-[10]-Asp-[3]-Glu (Fig. 6). The two iron binding sites at the FOC were shown to be highly conserved among Dps proteins, by which

they are referred to as canonical Dps (50, 88). It should be noted that multiple attempts of Dps crystallisation have been undertaken to confirm the di-iron binding site, but resulted in structures showing only a single iron coordinated at the binding site A (Fig. 6B) (81, 90–97). To our knowledge, only a single Dps crystal structure from *Borrelia burgdorferi* has been shown two simultaneously bind to two iron atoms at the FOC (Fig. 6C) (98). Based on these results it was concluded that the FOC binding site A exhibits a higher binding affinity as compared to site B that was often found empty or coordinating to a water molecule in numerous Dps crystal structures (90, 95, 99, 100). In a study on the two Dps from *B. anthracis* it was estimated that site B comprised an at least ~ 100 fold weaker Fe^{2+} binding affinity as compared to site A in both Dps. It was speculated that the FOC site B may gain affinity towards Fe^{2+} in the presence of O_2 or H_2O_2 (92).

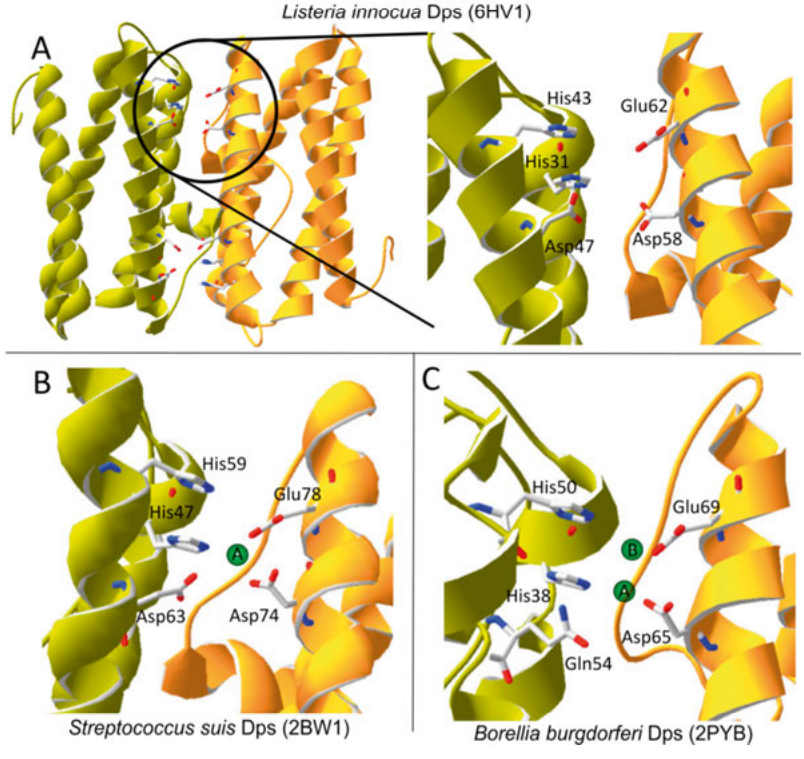

Figure 6 The FOC of Dps proteins in various iron-bound states. A. The dimeric interface of *Listeria innocua* Dps (LiDps) and zoom-in on its metal-free FOC (PDB: 6HV1) (74). B. The FOC of *Streptococcus suis* Dps (SsDps) (PDB: 2W1) binding to one Fe atom at FOC site A (90) and C. the FOC of *Borrelia burgdorferi* Dps (BbuDps) (PDB: 2PYB) binding to two Fe atoms (87). Fe atoms are shown in green spheres and binding sites A and B are indicated by respective letters. Highly conserved amino acids that commonly participate in metal coordination at the FOC shown in stick model. The two subunits of the dimer are shown in green and yellow colour.

When bound at the FOC, the Fe^{2+} ions are oxidised by either O_2 or H_2O_2, as both oxidants have been shown to be utilised by Dps proteins, but with a higher reaction rate for H_2O_2 as compared to O_2 (45, 46). The higher reactivity towards H_2O_2 is of special importance, since Dps proteins consume this specific ROS during the ferroxidase reaction ($2\ Fe^{2+} + H_2O_2 + 2\ H_2O \Rightarrow 2\ Fe^{III}(O)(OH) + 4\ H^+$, (101)) acting as an effective ROS-scavenger, similar to catalases or peroxidases (39, 101). When reacting with O_2, a small amount of H_2O_2 may be released as a by-product that will presumably be quickly reduced by further incoming Fe^{2+} into the Dps protein (101). In several studies it has been shown that Dps-deficient mutants from prokaryotes that contain only a single Dps protein are hypersensitive to externally-introduced oxidants such as peroxides (82, 102–104). It has been concluded that Dps proteins play an important role in coping with oxidative stress. To understand the physiological role of the Dps proteins from *N. punctiforme* the catalysed reactions at the FOC were a focus of this study.

The cyanobacterium *Nostoc punctiforme* and its five Dps

N. punctiforme is a filamentous cyanobacterium, in which vegetative cells contain the functional photosynthetic and carbon fixation machinery. Additionally, the vegetative cells are capable of differentiating into three distinct cell types under conditions that usually are not optimal for proliferation (105). They differentiate into (i) motile hormogonia that allows the cells to move in order to e.g. escape from disadvantageous conditions, (ii) spore-like akinetes that can outlast conditions of starvation, and (iii) heterocysts that can be formed under nitrogen starvation to enable N_2 fixation (105, 106). Heterocysts can account for ~ 5 - 10 % of the total amount of cells, usually organised in a well-defined interval pattern along the filament (Fig. 7). Every cell type has a specific function that ensures the survival under different environmental conditions.

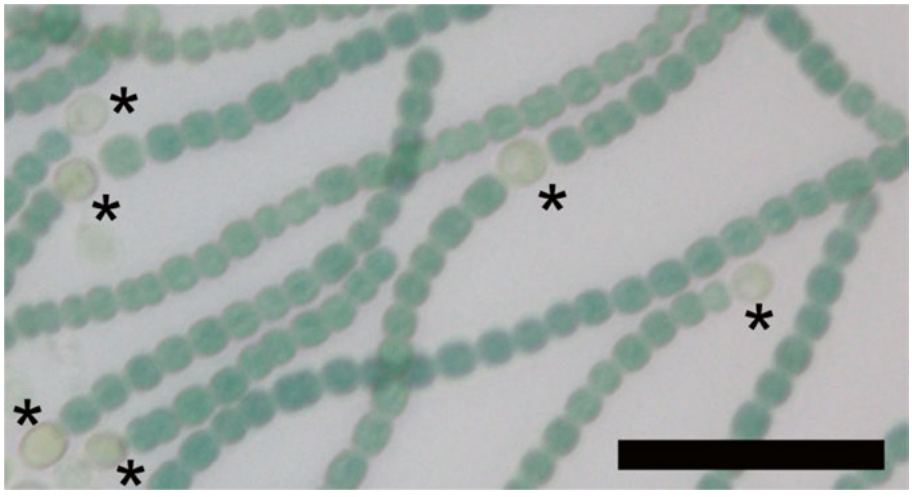

Figure 7 Microscopic picture of *Nostoc punctiforme*. In this culture of the filamentous cyanobacterium *N. punctiforme* between 5-10 % of the vegetative cells differentiated into heterocysts under the condition of N_2 starvation. The black bar represents the length of 25 µm. Heterocysts are indicated with asterisks.

Since *N. punctiforme* exhibits multiple cell types and an unusual high number of Dps proteins, it was hypothesised that each Dps might be linked to a certain condition or cell type. Different *in vivo* studies have been performed in our lab prior to this thesis to test this hypothesis. These results are summarised below, and in Table 1.

NpDps1. The transcript level of *Npdps1* (Npun_R3258) remained unchanged when cultures of *N. punctiforme* were treated with H_2O_2 indicating that NpDps1 is not involved in immediate oxidative stress response (50). A quantitative proteomic study showed a ~2.5 fold higher NpDps1 abundance in heterocysts as compared to the entire filament. However, a study performed in *Nostoc* sp. PCC 7120 has shown that All0458 (the homolog of Npdps1) is localised at the nucleoid of vegetative cells of a nitrogen supplemented culture, suggesting a possible involvement in DNA protection or nucleoid formation (107).

NpDps2. Transcriptomic analysis showed that only *Npdps2* was highly upregulated upon H_2O_2 stress, whereas the other *Npdps* transcripts remained unchanged as compared to the control condition (Table 1) (50). Furthermore, the NpDps2 overexpression strain could tolerate twice as high H_2O_2 concentrations as compared to the control strain (108). These results underlined the role of NpDps2 upon immediate peroxide stress and the lack of NpDps2 could not be compensated by any of the three catalases or various peroxidases in *N. punctiforme* (42). Also for the NpDps2 homolog *all4145* (93.9 %, sequence identity, Clustal Omega) (109) from *Nostoc* PCC 7120, a transcript

increase by ca. 6.5-fold was observed upon H_2O_2 stress indicating similar roles as for NpDps2. To resolve whether NpDps2 is specifically localised in the vegetative cells or in heterocysts, GFP fluorescence was utilised to report on the activity of the *Npdps2* promoter (50). GFP fluorescence was detected in both cell types, indicating *Npdps2* might be transcribed in both cell types. Shotgun proteomic data on the other hand indicated a comparatively lower level of NpDps2 in heterocysts as compared to the entire filament (Table 1) (110). Based on these results, NpDps2 was hypothesised to function mainly in vegetative cells detoxifying H_2O_2 as a first level defence mechanism during oxidative stress.

NpDps3. The promoter-GFP construct for *Npdps3* (Npun_R5701) indicated its transcription in both vegetative cells and heterocysts (50), similar to the results for *Npdps2*. Shotgun proteomics showed the highest relative amounts in heterocysts as compared to vegetative cells among all five NpDps proteins (110). As the transcript level of NpDps3 was not elevated during H_2O_2 exposure, and it did not have a crucial role for H_2O_2 tolerance, NpDps3 was suggested to have a general role for cellular growth (50). In *Nostoc* sp. PCC 7120 All1173, the orthologue of NpDps3, was localised at the nucleoid suggesting a possible involvement in DNA protection or nucleoid formation (107).

NpDps4. In an earlier study about the physiological role of the five Dps proteins in *N. punctiforme* it was found that NpDps4 clustered in a Dps subgroup dominated by N_2-fixing cyanobacteria (50). The physiological role of members of this cluster is fairly unexplored. In regards to protein localisation, a higher level of NpDps4 was found in heterocysts as compared to vegetative cells (110) and its transcript level was unchanged when the culture was treated with H_2O_2, as compared to the untreated one (50). Further sequence comparisons with the cyanobacterial Dps proteins from *Thermosynechococcus elongatus* (TeDpsA) and *Synechococcus elongatus* PCC 7942 (SeDpsA) indicated an atypical FOC composition with an additional His, whereas canonical Dps proteins possess a conserved Asp (50). A biochemical study on the TeDpsA suggested that Zn^{2+} would act as a cofactor at the FOC to increase its oxidant preference towards O_2 (51). However, the authors of that study claimed that Zn^{2+}-free protein material has never been obtained for experimental verification and the function of the two additional His at the FOC remained unknown. *T. elongatus* is a diazotrophic cyanobacterium, but yet no linkage between nitrogenase and TeDpsA has been suggested. *S. elongatus* PCC 7942 on the other hand is a non-diazotrophic cyanobacterium (111) speaking against the idea of these atypical Dps to be specifically involved in supplying Fe to the nitrogenase.

NpDps5. The promoter-GFP construct for *Npdps5* indicated its specific transcription in heterocysts, while no fluorescence was detected in vegetative cells (50). Interestingly, *Npdps5* is located directly upstream of a gene annotated as an iron permease (Npun_F6213), which suggests NpDps5 to be important for iron storage, putatively only in heterocysts (50). A transcript operon study confirmed the co-expression of *Npdps5* with *Npun_F6211* and the *Npun_F6213* gene, supporting the NpDps5 involvement in iron homeostasis. The NpDps5-deletion mutant ΔNpun_F6212 showed a lower growth at higher light intensities of 70 and 200 µmol $m^{-2} s^{-1}$, as compared to wildtype under diazotrophic conditions (112). These results implied that NpDps5 is required to handle light stress, while the overexpression of NpDps5 enhanced the tolerance to H_2O_2 (108). A recent study has shown that heterologous over-expression of all3940, an orthologue of NpDps5 from *Nostoc* PCC 7120, leads to an increased tolerance against nutrient limitation and different abiotic stresses, including oxidative stress in *E. coli* (113).

As mentioned above, Dps proteins have been shown to increase bacterial robustness against oxidative stress (82, 102–104) and might be advantageous for finding molecular solutions to cope with elevated O_2 concentrations in photobioreactor systems.

However, the mechanistic understanding of the different biochemical reactions within Dps that are important for oxidative stress and iron homeostasis is rather unclear. Knowledge of the structural and biochemical properties of the Dps will be needed to guide us towards a more detailed understanding of their individual and perhaps collaborative physiological roles. This is of special importance for systems, where multiple ferritin-like proteins coexist in one bacterium.

Table 1 Overview on the properties of the five Dps from N. punctiforme. Not determined (n.d.).

	NpDps1	NpDps2	NpDps3	NpDps4	NpDps5
relative protein abundance heerocyst:entire filaments (110)	2.47	0.66	9.1	4.69	1.89
fluorescence from promotor-GFP constructs in NH_4^+ conditions (50)	n.d.	in vegetative cells	in vegetative cells	n.d.	no fluorescence observed
fluorescence from promotor-GFP constructs under N_2 deprivation (50)	n.d.	in vegetative cells & heterocysts	in vegetative cells & heterocysts	n.d.	in heterocysts
transcript level increase of the Npdps gene after 30 min of H_2O_2 exposure; H_2O_2-treated:non-treated culture (50)	1.1	25	0.84	0.52	0.99

Aim

The aim of the work presented in this thesis can be summarised in three points:

1. To determine the role of each of the five NpDps in oxidative stress protection and iron regulation with the purpose to evaluate their potential for increasing the robustness of cyanobacteria in photobioreactor systems.
2. To uncover a cultivation condition that reduces cellular proliferation for the benefit of production, in order to implement this culture condition in a biofilm reactor for H_2 production.
3. To design and manufacture a biofilm photobioreactor that could serve as a low-energy input system for cyanobacterial H_2 production.

The research and discussion part of this thesis consists of three parts.

In an introductory part, I present and discuss a novel conceptional design of a biofilm photobioreactor for the purpose of indirect photolysis. It is a vision that addresses several challenges in our strive to develop a more efficient cyanobacterial H_2 production system and takes results and concepts from chapter I and II into account.

Chapter I. Based on the results from biochemical investigations, I am discussing the potential of a group of Dps proteins to increase the tolerance to oxidative stress. The objective is to utilise Dps proteins in cyanobacterial H_2 production systems. The results in this chapter cover research presented in paper I, II and III, together with two sections exclusively presented in this thesis, and describe how the first aim in the list will be accomplished.

Chapter II. *Nostoc* PCC 7120 Δ*hupW* was set under iron starvation to evaluate this cultivation strategy for the purpose of H_2 production. It describes how the second aim in the thesis will be achieved. The objective was the reallocation of photosynthetic energy from cell growth to cellular storage that can be used to enhance H_2 yields. Chapter II covers the research presented in paper IV and an additional section concerning manufacturing a biofilm photobioreactor (exclusively in R&D of this thesis).

Results and Discussion

A novel concept for enhanced H_2 production from cyanobacteria

In photobioreactor systems cyanobacterial photosynthesis can lead to toxic concentrations of O_2, which can impair cellular mechanisms on different levels (33, 34, 39, 40). Attempts to insert and overexpress O_2-svavenging and ROS detoxifying enzymes have been considered to protect cyanobacteria producers from O_2 and oxidative stress (12). Based on results from biochemical investigations described in thesis chapter I, I discuss the potential of a group of Dps proteins to increase the tolerance against oxidative stress. The aim is to implement this strategy in H_2 producing cyanobacteria.

In the field of photobiological H_2 production new strategies to enhance H_2 production yields are required. For this thesis a novel conceptional design is presented that addresses several challenges in the process of cyanobacterial H_2 production. In the past years the great energy input into photobioreactors for the purpose of low-cost products e.g. biomass or fuels such as H_2 has been identified to be an obstacle for economic viability (25). The circulation of the suspension cultures to reach an optimal distribution of light, and the use of expensive material for the construction of photobioreactors create great costs and need constructive revision (25). In a pilot plant for the production of biomass, the liquid circulation was estimated to consume about ~ 54 % of the total power of the process, representing a significant cost factor. Innovations with reduced costs may enter the upscaling process for the photobiological H_2 production that could contribute to a carbon-free society.

In this thesis I present a new concept that uses cyanobacterial biofilms for the production of H_2. I hypothesise that biofilms do not require energy-intense liquid circulation and therefore could be a cheap alternative to photobioreactors using suspension cultures. A novel design for a biofilm photobioreactor is proposed in chapter II. Almost no data is available about cyanobacterial growth rate inside biofilms and how they are affected by biofilm formation. Nevertheless, there is no indication that microbial growth is arrested in microbial biofilms and one may assume that growth rates could be similar to those in suspension cultures (114–116). To control the biofilm thickness for optimal photosynthetic production, mechanism to prevent ex-

tensive growth must be considered. If not controlled, biofilms might simply overgrow the photobioreactor system. One possibility is to restrict cellular growth of the culture. To accomplish that, we argue that a halted state of growth must be initiated and retained throughout the H_2 production process. In this study we chose a nutrient-limited strategy that could impair growth, which could be useful to implement into biofilm photobioreactors, which is discussed in chapter II.

As a side-effect, I hypothesise that impaired growth could reallocate more photosynthetic energy towards the biosynthesis of photobiological fuel such as H_2. Recent reviews on the manipulation of glucose storage and photobiological fuel production formulated similar conclusions as efforts that impaired glycogen storage in cyanobacteria did majorly not result in enhanced fuel synthesis (6, 14).

Vision. In this thesis I propose the following novel concept for potentially cheaper and enhanced H_2 production (Fig. 8): This concept includes a cyanobacterial biofilm that is integrated in a photobioreactor chassis for the purpose of H_2 production. The cyanobacterial producers are of filamentous and heterocystous origin. Heterocysts display an optimal chassis for indirect photolysis processes, but to make this a reality, H_2-producing enzymes such as hydrogenases or entire photo fermentative pathways have to be introduced by synthetic biology. In the biofilm photobioreactor, the culture is entirely immobilised and gas exchange takes place through a membrane that stabilises the film. Besides technical O_2 extraction, the toxicity of elevated O_2 conditions may be reduced by the genetic introduction of a resistance cassette that could consist of Dps proteins or other ROS-protectants. CO_2 inside the system is intracellularly recycled by the accumulation of sucrose via carbon fixation and degradation of sucrose into CO_2 and H_2. H_2 and O_2 have to be extracted from the system to be used as CO_2-emission free fuel components.

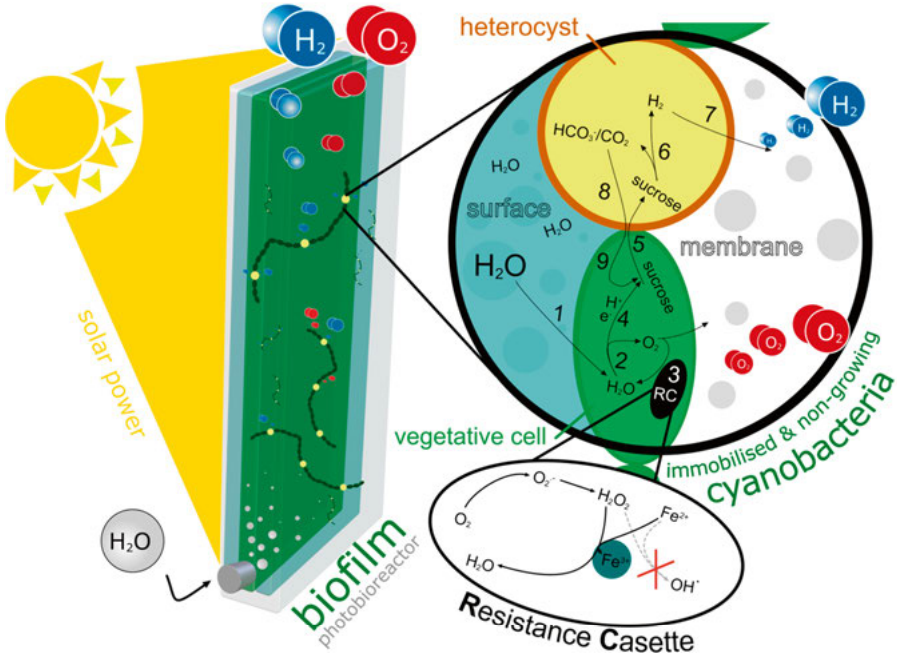

Figure 8 The conceptional design of a H_2-production system from cyanobacterial biofilms in a non-proliferating physiological state. Sunlight delivers solar energy to a photobioreactor system that contains a biofilm. Photosynthesis requires the re-supply of water, while H_2 and O_2 gasses are extracted from the system. Zoom in on the surface of the biofilm onto a molecular level: 1. Water diffuses from the humid immobilisation surface into the vegetative cells of the filamentous and heterocystous cyanobacterium. 2. Photosynthesis drives water splitting reaction and produces reductive power (e^-), H^+ and O_2. O_2 escapes from the cells into the membrane or forms H_2O_2 in a reactive oxygen species reaction cascade, which could be detoxified by an additional resistance cassette (RC), genetically introduced into the cyanobacterium. The RC is a ROS-capturing protein e.g. a Dps protein, which displays also an iron storage protein. 4. Carbon fixation leads to the accumulation of glucose and sucrose. 5. Sucrose is transported into heterocysts containing a microoxic environment. 6. Sucrose is degraded by an artificially introduced photo fermentative pathway into HCO_3^-/CO_2 and H_2. 7. H_2 leaves the cells, diffusing through a membrane and is collected to serve as a fuel. 8. HCO_3^-/CO_2 is recycled in the carbon fixation mechanism to form sucrose. The cyanobacteria are immobilised on a surface and not agitated by an energy-intense mechanism. A cultivation strategy is applied that resulted in a halted state of growth and biomass accumulation is restricted, e.g. by iron limitation.

Chapter I

All five NpDps proteins form high multimeric protein complexes (Paper I & III)

Based on the structural information from more than 30 different Dps crystal structures, Dps proteins generally assemble into a dodecameric multimer (8). This dodecamer is thought to be the only form that guarantees efficient iron storage, but during the past decades various Dps proteins have been purified that comprised different multimeric forms besides the dodecamer such as dimers, trimers and hexamers (52, 54, 117, 118). Some of the intermediate forms comprised different functions as compared to the dodecamer. For example, the biochemical analyses on the Dps1 from *Deinococcus radiodurans* showed differential DNA-binding profiles for its dimeric and dodecameric forms, but the capacity for DNA-aggregation was only observed for the dodecamer (83, 119). It remains unknown whether these intermediate forms are active Dps complexes *in vivo*.

In this work, the five Dps proteins from the cyanobacterium *N. punctiforme* were purified to identify their physiological function and whether they could potentially display candidates for increasing the robustness of the cells towards oxidative stress in production systems. In order to gain insights on their multimeric state after the proteins were overexpressed and purified, non-denaturing PAGE (polyacrylamide gel electrophoresis) was utilised. A dodecameric form enables the full function of the Dps in terms of Fe^{2+} oxidation and storage, whereas the formation of the Dps-typical dimer allows Fe^{2+} oxidation, as the ferroxidase center (FOC) is formed at the dimeric interface, but does not enable iron storage. All five NpDps proteins were observed to assemble into multimeric forms of at least trimers, and differences in their multimeric composition were observed (Fig. 9). Based on the molecular mass, NpDps1 and NpDps2 were identified in their putative trimeric and pentameric forms, respectively. In theory, these multimers could be lacking the active interface of the dimer as various complexes could be formed that do not require the Dps-typical dimer. NpDps3, NpDps4 and NpDps5 on the other hand formed higher multimeric forms of at least hexamers and likely comprise active FOC in their structures. Additionally, NpDps5 was found to form a putative tetramer. The results of the non-denaturing PAGE provided

the first indication of differential multimerisation behaviour among the five NpDps proteins.

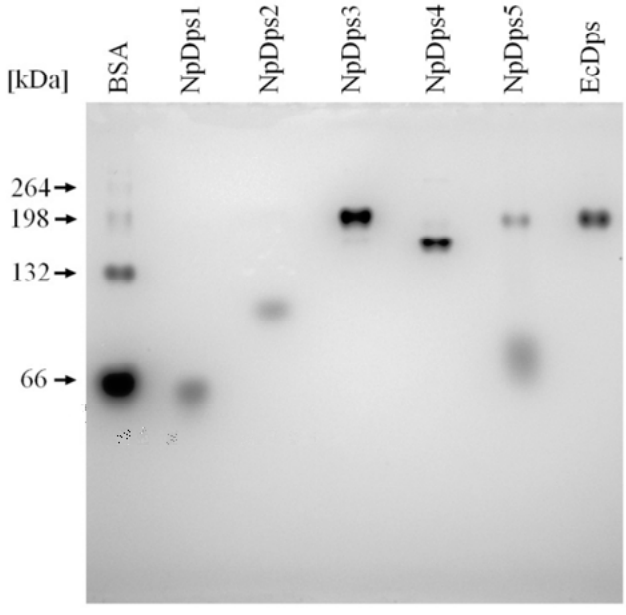

Figure 9 Multimerisation of NpDps1, NpDps2, NpDps3, NpDps4, NpDps5 and *E. coli* Dps (EcDps) analysed by non-denaturing PAGE. The theoretical molecular masses of putative dodecamers were 255 kDa for NpDps1, 234 kDa for NpDps2, 266 kDa for NpDps3, 263 kDa for NpDps4, 212 for NpDps5 and 239 kDa for EcDps. Additionally, the different native forms of bovine serum albumin (BSA) were used to estimate the approximate molecular masses. The pH of the gel and that of the running buffer was 8.5 and 8.0, respectively. The gel was stained with colloidal Coomassie.

Since it was aimed to investigate the enzymatic function of the five NpDps in solution via spectroscopic methods, the stability of the Dps proteins was investigated with dynamic light scattering (DLS). DLS represents a non-invasive technique that has been used to analyse the particle size of Dps multimers in solution (120, 121). Via DLS, insights on the Dps multimer stability at various conditions can be gained. In this experiment, all Dps proteins were analysed at pH 3.0, 5.0, 6.0, 7.0, 8.0, and 9.0 using different buffer compounds to find at least one suitable condition, at which all the five NpDps could be analysed in an identical setup, thus enabling direct comparisons in an enzymatic assay.

The DLS analysis revealed that NpDps3, NpDps4 and NpDps5 formed stable multimers at a pH range between pH 5.0 to pH 8.0, whereas NpDps1 and NpDps2 were stable at more acidic pH conditions (Fig. 10). This was in agreement with the prior results from the non-denaturing PAGE, performed

at pH 8.0 - 8.5, in which NpDps1 and NpDps2 comprised multimers of lower molecular weight, as compared to NpDps3, NpDps4 and NpDps5. We concluded that all NpDps possessed an individual pH range to be physiologically active in *N. punctiforme*. Among the investigated pH conditions, pH 6.0 seemed to represent a suitable condition for enzymatic studies under identical experimental conditions that guarantee multimer preservation.

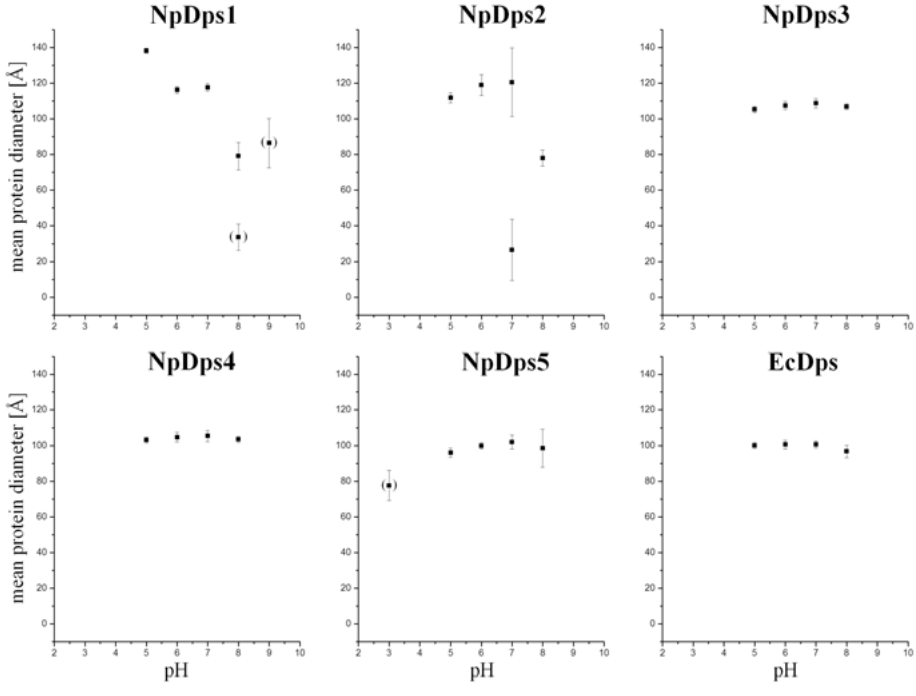

Figure 10 Dynamic light scattering (DLS) on NpDps1, NpDps2, NpDps3, NpDps4, NpDps5 and EcDps at different pH conditions. The hydrodynamic diameters of all protein species are displayed as a mean of the average hydrodynamic diameter from each experimental series in Å at pH 3.0, 5.0, 6.0, 7.0, 8.0, and pH 9.0. Protein complexes with a lower peak occurrence than 1% (number related) are not displayed, whereas those with occurrence between 1 and 10 % are shown in parentheses. The *E. coli* Dps (EcDps) served as a control. Mean +/- S.E. protein diameters are given as error bars.

Previous gel electrophoresis and DLS analyses of the NpDps protein material showed that each of the NpDps formed multimeric complexes and were individually affected by the pH condition. However, both analytical techniques did not suffice to specify the multimeric state of the Dps proteins in solution. This is of importance as the multimeric form of a Dps protein can determine its functional capacities, as a Dps-typical dimeric interface allows the formation of the FOC and the dodecamer additionally enables iron storage (8). Therefore the protein material was subjected to gel filtration that

allows for a classical molecular mass determination at pH 6.0 and pH 8.0. Both pH conditions were used to analyse the degree of multimerisation and the possible transition of a higher multimeric state into a lower one for NpDps1, NpDps2 and NpDp5 at a more basic condition. The results of gel filtration supported the observations that were made using non-denaturing PAGE and DLS. At pH 6.0 NpDps1 and NpDps2 were found to comprise a higher multimeric relative ratio of multimers such as an 11-subunit complex as compared to pH 8.0, while no difference was observed for the multimer stability of NpDps3, NpDps4 and NpDps5. All these three Dps formed multimeric complexes of octamers and higher forms at both pH conditions (Fig. 11).

Interestingly, the smallest multimeric state that could be detected was of dimeric or trimeric nature and they might represent the more favourable multimeric forms under basic conditions. Dimeric and trimeric Dps forms have often been observed (52, 54, 117, 118) and referred as to the building blocks of the Dps dodecamer. Monomeric forms of Dps proteins were not observed that would structurally not allow enzymatic activity. Only some studies report on the identification of monomeric Dps, mostly at more acidic pH conditions or in combination with point mutations at the Dps assembly interfaces (75, 122, 123).

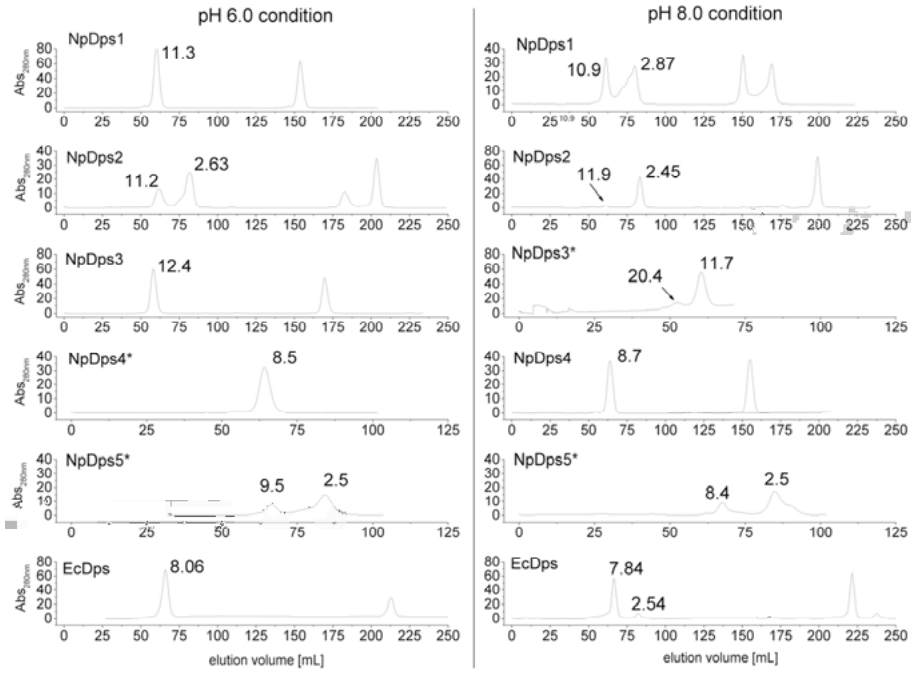

Figure 11 NpDps multimerisation studied at different pH conditions. Gel filtration profiles of recombinant NpDps1, NpDps2, NpDps3, NpDps4, NpDps5 and EcDps at two pH conditions: pH 6.0 (10 mM MES, 150 mM NaCl) and pH 8.0 (10 mM Tris, 150 mM NaCl) at 4°C using a HiLoad 16/600 Superdex 200 column. Proteins (ca. 0.35 – 0.5 mg per run) were equilibrated at given conditions for at least 30 min prior gel filtration at 4 °C. The absorption units at 280 nm are in mAU. Two subsequent injections for each protein are shown, except for NpDps3 and NpDps4 at both pH conditions and for NpDps5 at pH 8.0. EcDps served as a control for NpDps multimerisation. Numbers above the peaks (or indicated with arrow) show the predicted multimeric state (accurate within 5%) averaged over the two subsequent gel filtrations (* except for NpDps4 and NpDps5 at both pH conditions and except of NpDps3 at pH 8.0, for which only one run was performed).

In summary, at pH 6.0 all Dps proteins formed a multimer ranging between eight to twelve subunits that ensure the formation of the FOC and allow for spectroscopic analysis. It should be noted that no information on the intracellular pH in the multicellular cyanobacterium *N. punctiforme* is available and that pH 6.0 might deviate from the physiological pH, in which a specific NpDps is active. Nevertheless, the pH in different cellular compartments in cyanobacteria showed a strong dependence on photosynthesis due to proton translocation that takes place across the thylakoid membranes (124, 125). Alternations of the light intensity during the day are thought to cause significant pH variations, which might hypothetically regulate a pH-dependent Dps decomposition and therefore affect the functions of specific NpDps proteins. Dps proteins have been known to comprise different functions such as their ferroxidase capacity and DNA-binding properties. Both of these functions

were investigated in this study. While for the ferroxidase capacity at least the Dps-typical dimeric structure is required, DNA-binding requires in theory no Dps complex formation, if DNA-binding originates from their lysine-riche N- or C-terminal sequences.

The three canonical Dps: NpDps1, NpDps2 and NpDps3 (Paper I)

Earlier investigations of the five NpDps proteins have resulted in distinct sequence-based categorisation (50). NpDps1, NpDps2 and NpDps3 shared high similarities with canonical Dps proteins possessing a conserved FOC motif His-[11]-His-[3]-Asp/Glu/Gln-[10]-Asp-[3]-Glu (50). NpDps4 and NpDps5 were found to deviate from this pattern and were considered to be of atypical nature. As a result of this structural differentiation, we discuss the physiological role of the three canonical Dps separately from NpDps4 and NpDps5. The predicted tertiary structure of the three canonical NpDps, based on the protein homology/analogy recognition engine 2 (Phyre2) (126), revealed high structural similarity (Fig. 12). Models of the NpDps1, NpDps2 and NpDps3 comprise the classical Dps protein fold with a four- helix bundle including the BC helix within the long loop connecting helix AB with helix CD.

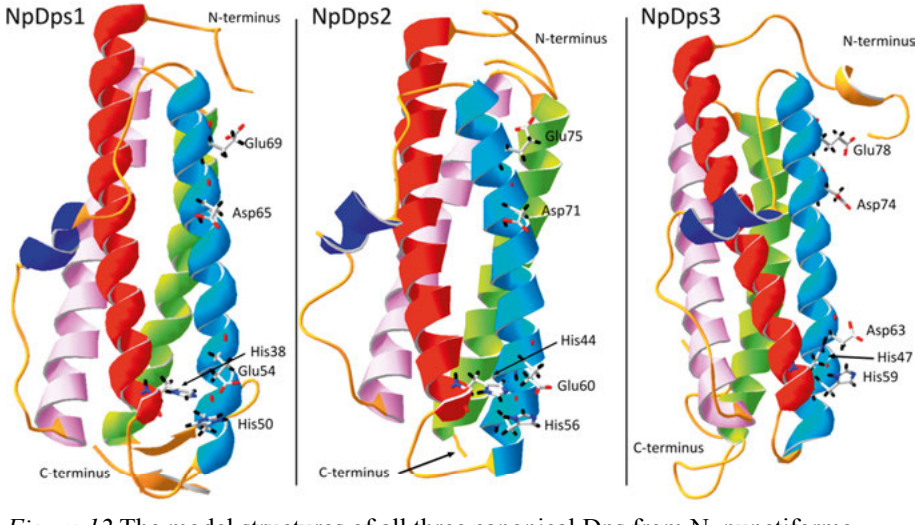

Figure 12 The model structures of all three canonical Dps from N. punctiforme. Model structures for NpDps1, NpDps2 and NpDps3 created using the web-based protein homology/analogy recognition engine 2 (126). Helices A (red), B (light blue), BC (dark blue), C (pink) and D (light green) displayed. Amino acids conserved among canonical Dps for metal binding at the FOC shown as stick model. N- and C-terminal sequences labelled.

In earlier studies, the NpDps2 protein was strongly associated with H_2O_2 detoxification (50). In this thesis it was aimed to verify whether the purified NpDps2 could utilise H_2O_2 as an effective oxidant. Additionally, studies on NpDps1 and NpDps3 showed that both proteins could not compensate for the lack of NpDps2, indicating that NpDps1 and NpDps3 were not crucial in response to elevated levels of H_2O_2 (50). Whether this finding was correlated to an inability to use H_2O_2 as an oxidant was analysed. Spectroscopic experiments were performed to monitor Fe^{2+} oxidation at 310 nm under aerobic conditions in the absence or presence of the three canonical NpDps, testing their ability to utilise O_2 for Fe^{2+} oxidation. The addition of H_2O_2 should show whether the NpDps catalyse the reaction between Fe^{2+} and H_2O_2.

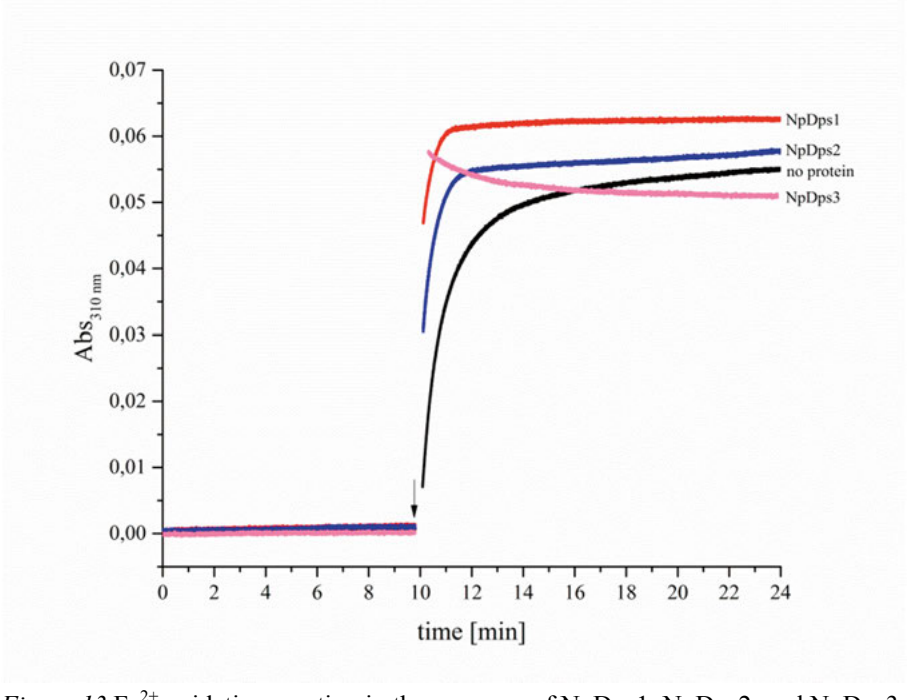

Figure 13 Fe^{2+} oxidation reaction in the presence of NpDps1, NpDps2, and NpDps3. Absorbance measured at 310 nm corresponds to the formation of the ferric iron in the presence of NpDps1 (red trace), NpDps2 (blue trace), NpDps3 (pink trace), and for the no protein control (black trace). 0.5 µM of each NpDps protein was mixed with 24 µM Fe^{2+} (48 iron ions per Dps dodecamer), at time 0 min and the absorbance was analysed for 10 min, before addition of 16 µM H_2O_2 as indicated by the arrow. Reactions were performed in 5 mM succinate buffer, pH 6.0, 50 mM NaCl, at room temperature and under aerobic conditions.

The spectroscopic analysis was performed at pH 6.0, at which a high multimeric state of each of the three NpDps proteins was previously found and could guarantee the ferroxidase activity of each NpDps protein. In these multimeric complexes, the formation of the FOCs would allow an enzymatic

investigation in regards to Fe^{2+} oxidation capacities as shown for many Dps proteins (51, 78, 89, 92, 127, 128).

The results revealed that none of the three NpDps proteins utilised O_2 for Fe^{2+} oxidation under the chosen conditions, but they used H_2O_2, as the Fe^{2+} oxidation was faster in the presence of the three NpDps as compared to the control (Fig. 13). This finding was surprising, as NpDps1 and NpDps3 could not compensate for the lack of NpDps2 to protect the culture from exogenously added H_2O_2 (50). Nevertheless, the results suggest that these two NpDps might share the role of H_2O_2 detoxifiers, as previously shown for NpDps2, but maybe under yet unknown physiological conditions. The NpDps1 homolog from *Nostoc* PCC 7120, encoded by the gene *all0458* (83.8 % sequence identity, *Clustal Omega* (109)), was found to be induced under low-temperature conditions (107). This might imply that under a similar condition NpDps1 could be active to protect the cell from H_2O_2. The All1173 from *Nostoc* PCC 7120, the protein homologue to NpDps3 (79.3 % sequence identity, Clustal Omega (109)), was observed to protect DNA from the Fenton reaction (117), which indicates its capacity to consume H_2O_2 for the Fe^{2+} sequestration process, similar to NpDps3, but under which physiological condition remains unknown.

To conclude, all three NpDps can utilise H_2O_2 and therefore display interesting candidates to be implemented in cyanobacterial cultures to protect them from oxidative stress that is promoted under elevated O_2 concentrations.

Two of the three canonical NpDps bind to DNA (Paper I)

Since 1992, more than 20 DNA-binding proteins from starved cells (Dps) have been investigated in regards to their possible role in DNA-binding and protection. For more than half of these proteins, the capability to bind to DNA was not observed (Table S1). For those that bind to DNA, a clear and conserved DNA-binding motif has not been found - only a tendency, namely the possession of more positively charged amino acids in the N- or C-terminal sequences that enables ionic interaction with DNA, was identified. To identify the physiological function of the five NpDps proteins, the ability to bind to DNA could indicate a role in DNA protection or nucleoid formation.

Except of NpDps1, NpDps2 and NpDps3, were found to bind to DNA in a pH dependent manner. These results were based on electrophoretic mobility shift assays (EMSA). Notably, the GFP fusion protein of All0458, the homolog of NpDps1, was found to localise at the nucleus in *Nostoc* PCC 7120 and therefore a role in DNA protection was suggested (107). As identified in an

earlier study on the five NpDps proteins, only NpDps3 possesses a lysine-rich C-terminal tail ($KxxKxxxxxK_{end}$) that supports ionic interaction with DNA (50) (Table S1), similar to the C-terminus ($KxxxxKxRRKxx_{end}$) of Dps1 of *M. smegmatis* (MsDps1) (75). The NpDps3-homolog All1173 from the filamentous and heterocystous cyanobacterium *Nostoc* PCC 7120 was not observed to bind to DNA at pH 8.0, a condition at which also all NpDps proteins did not show DNA-binding properties (data not shown) (117). Interestingly, the fusion protein GFP-All1173 co-localised at the nucleus in *Nostoc* PCC 7120 indicating a role for DNA nucleoid formation or DNA protection (107). Except of the lysine-rich C-terminal tail of NpDps3, the canonical NpDps terminal sequences were found to contain none or at most two positively charged amino acids (Table S1). This low amount of positive charges likely did not relate to DNA-binding, as for several non-DNA-binding Dps two or more positively charged amino acids can be found in their termini (Table S1). Another known mechanism that could facilitate DNA-binding is related to the overall surface charge as shown for Dps from *H. pylori* (79), but was not investigated for the NpDps in this study. Whether the NpDps2 and NpDps3 in *N. punctiforme* comprise a physiological role in DNA nucleation remains unknown, but they display candidates for future investigation, as the process of cyanobacterial nucleoid formation is largely unknown (129).

The Dps protein annotation implied DNA-binding properties for all the members of the Dps class, but this annotation should be re-considered in the light of the past decades of Dps research. Besides DNA-binding, functional studies on members of this Dps protein class quickly revealed their role in detoxifying H_2O_2 and Fe homeostasis. Based on their similarities to ferritins, they have been referred to as miniferritins (92), which might be a more appropriate annotation than the abbreviation Dps. Besides the three canonical NpDps, *N. punctiforme* comprises two additional Dps proteins, and the physiological function of NpDps4 displays a focus of this study.

NpDps4 – the Dps with an atypical His-type FOC (Paper II)

In earlier studies, the protein sequence of NpDps4 indicated distinct deviations from the conserved FOC motif that is commonly found in canonical Dps (50). The FOC in NpDps4 was suggested to comprise a His-pronounced character, similar to the DpsA from *Thermosynechoccocus elongatus* (TeDpsA) (51). Biochemical investigations on the enzymatic capacity of TeDpsA revealed a pronounced use of O_2 for Fe^{2+} oxidation catalysis as compared to many other Dps proteins. The atypical FOC composition of

TeDpsA, but also its putative enzymatic modulation by Zn^{2+} was suggested to be linked to the distinct oxidation capacity.

Whether similar characteristics could also be found in NpDps4 that could give insights on the physiological function of the protein, a thorough structural investigation via crystal structure analysis was initiated. The crystallographic data on NpDps4 revealed a dodecameric structure that consists of twelve identical subunits, which is typical for Dps proteins (8) and it verified the existence of the predicted atypical FOC, similar to TeDpsA (Fig. 14). The His78 exchanged for the conserved Asp that can be found among canonical FOC and the His 164, involved in a Dps-atypical metal binding at binding site B, originated from a third monomer. These results supported our hypothesis that both cyanobacterial proteins, NpDps4 and TeDpsA, share similar protein structures that exclude them from canonical Dps proteins (8, 51). The FOC of NpDps4 was found to bind to two Fe atoms at the FOC binding site A and B, and Zn^{2+}-soaked crystals showed one Zn atom at binding site A. This observation was different from the TeDpsA that showed a persistent binding of one Zn atom at the FOC site A, whereas at site B one Fe or Zn atom can be found (51).

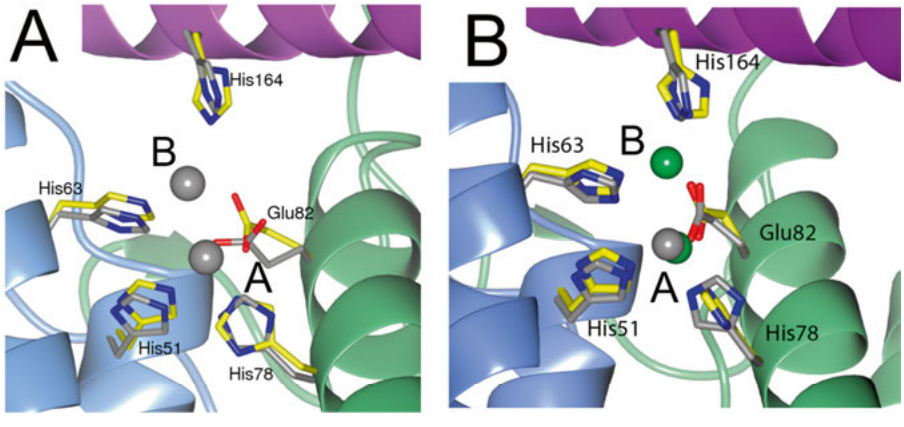

Figure 14 Metal binding at the FOC of NpDps4. A. Superposition of the amino acids involved in the formation of the NpDps4 FOC of the Fe^{2+}-soaked structure (amino acids and coloured in yellow, grey spheres indicate the Fe atoms, PDB: 5HJH) with the metal-free NpDps4 structure (amino acids coloured in grey, PDB: 5HJF). All amino acids labelled. B. Comparison of Zn^{2+}-binding at the FOC between NpDps4 and TeDpsA. Superposition of the amino acids involved at the FOC in the Zn^{2+}-soaked NpDps4 structure (amino acids labelled and coloured in yellow, Zn atom in grey, PDB: 5I4J) with the Zn^{2+}-soaked TeDps4 structure (amino acids coloured in grey, Zn atoms in green, PDB: 2VXX) (51). The metal coordination sites of the FOC are indicated with the letters A and B.

The observation that two Fe atoms coordinate at the FOC is rare in the field of Dps research as it was solely observed for the Dps from *Borellia burgdor-*

feri (98). While FOC site A has been frequently shown to bind to one Fe atom, the metal binding site B has been found to be empty or filled by a water molecule (90, 95, 99, 100). It was concluded that site A is the high affinity binding site at the FOC, whereas FOC site B comprises only a loose coordination to the second Fe atom (92).

To determine whether a similar oxidant preference could be observed for NpDps4 as found in TeDpsA, a spectroscopic analysis was performed using a similar setup as the one used for NpDps1-3. The results showed that NpDps4 catalysed the redox reaction between Fe^{2+} and O_2, but a catalytic effect on the reaction between Fe^{2+} and H_2O_2 was not observed in the presence of NpDps4 (Fig. 15). This was in contrast to the results presented for TeDpsA, in which H_2O_2 was utilised as an oxidant, but at an approx. 2-fold higher rate as compared to O_2 (51). Since the earlier *in vivo* experiments showed no change in the transcript level of *Npdps4* upon H_2O_2 addition to a culture of *N. punctiforme*, the spectroscopic results supported our hypothesis that NpDps4 is not involved in H_2O_2 detoxification. Only a single other Dps protein, the BaDps1 from *Bacillus anthracis*, was found to be restricted to O_2 as the only oxidant (91). However the FOC of BaDps1 is of canonical nature indicating that the His-type FOC of NpDps4 might not be the only reason for its atypical oxidant preference. Additionally, *B. anthracis* possesses another Dps protein, the BaDps2, which could use both oxidants O_2 and H_2O_2 (91). Whether the two Dps from *B. anthracis* work in concert remains unclear, but *N. punctiforme* comprises three canonical Dps that utilise H_2O_2 and thus complement the function of the O_2-consuming ferroxidase activity in NpDps4.

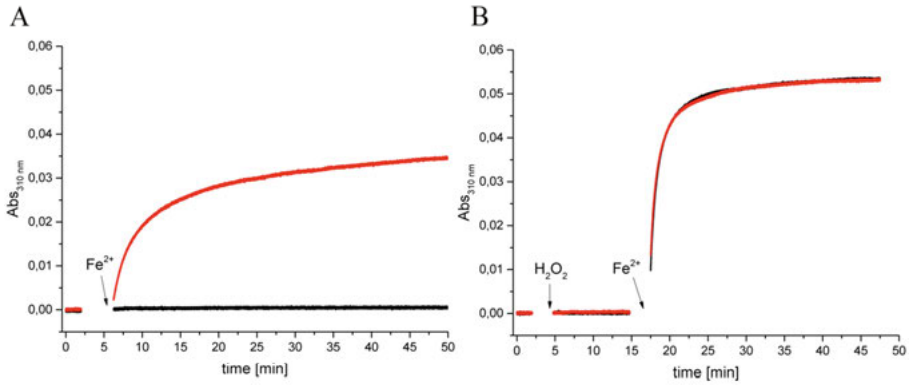

Figure 15 NpDps4 catalyses the O_2-mediated Fe^{2+} oxidation, but no indication for utilising H_2O_2 as an oxidant was found. Absorption spectroscopy following the wavelength at 310 nm to monitor the formation of Fe^{3+} species over time. A. In the absence of NpDps4, 24 µM Fe^{2+} was added to the reaction mixture (black graph). In the presence of 0.5 µM NpDps, 24 µM Fe^{2+} was added to the reaction mixture (red graph). B. In the absence of the protein 16 µM H_2O_2 and 24 µM Fe^{2+} were added (black graph). In presence of 0.5 µM NpDps4, 16 µM H_2O_2 and 24 µM Fe^{2+} were added (red graph). The reaction mixture contained 5 mM succinate buffer at pH 6.0 and 50 mM NaCl under aerobic conditions. All chemical additions are highlighted with arrows. Protein absorbance was set to zero. Time axis was reconstructed from subsequent absorbance traces, because spectra were recorded after each chemical addition. Two experimental replicates were performed for each reaction; the same NpDps4 protein material as for metal-free crystal structure determination was utilised.

In conclusion, the high structural similarities between NpDps and TeDpsA implied similar functions for both cyanobacterial proteins. In contrast to TeDpsA, NpDps4 lacks the capacity of utilising H_2O_2 for Fe^{2+} oxidation. Furthermore, when Zn^{2+} was added to NpDps4 it lost its function to catalyse the O_2-mediated Fe oxidation (Paper II). A similar inhibitory effect was observed for other Dps e.g. the Dps from *Deinococcus radiodurans* (DrDps1) (83), the Dps from *Listeria innocua* (LiDps) (130) and the Dps from *Streptococcus suis* (SsDps) (131). In TeDpsA on the other hand the Zn^{2+} is suggested to act as a cofactor at the FOC to increase its oxidant preference towards O_2 and might represent an exception.

As we were interested in whether the His-type FOC of NpDps4 and TeDpsA can be found in various cyanobacterial Dps, a broader sequence alignment study was conducted. We found Dps containing the His-type FOC in many cyanobacterial species and detected no boundaries in morphology or physiological capacity (Paper II). Unicellular as well as filamentous, marine strains and fresh water species, and heterocystous and non-diazotrophic cyanobacteria can possess a Dps with a His-type FOC. We concluded that while the canonical Dps from *N. punctiforme* comprise a role as H_2O_2 detoxifiers,

NpDps4 is involved in cyanobacterial metabolism, which is shared by all cyanobacteria e.g. iron homeostasis. As we found it to be more abundant in heterocysts, NpDps4 could represent a Fe storage protein for iron-intense complexes such as nitrogenases or PS I (48, 49).

As NpDps4 was found to be an O_2-consuming protein, it might be an interesting candidate to maintain the microoxic environment in heterocysts, when cultures are grown under elevated O_2 concentrations. A similar approach was taken in a study, in which an algal hydrogenase was co-expressed with the O_2-consuming enzyme cyanoglobin in heterocysts (12). Heterocysts are known to sustain a microoxic environment by an increased rate of respiration as compared to the vegetative cells, a non-O_2 producing photosystem II and multiple cell walls impeding O_2 diffusion from the outside (132). However, these mechanisms might not suffice when cultures are grown in closed photobioreactors with higher O_2 concentrations than air-saturated conditions.

In experiments to identify a possible DNA-binding property of NpDps4 using EMSA and fluorescence resonance energy transfer (FRET), NpDps4 was found to bind to DNA in a pH-dependent manner (Paper III). Even though Lys-rich N- or C-terminal sequences are not present in NpDps4 that could explain these results (Table S1), surface interaction of NpDps4 with DNA cannot be out-ruled, as found for the Dps from *H. pylori* (79). Whether DNA can be protected by NpDps4 from the Fenton reaction is questionable, as no indication of H_2O_2 utilisation by NpDps4 was found. NpDps4 may still deprive the reaction from its reaction partner Fe^{2+} due to iron incorporation. By utilising FRET to determine protein-protein interactions, we also searched to identify a possible ferredoxin partner that could enable electron transfer to the Fe^{3+} core of NpDps4 to release Fe^{2+} (Paper III). The mechanism of iron release from Dps proteins has not been resolved yet and further analysis is required to understand the Dps integration into iron homeostasis.

The atypical NpDps5 - a Dps-like protein? (Exclusively in the R&D part of this thesis)

Based on earlier sequence comparison, NpDps5 was found to cluster with bacterioferritins and not with Dps proteins (50). Further sequence analysis revealed that its FOC was likely to be found buried inside monomeric structures, a structural characteristic for Ftn and Bfr.

In the field of Dps proteins, a small Dps subgroup has been identified that was annotated as Dps-like proteins (DpsL). DpsL, mainly identified from three prokaryotes, the archaea *Pyrochcoccus furiosus* (PfDpsL) (133) and

Sulfolobus solfataricus (SsDpsL, PDB: 2CLB) (134) and from the bacterium *Bacteroides fragilis* (BfDpsL, PDB: 2VZB) (80), comprise the dodecameric structure of a Dps (80, 134), but the FOC is located inside the monomeric subunit, similar to the observation made in NpDps5. DpsL also contained the Dps-specific BC helix and did not exhibit the short E helix that usually can be found among Bfr/Ftn (45). It has been suggested that they resemble a primitive common ancestor for the entire ferritin-like protein (Ftn–Bfr–Dps) family (88). A sequence comparison of these Dps-like proteins to NpDps5 revealed that NpDps5 is likely a member of this small subgroup.

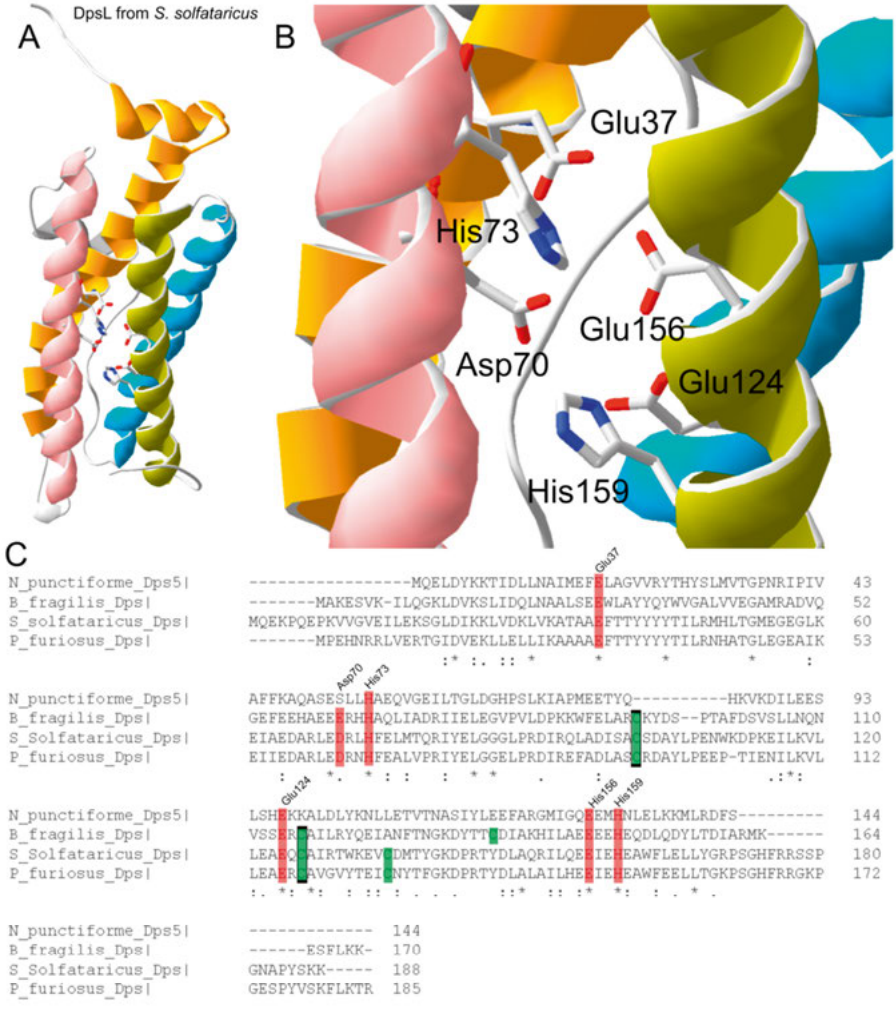

Figure 16 The NpDps5 shares similarities to Dps-like proteins (DpsL). A. crystal structure of the DpsL from *Sulfolobus solfataricus* (PDB: 2CLB) and B. zoom in on its FOC, buried within the monomer. Amino acids of the FOC highlighted with stick models and labelled. C. Sequence comparison of NpDps5 with the DpsL protein from *Bactereoids fragilis* (B_fragilis_Dps), *Sulfolobus solfataricus* (S_solfataricus_Dps) and *Pyrococcus furiosus* (P_furiosus_Dps) performed with the web-based software Clustal Omega (109). Amino acids involved in metal binding at the FOC in *S. solfataricus* highlighted with their labels. Red colour marks the identical amino acids involved in FOC formation among the sequences. All Cys highlighted in green and functional Cys are additionally boxed in black colour (134).

The sequence of NpDps5 shares high similarities to the three representative DpsL proteins and all amino acids for the formation FOC are present in NpDps5, except of NpDps5 containing a Ser53, where a Asp or Glu can be found in the three DpsL. The adjacent Glu54 in Npdps5 might compensate for this missing Asp at the FOC, while similarly a Glu was also found in the

Dps-L protein sequences. In contrast to NpDps5, all three DpsL protein sequences contain three Cys, of which two have been identified to be highly conserved. These two Cys have been found to form a di-sulphide bond acting as a gate keeper for an additional Fe pore, which connects the protein exterior directly to the buried FOC inside each monomer (80). NpDps5 does not contain a Cys in its sequence, which departs it from the DpsL protein class.

Furthermore, biochemical data on the three representative DpsL-proteins has indicated a role in H_2O_2 detoxification for SsDpsL and BfDpsL, as their transcript levels increased upon H_2O_2 treatment (80). For PfDpsL it was found that it had the capacity to catalyse the Fe^{2+} sequestration reaction utilising H_2O_2 and therefore it has been suggested to be involved in ROS protection (133). In contrast to these results, the transcript level of *Npdps5* kept unchanged when *N. punctiforme* was treated with H_2O_2 (50). Furthermore the ΔNpun_F6212 did not show a significant difference in growth as compared to wildtype cells after the addition of 0.5 mM H_2O_2 under diazotrophic conditions (112). The NpDps5 overexpression mutant on the other hand showed a higher resistance against H_2O_2 treatment (108). The function of NpDps5 remains unclear in *N. punctiforme*, but it may comprise a specific role in heterocysts, as the fluorescence of GFP coupled to the *Npdps5*-promoter was only observed in this cell type. Information on the enzymatic capacities of NpDps5 is required to identify its physiological function and whether it could be used in resistance cassettes in future cyanobacterial production systems.

Similar to NpDps4, we analysed the capacity of NpDps5 to bind to DNA and ferredoxins (paper III). Also NpDps5 binds to DNA in a pH-dependent manner, but it remains unknown whether this implies a function in DNA nucleoid formation or DNA protection. Further studies on the iron release mechanism of NpDps5 with its putative ferredoxin partners that we identified could lead to further understanding in how Fe^{2+} is being released from Dps proteins (Paper III).

Insights into ferritin-like systems in prokaryotes (Exclusively in the R&D part of this thesis)

Many prokaryotes have been discovered to possess only a single Dps protein (8) such as *Escherichia coli*, *Streptococcus suis* and *Listeria innocua*, whereas the cyanobacterium *Nostoc punctiforme* contains five Dps (50). Besides Dps proteins, prokaryotes can exhibit two other types of ferritin-like proteins, namely bacterial ferritins (Ftn) and bacterioferritins (Bfr). The di-

versity of the composition of ferritin-like proteins in prokaryotes can be vast and has barely been analysed in the field. To understand intracellular iron homeostasis, the analysis of the entire set of ferritin-like proteins within the prokaryote has gained little attention in the past years (135, 136).

In this study we present an overview of the many ferritin-like protein compositions of those prokaryotes of which at least one Dps protein has been investigated since 1992. For protein identification and classification, sequence annotations from cyanobase (137) and kegg databases (https://www.kegg.jp/) as well as the web-based sequence comparisons tool Clustal Omega (138) and protein model software Phyre2 (126) has been utilised. This overview contains also information about the origin of the prokaryote, in some cases highlighting its habitat (Fig. 17). Frequently, structural and functional comparisons between Dps proteins from different prokaryotes have been undertaken, irrespectively to their life style or their equipped ferritin-like protein composition. I hypothesise that a fundamental mechanism underlies each of the identified ferritin-like protein compositions. Comparing Dps proteins among prokaryotes that comprise a similar ferritin-like protein composition may contribute to the understanding of ROS-protection and iron homeostasis. This overview on the little data that exist on ferritin-like systems may function to identify physiological patterns in future Dps research.

Four major observations can be summarised as the following:

Firstly, based on this overview, the composition of ferritin-like proteins in prokaryotes is surprisingly diverse. While many prokaryotes contain only a single ferritin-like protein, namely a Dps protein, also multiple Dps proteins can be possessed by a prokaryote such as two Dps, three Dps and five Dps. Four Dps proteins in a single prokaryote may exist, but to my knowledge no correspondent organism has been identified, yet. On the other hand, a prokaryote which only contains a single or multiple maxiferritin(s) with no additional Dps protein has also not been discovered, yet. Additionally, prokaryotes that contain ferritin-like sets such as 1-Dps-1-maxiferritn, 1-Dps-2-maxiferritins as well as 2-Dps-1-maxiferritin, 2-Dps-2-maxiferritins and 3-Dps-1-maxiferritin can be found. The maxiferritin may either resemble a Bfr or a Ftn, dependent on the prokaryote. It should be noted that the differentiation between a Bfr and a Ftn on the basis of protein sequences is sometimes difficult, as a continuum of sequence similarities exist (44). Differentiations between a Ftn and Bfr could be made upon the existence of a Met at position 52 (in reference to the Bfr sequence from *E. coli*) that usually serves to identify the possibility to complex a porphyrin structure. The coordinated porphyrin has been shown to enable electron transfer to the iron core in Bfr (139, 140).

Secondly, it is apparent that half of the studied Dps proteins originate from pathogenic bacteria dominating the focus of the Dps research field since their discovery (43). Some of these pathogens such as *Borrelia burgdorferi* (98)*, Treponema pallidum* (141)*, Yersinia pestis* KIM10 and *Vibrio cholera* (142) (Fig. 17) are directly connected to the human diseases borreliosis (lyme disease), syphilis, pest and cholera, respectively. Some studied Dps proteins originate from bacteria found in human tissue e.g. *Staphylococcus aureus* (85) and *Mycobacterium smegmatis* (52). Others have been investigated from the radio tolerant species *Deinococcus radiodurans* (77) and *Kineococcus radiotolerans* (127) or from the archaea *Halobacterium salinarum* (143) and *Sulfolobus solfataricus* (134). Concerning their different lifestyles, it is unknown to what extent functional knowledge about the Dps protein from a pathogenic bacterium or archaea can be transferred to a cyanobacterial Dps. To what extent mechanisms such as iron homeostasis, ROS protection and DNA-condensation in a cyanobacterium resemble those from a pathogen has not been the focus of any Dps research.

Thirdly, the studied cyanobacterial Dps proteins originate from cyanobacteria that clearly have different sets of ferritin-like proteins. While *T. elongatus* exhibits two Dps proteins and one putative bacterioferritin (51, 89), *Synechococcus* sp. PCC 7942 (144–146) and *Trichodesmium erythraeum* (147, 148) possess two Dps proteins and no maxiferritin. On the other hand *Synechocystis* PCC 6803 possesses one Dps (135, 136) and two maxiferritins. It should be noted that little data exist on cyanobacterial maxiferritins and evidence to their existence is mostly derived from gene annotation and/or sequence comparisons.

Fourthly*, N. punctiforme* and *Nostoc* PCC 7120 (107, 117) comprise the greatest known number of ferritin-like proteins among all investigated prokaryotes. The possession of numerous ferritin-like proteins might be required for distributing iron to the iron-demanding proteins involved in photosynthesis and N_2-fixation. In contrast to that argumentation, for the diazotrophic *Trichodesmium erythraeum* only two Dps proteins and no further maxiferritin was found. Furthermore, it should be noted that *Streptomyces coelicolor*, *Mycobacterium smegmatis* and *Bacillus anthracis* do contain four ferritin-like proteins and none of these prokaryotes possess an iron-demanding photosynthetic machinery or nitrogenase. It could be concluded that there are no obvious correlations of the number and composition of the set of ferritin-like proteins and the physiology and/or life style of individual bacteria. It remains uncertain why prokaryotes, cyanobacterial or non-cyanobacterial, need such a diverse set of ferritin-like proteins at all.

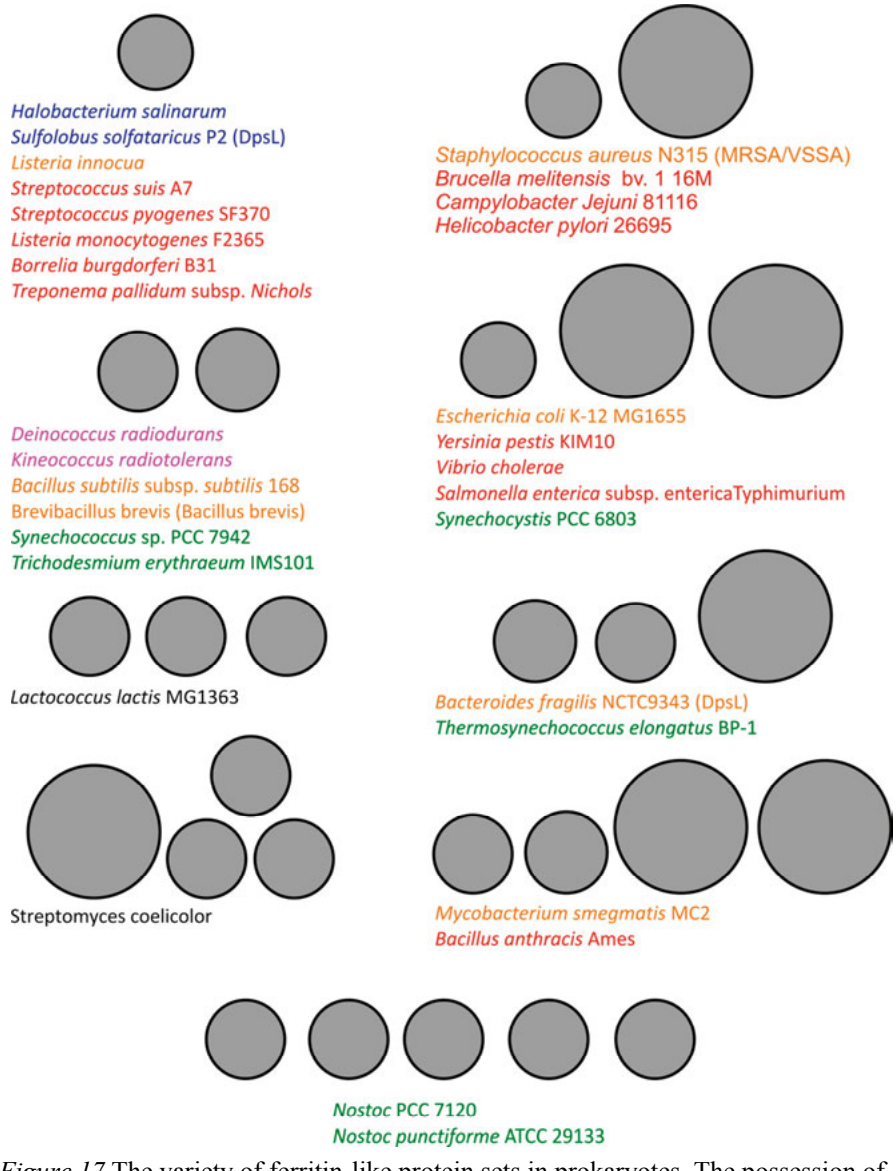

Figure 17 The variety of ferritin-like protein sets in prokaryotes. The possession of Dps proteins and maxiferritins (Ftn or Bfr) symbolised by small and large circular silhouettes in grey colour, respectively. The names of the prokaryotic species are indicated underneath each ferritin-like composition. Species names are coloured in blue for archaea, in pink for radio resistant bacteria, in yellow for bacteria related to human tissue, in red for human pathogens, in green for cyanobacteria and in black with no further specification. Existence of Dps and maxiferritins from cyanobase (137), the kegg database (https://www.kegg.jp/) supported by the web-based sequence comparisons tool Clustal Omega (138) and the protein model software Phyre2 (126).

Chapter II

Fe limitation decreases growth of *Nostoc* PCC 7120 Δ*hupW* (Paper IV)

The induction of iron deprivation in diazotrophic cyanobacteria has been observed to decrease growth rates and increase the accumulation of carbon-based storage compartments such as glycogen (58–64). A decreased growth and the accumulation of fixed carbon could be important parameters to reallocate more photosynthetic energy to H_2 production. It was tested whether similar results could be obtained for the potent H_2 production mutant *Nostoc* PCC 7120 Δ*hupW* in a cultivation experiment over four weeks. Phenotypical characteristics of the culture that could give visible insights into cellular proliferation were documented by photography. A four week cultivation period was chosen to evaluate whether Fe limitation could be used for the purpose of future H_2 production in long term processes.

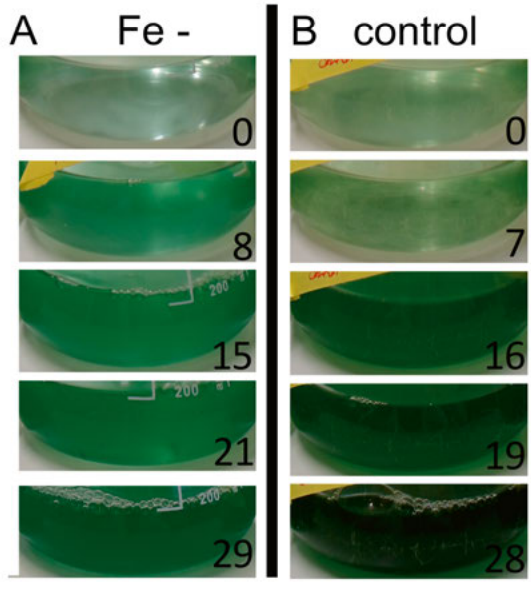

Figure 18 Nostoc PCC 7120 Δ*hupW* grown under Fe limitation indicated decreased cyanobacterial growth and a distinct pigmentation pattern as compared to the control culture. Images of cultures grown in A. iron-limited (Fe -) and B. control medium. The cultivation day is indicated by a number in each picture. All cultures were grown at 20 µmol photons m^{-2} s^{-1} (12 h light/12 h darkness), 100 rpm agitation at 25 °C for approximately four weeks.

Over the four week experiment, the Fe-limited cultures showed a visibly slower growth as compared to the wild-type, as its colour was less intense throughout the cultivation (Fig. 18). The slower growth under Fe limitation is a typical phenotype, frequently reported for iron-starved cyanobacteria and also for the wildtype of *Nostoc* PCC 7120 (56, 57, 63, 64). Any indication for a completely arrested state of growth was not observed as the blue-green colour of the Fe-limited cells gradually increased in its intensity.

The analysis of the visible phenotypic characteristics during the long-term cultivation of *Nostoc* PCC 7120 Δ*hupW* gave qualitative insights on the decreased cyanobacterial growth and differential pigmentation under Fe limited conditions. To quantitatively compare the growth under Fe-limited conditions to the control, spectroscopic methods were used to determine the optical density at 800 nm (OD_{800nm}) and the chlorophyll a concentration (Chl a).

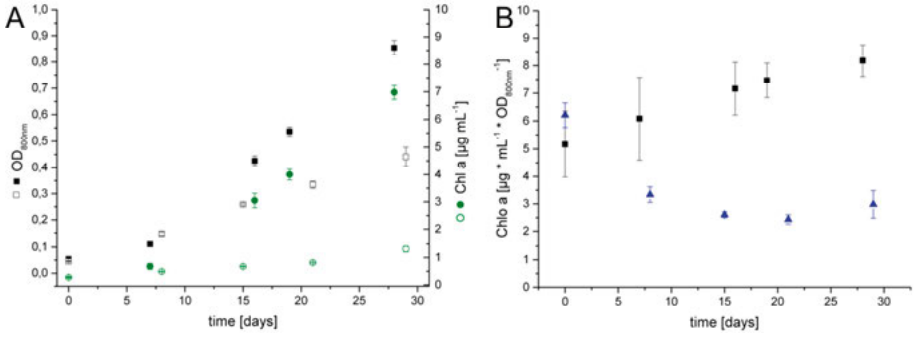

Figure 19 Growth curves and the specific chlorophyll concentration of the *Nostoc* PCC 7120 Δ*hupW* in diazotrophic conditions under Fe limitation and control condition. A. Optical density at 800nm (OD_{800nm}) and chlorophyll a concentration (Chl a) in µg mL^{-1} versus cultivation time. OD_{800nm} displayed under iron-limited (empty black squares) and control condition (filled black squares). Chl a displayed under iron-limited (empty green circles) and control condition (filled green circles). B. The specific Chl a concentration (Chl a concentration divided by OD_{800nm}) plotted against the cultivation time. Fe-limited (blue triangles) and control (black squares) condition displayed. All cultures were grown at 20 µmol photons m^{-2} s^{-1} (12h light/12 h darkness), 100 rpm agitation at 25°C for approximately four weeks. Each data point represents a biological triplicate with technical duplicate and the error bars indicate the standard deviation.

The spectroscopic analysis revealed that the Fe-limited cultures reached a final ~ 1.9 fold and 5.3 fold lower OD_{800nm} and Chl a concentration as compared to the control cultures, respectively (Fig. 19). The growth of *Nostoc* PCC 7120 Δ*hupW* can be significantly impaired by Fe limitation, but based on its gradual and linear increase of the OD_{800nm} and Chl a concentration, a halted state of growth was not reached. This is in agreement with a study on *Nostoc* PCC 7120 wildtype cultures that showed a continuous, but slow proliferation under Fe-starvation for 90 days (57). The final specific Chl a concentration of the Fe-limited culture was ~ 2.8 fold smaller as compared to in the control cultures. I hypothesised that a lower specific chlorophyll concentration indicates a larger amount of cellular debris or an accumulation of intracellular storage compartments, which both could increase the scattering properties of the samples at 800 nm (149). Regular microscopy during the four weeks of cultivation was conducted to evaluate this hypothesis.

Under Fe limitation *Nostoc* PCC 7120 Δ*hupW* accumulates higher levels of carbohydrate storage compounds (Paper IV)

Microscopic parameters such as the filament length, heterocyst frequency, the accumulation of storage compartments, the rate of cell death etc. could

all potentially affect the H_2 production capacities, but has only recently been studied (150, 151). The lower specific Chl a concentration in the Fe-limited cultures indicated an increased level of cellular debris or the accumulation of storage compounds that could be verified by microscopic analysis.

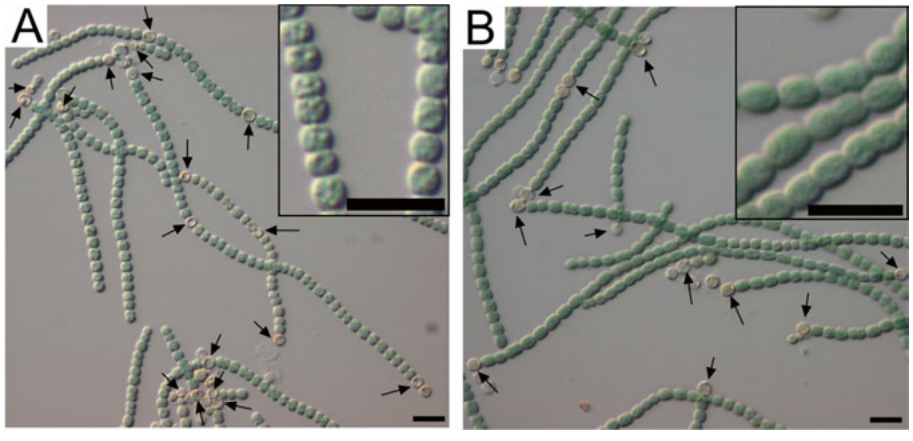

Figure 20 The limitation of Fe resulted in an accumulation of storage compartments. Microscopic images of a A. Fe-limited culture (Fe -) on day 21 and B. control culture on day 28. Image blow-ups give insights on the accumulation of cellular storage compartments under iron limitation as compared to the control conditions. Microscopic images from the cultures over the full cultivation time can be accessed from the web deposit: http://dx.doi.org/10.17632/hs8kkr6mgg.1. All black bars represent a length of 10 µm and arrows indicate heterocysts.

Based on the microscopic images, the filaments of the Fe-limited cultures were long and contained heterocysts, similar to the control (Fig. 20). The vegetative cells under Fe limitation contained small particles of a size of up to 1 µm, which were barely observed in the control cultures. The amount of cellular debris or dead cells was found to be similar in both conditions. Therefore, the 2.8 fold decreased level of the specific Chl a concentration in the Fe-limited cultures is likely due to the increased amount of storage particles under the Fe-limited conditions that increased the scattering properties of the samples (149).

To verify the nature of these particles, a quantification of the specific carbohydrate concentration (mg carb Chl a^{-1}) at the end of the four week cultivation was performed. The specific carbohydrate concentration was 4.5 fold higher in the Fe-limited cells (2.2 mg carb μg^{-1} Chl a^{-1}) as compared the control samples (0.49 mg carb μg^{-1} Chl a^{-1}). The accumulation of carbohydrate storage compartments has been frequently observed for filamentous cyanobacteria under Fe starvation (56). The stored photosynthetic energy in glycogen is required to be reallocated to the biosynthesis of H_2 (14). Therefore, the implementation of a foreign H_2-producing hydrogenases or a complete photo

fermentative pathway could be used for enhanced H_2 production (12, 152). Due to their O_2-sensitivy, heterocysts could a suitable chassis, since these cells comprise a microoxic environment enabling the function of the enzymes. The microscopic investigation of the Fe-limited cultures indicated heterocyst-containing filaments over the whole period of cultivation, and indicates that this cultivation strategy is suitable for H_2 production purposes.

Heterocysts are retained at high frequencies under Fe limited conditions (Paper IV)

For a stable H_2 production, heterocysts must be retained throughout the cultivation time (150, 151). If cultures lose their heterocysts during a short time, they would need to be exchanged by a heterocyst-containing culture, which increases the cost of this process. Therefore, a H_2 production system that runs for many months would be desirable in order to reduce maintaining costs. Based on microscopic images of the Fe-limited cultures, quantitative information about the heterocyst frequency throughout the four weeks of cultivation was collected.

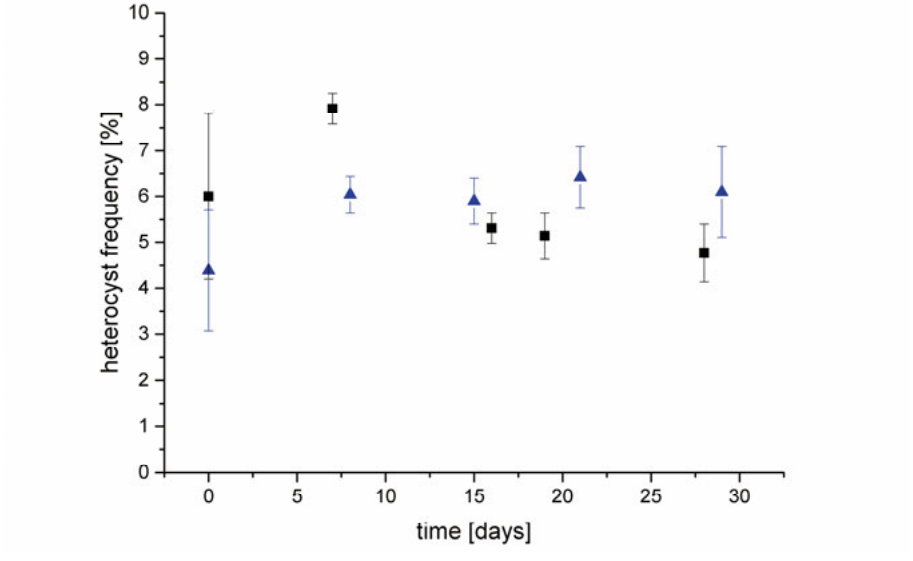

Figure 21 The heterocyst frequency was retained at high levels in the Fe limited cultures (blue triangles), similar to the controls (black squares). Heterocyst frequency [%] over the cultivation time in Fe-limited and control cultures. Except of day zero, all data points represent > 3000 counted cells (vegetative cells and heterocysts) from three biological triplicates (count of > 1000 per replicate) and the error bars indicate the standard deviation. For data points on day zero > 1000 cells were counted from the inoculation culture that was grown under control conditions. The standard deviation was set to 30 %, the highest experimentally observed one.

The Fe-limited culture possessed a high heterocyst frequency ranging from ~ 5.9 % to 6.4 % during the last three weeks of cultivation (Fig. 21). In agreement with this observation, also the diazotrophic cyanobacterium *Calothrix parietina* possessed an increased heterocyst frequency under iron starvation (64). A retained high heterocyst frequency is desirable for a long term production process of H_2 from indirect photolysis processes (9).

To conclude, the Fe limitation was found to be a suitable cultivation strategy as glycogen storage was built up, growth was impaired and heterocysts were retained for potentially enhanced H_2 production. Further efforts to reallocate the photosynthetic energy towards H_2 inside the heterocysts are required.

Manufacturing biofilms in closed photobioreactors for H_2 production (Exclusively presented in this thesis)

Photobioreactors have majorly been designed to constantly circulate a liquid culture medium for optimal light conditions. Acién et al. estimated that ~ 54 % of the energy input was due to the use of pumps circulating the liquid inside a microalgal pilot plant for feed production (25). Energy input always adds to the cost of the production and if low-price commodities are being produced, these costs significantly determine the economic viability of the process. Therefore, efforts to develop an economically viable H_2 production need to be intensified in order to increase the probability that photobiological H_2 production could contribute to the global decarbonisation of the transport sector.

The majority of the energy input in conventional photobioreactors containing suspension cultures is due to mixing and liquid circulation. Thus, I propose a novel design of a photobioreactor, in which liquid circulation is not required. The design is inspired by microbiological mats in nature (153) and the recent studies on biofilm photobioreactors for the purpose of photo fermentation. However, photo fermentative bacteria require a constant supply of organic compounds and thus liquid circulation is commonly integrated in these systems to feed the biofilm (154–156). While in conventional photobioreactor systems biofilm formation is undesired (157), the here presented design of the photobioreactor consists of an immobilised culture with no intention of liquid agitation (Fig. 22).

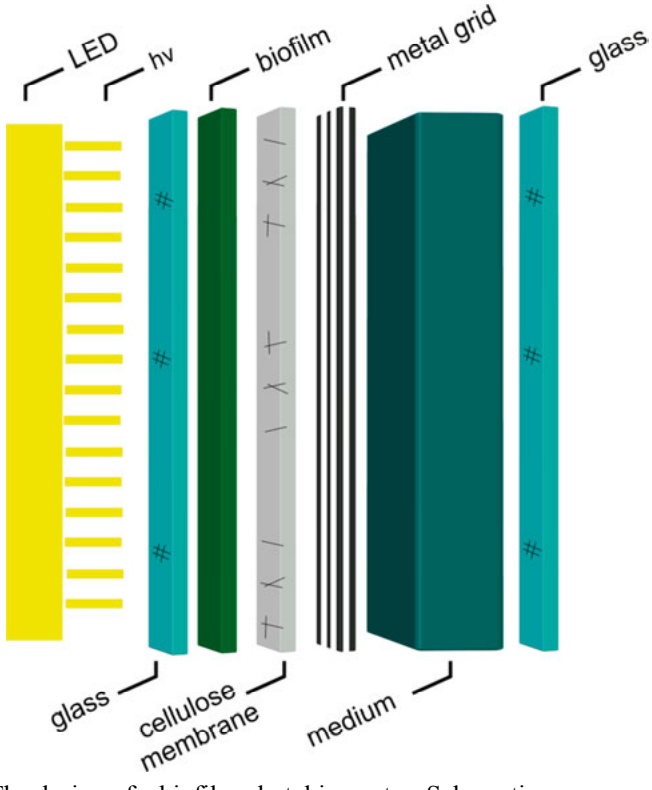

Figure 22 The design of a biofilm photobioreactor. Schematic sequence of the inner compartments in a biofilm photobioreactor orientated to the artificial light source LED.

A flat panel design was chosen and a cyanobacterial culture is required to be inserted into the photobioreactor chassis. Therefore, the culture is immobilised on the glass surface inside the bioreactor chassis. The biofilm is direct contact to a cellulose membrane to supply water for photosynthesis. A metal grid supports the stability of the cellulose membrane on the biofilm.

Two different methods to transfer a cyanobacterial culture onto the glass surface to form a biofilm have been tested. The first method comprises a natural cell sedimentation step, in which the cyanobacterial culture of about 200 mL was concentrated in four 50 mL Falcon tubes to a volume of about 30 mL (Fig. 23). A 7-fold concentration within 120 min was possible to obtain. This concentration step was necessary to decrease the culture volume to be immobilised on the glass surface and enable a drying step to form a solid biofilm.

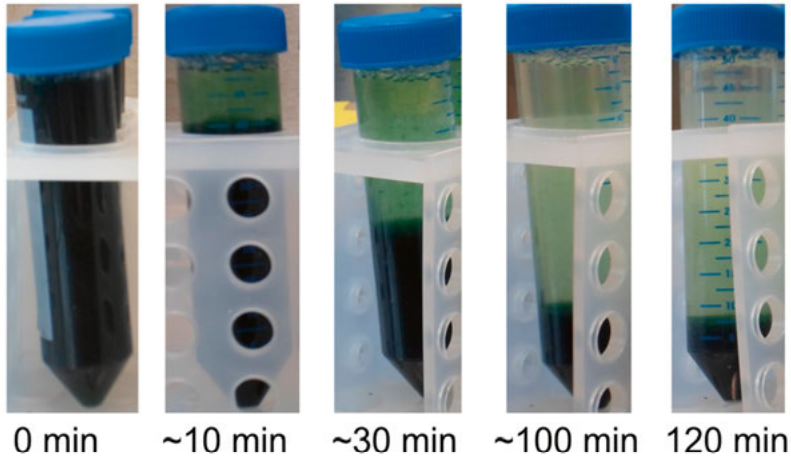

Figure 23 The gravity-driven sedimentation process in ~ 50 mL culture of *Nostoc* PCC 7120 Δ*hupW*.

The dense culture slurry obtained by the gravity-driven sedimentation process was applied onto the glass surface (Fig. 24, A). To confine the biofilm, slices of gelatine were used. A subsequent drying process generated a homogenous biofilm (Fig. 24, B-C). However, there were several drawbacks using this method to form a biofilm. The biomass transfer efficiency (based on OD_{800nm}) from the culture onto the glass surface reached between 65 – 75 %, while a significant amount of cell material could not be concentrated by the sedimentation process (Fig. 24 D). Filaments of short length between one to three cells per filament were microscopically identified in the supernatant after sedimentation (data not shown). Other cell residues could not be transferred as they were lost inside the pipette used for the transfer. Furthermore, long biofilm drying processes between 6 - 10 h were required dependent on the final culture slurry volume for the transfer. During photobioreactor assembly, the biofilm was vulnerable to deformation (Fig. 24 E) when e.g. the cellulose membrane and metal grid were inserted for the purposes of immobilisation and stability. If the optimal drying time was exceeded, a blue substance was extracted from the cells when filling the photobioreactor with the culture medium (Fig. 24 F). Based on spectroscopic analysis, this blue substance was likely phycobilisomes, putatively extracted by the cells upon osmotic stress (data not shown).

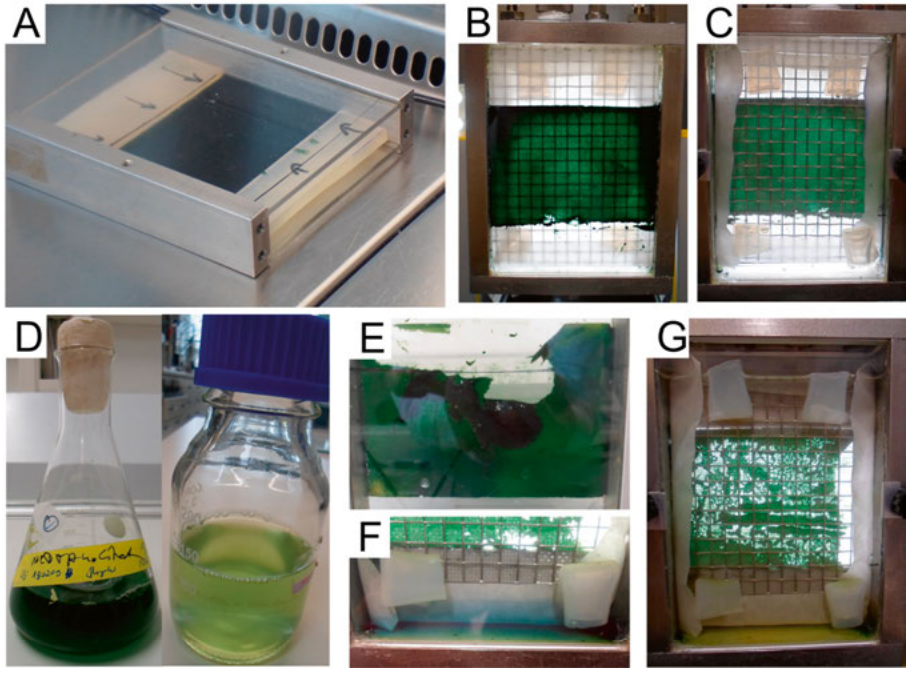

Figure 24 Advantages and disadvantages in biofilm formation using the sedimentation process. The sedimentation process allows for A. homogenous biofilm formation, confined by two galantine slices, inside the photobioreactor chassis with views on B. the front side and C. the back side of the biofilm photobioreactor. The sedimentation process from a D. culture (D. left) leads to biomass losses as the supernatant contains cells that are not transferred onto the biofilm (D. right). The biofilm is E. physically vulnerable to the insertion into the reactor chassis, F. too long drying processes and G. gas bubble formation in between the glass surface and the biofilm that caused stress and the loss of biofilm homogeneity, respectively.

The application of culture slurry onto the glass surface was found to be disadvantageous, as it comprised biomass loss and the risk of osmotic stress. Therefore, a second approach, a filtration process, was attempted for a more efficient biofilm formation. In this process it was aimed to decrease the drying time and increase the biomass transfer efficiency. Instead of sedimentation, the cells were directly transferred onto the cellulose membrane that was used in the reactor design for stabilising the biofilm (Fig. 25). This filtration process required between 30 – 40 min for a 200 mL culture and decreased the biofilm preparation time by at least 5 h as compared to the sedimentation process. In sum, the risk of non-optimal drying times that would lead to osmotic destruction of the cells upon the contact with the culture medium was reduced.

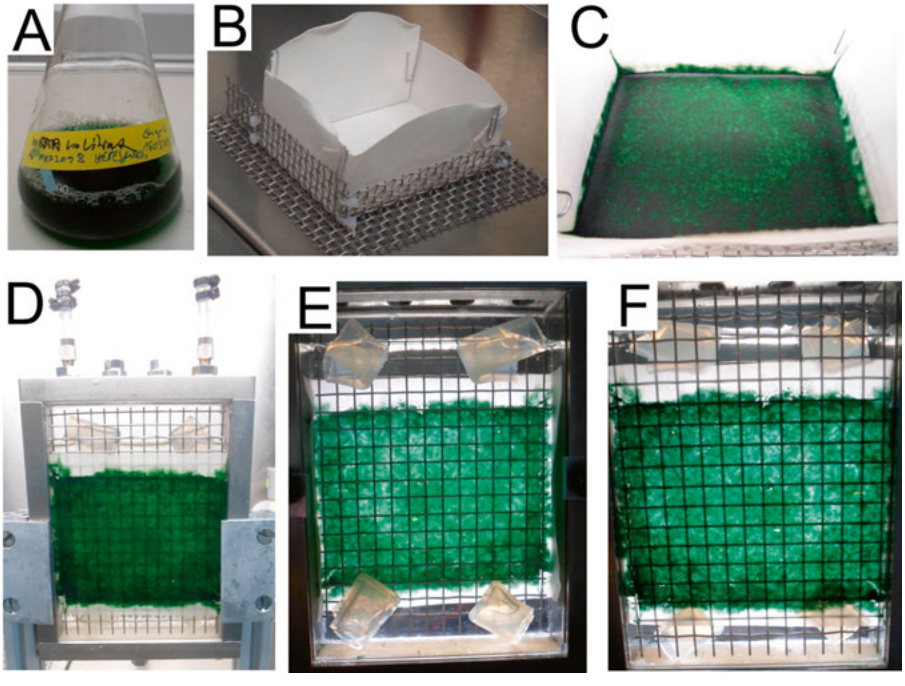

Figure 25 Biofilm formation with the filtration process. The A. original cyanobacterial culture *Nostoc* PCC 7120 Δ*hupW* is directly transferred onto a B. cellulose filtrate paper folded in a metal grid holder to receive the C. cyanobacterial biofilm. After the insertion of the biofilm into the D. photobioreactor with the view on E. the back side and F. the front side of the reactor chassis.

Using the filtration process, biomass transfer efficiencies (based on OD_{800nm}) between 92.0– 99.9 % were reached, which was a significant improvement as compared to the sedimentation-based process. Short filaments containing one to three cells were microscopically identified in the collected filtrate and thus both biofilm formation techniques could not guarantee a complete culture transfer. During the assembly, there was a lower risk to physically damage the biofilm as compared to the previous method. Both biofilm formation techniques were based on the same design to immobilise the biofilm directly onto the glass surface and it was observed that immediate gas production, putatively O_2 from photosynthesis, resulted to biofilm deformation within 12 h (Fig. 26).

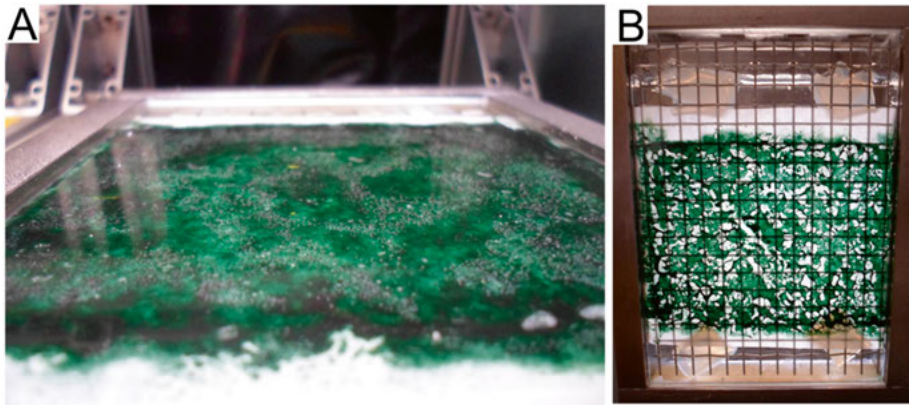

Figure 26 The effect of illumination on the biofilm homogeny. A. small gas bubbles appear between the glass surface and the biofilm upon illumination (~20 µmol m^{-2} s^{-1}) and lead to B. biofilm deformation and the loss of homogeneity within the 12h.

Biofilm deformation decreases the effective area of illumination, while on the other hand a homogenous biofilm would guarantee an even distribution of the light onto the photobioreactor surface and is therefore desired. A new design was developed to mitigate the effect of evolving gas that deformed the biofilm. In this optimised design, the biofilm is not immobilised onto the glass surface, but covered by a transparent silicon membrane on the illuminated side and by the cellulose membrane on the non-illuminated side. While the cellulose membrane allows for an efficient and quick biofilm formation, the silicon membrane could allow for a continuous gas exchange and prevent the deformation of the biofilm.

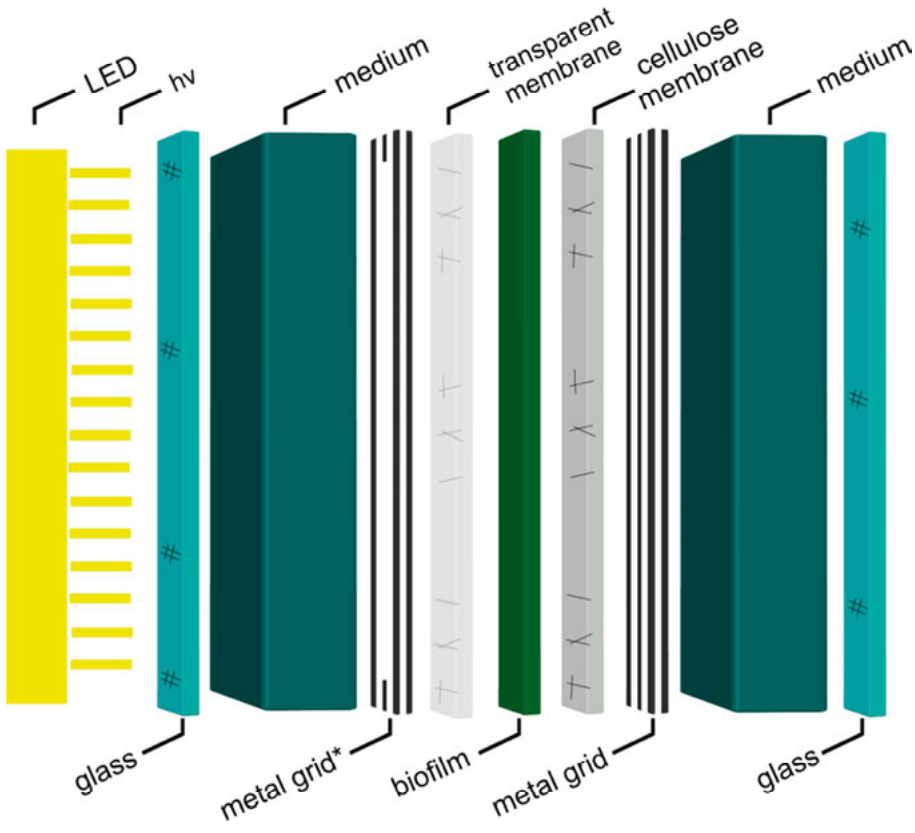

Figure 27 The design of the optimised biofilm photobioreactor. Schematic sequence of the inner compartments in a biofilm photobioreactor orientated to the artificial light source LED. * The metal grid comprises an opening for optimal light penetration on the biofilm.

Both membranes are re-enforced by two metal grids that are clammed with four silicon rubber tubes into the case stabilising the embedded biofilm (not shown). The use of the cellulose membrane enables the previously described filtration process to form a homogenous biofilm. The metal grid facing the illuminated area of the biofilm is decreased to a minimal material, but still supported the stability of the biofilm (Fig. 28A).

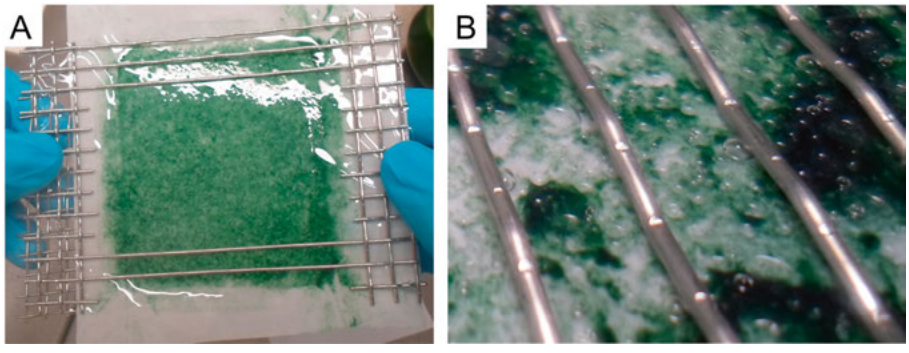

Figure 28 The assembly of the optimised biofilm using a transparent silicon membrane. The biofilm is A. covered by the silicon membrane and B. upon light illumination (~20 µE m^{-2} s^{-1}) bubble formation was observed on top of the membrane inside the biofilm photobioreactor.

When assembled, the cyanobacterial biofilm was observed to form gas bubbles immediately upon illumination as previously observed. Most of these gas bubbles were formed on the membrane facing the LED. Biofilm distortion caused by these bubbles was not observed using the silicone membrane as compared to previous attempts for biofilm immobilisation on the glass surface. The use of a silicone membrane also enabled to sporadically observe H_2 production by gas chromatography (data not shown). In contrast to suspension cultures, the H_2 evolution from the biofilm was not continuous during illumination (data not shown). Gas bubbles on top of the silicone membrane were observed to stay on the surface and could explain the discontinuity of the H_2 evolution. Further developments of the shown prototype are required to enable the enrichment of the gas phase with H_2. A focused gas stream directed towards on the area of bubble accumulation could facilitate gas exchange. This optimisation could support a constant H_2 harvest and O_2 removal from the system. Similar gas exchange units are commonly installed in conventional photobioreactors to extract O_2 from the system (25).

Throughout the bioreactor tests, the cells were observed to proliferate in the biofilms; in long-term experiments even outgrowing the biofilm while cells accumulated in the bioreactor chassis. An economic analysis on the biofilm was not foreseen or conduced in this study, as this would require upscaling the systems. Nevertheless, the developed system appears to be economically promising due to the lack of liquid circulation that increases substantially the production costs.

Summary, conclusion and future directions

In thesis chapter I, the five Dps from *N. punctiforme* have been investigated to identify their physiological function. After overexpression and purification we collected information on their multimeric state and verified that all NpDps could be subjected to further enzymatic analysis. While NpDps1, NpDps2 and NpDps3 were observed to catalyse the reaction between H_2O_2 and Fe^{2+}, the previous role of NpDps2 in immediate response to H_2O_2 was verified.

Whether these three canonical NpDps can be used in cyanobacterial production systems to cope with elevated O_2 concentrations needs to be investigated, but they all comprise the necessary enzymatic function to detoxify H_2O_2, a product of the reactive oxygen species reaction cascade that is harmful to the cells.

In contrast to NpDps1-3, NpDps4 was found to catalyse the reaction between O_2 and Fe^{2+} and no indication of detoxifying H_2O_2 was found. NpDps4 comprised a special His-type FOC that was found in many different cyanobacterial Dps proteins and further investigation of its role in the atypical enzyme activity needs to be further analysed. Therefore, point mutations on the His-type FOC in Npdps4 could be inserted to modulate and study the Fe^{2+} oxidation reaction. This could give insights on how the FOC structure affects the enzyme's capability to utilise O_2, or H_2O_2 as shown for canonical Dps.

Whether NpDps4 could be used as a resistance protein to protect cyanobacterial producers inside photobioreactor systems needs to be investigated. Inserted into heterocysts, it could contribute to the natural mechanisms to maintain the microoxic environment. How intracellular O_2 concentrations in heterocysts are affected in photobioreactor systems with elevated O_2 levels is unknown.

We have found potential ferredoxins that NpDps4 and NpDps5 might interact with, but further investigations on the possible electron transfer from these ferredoxins to the NpDps proteins are required. These studies could give answers on how the release of iron from Dps proteins is triggered to fully understand their role in iron homeostasis.

In the 2nd chapter of the thesis, the limitation of Fe and its effect on cultural proliferation, carbohydrate accumulation and heterocyst frequency were studied. While Fe limitation did not fully cease growth inside the culture of *Nostoc* PCC Δ*hupW*, it displays a promising cultivation strategy to investigate the reallocation of photosynthetic energy into the biosynthesis of H_2. The initiation of a co-limitation of other nutrients might be useful to stop cellular proliferation. Over four weeks of cultivation time, the heterocyst frequency remained on a high level of ~ 6 %, which is an essential prerequisite for H_2 production from heterocystous cyanobacteria. Further long term experiments need to be conducted and higher illumination levels need to be applied to evaluate the potential of the cultivation strategy for outdoor use. Nevertheless, hydrogenases or entire photo fermentative pathways have to be inserted into the heterocyst metabolism for ultimate H_2 production. This requires the techniques of synthetic biology. The reallocation of carbon storage could then be monitored and improved towards the production of the desired compound.

Little is known about cyanobacterial biofilms and how they could be used for H_2 production. The here presented study discusses practical aspects about a novel design for a cyanobacterial biofilm photobioreactors. The biofilm can be formed using a filtration method that guarantees a high biomass transfer efficiency from a liquid However, the presented design requires further improvements in regards to efficient gas exchange. If continuous photobiological H_2 production can be established during light conditions, the upscaling of the reactor is required to analyse the system from an economical point of view. Non-proliferating and efficient H_2-producing cyanobacteria are then required to be analysed economically to compare with conventional systems.

Finally, it remains to be investigated whether both strategies to enhance cyanobacterial H_2 production can be combined in one setup. The cultivation under Fe limitation to impair growth might affect the capability of genetically introduced Dps proteins for an enhanced robustness during oxidative stress. Too little is known about how Dps proteins manage iron homeostasis inside the cells, especially in *Nostoc* cultures that contain an unusually high number of five Dps proteins.

Sammanfattning på Svenska

Klimatförändringarna är ett stort globalt hot. Vi vet med säkerhet att den ökning av koldioxid som sker i atmosfären grundas i vårt bruk av fossila bränslen med start under den industriella revolutionen. För att begränsa den klimatpåverkan som vår energikonsumtion leder till behöver vi gå från fossila bränslen mot förnybara alternativ. Vätgas är en alternativ energibärare som av många anses vara nödvändig för denna övergång. Vätgasförbränning ledar inte till ökad koldioxidhalt eftersom vatten är den enda avgas som bildas vid förbränning. Vätgas producerat av cyanobakterier är ett intressant förnybart alternativ som har utforskats under flera decennier. Med hjälp av genteknik och genom förbättring av odlingsförhållanden har man lyckats optimera H_2-produktionen. De stora forskningsansträngningarna har resulterat i en omvandling av solenergi till H_2 med en effektivitet på 4,0%, vilket är långt från dess teoretiska maximum.

I två separata kapitel beskriver jag nya koncept för att förbättra fotobiologisk H_2-produktion från cyanobakterier. Cyanobakterier är fotosyntetiserande prokaryoter som endast behöver solenergi, vatten, koldioxid från luften och små mängder näringsämnen för tillväxt och biosyntes av exempelvis H_2. I cyanobakterier finns två enzym som kan bilda vätgas; hydrogenas och nitrogenas. För att en robust produktion av vätgas ska bli en framtida realitet måste både cellens metabolism och odlingsprocesser förändras och optimeras.

För biotekniska applikationer av cyanobakterier så används ofta fotobioreaktorer. En utmaning är att syrgasnivåerna i dessa reaktorer ökar på grund av cellernas fotosyntes vilket leder till att mängden av reaktiva syrearter (ROS) ökar. I en fotobioreaktorodling behöver ROS-halterna kontrolleras för att inte en oxidativ stress som kan leda till en kollaps av hela odlingssystemet ska uppkomma. Cyanobakterier i släktet *Nostoc* har använts som modellorganismer för att studera och utveckla vätgasproduktion från heterocyster, som är en celltyp med låg syrgashalt där kvävefixering och vätgasproduktion kan ske. Min forskningen har haft syftet att karaktärisera mini-ferritiner (Dps) i *Nostoc*. Dessa antas fungera i skydd mot ROS, samt i cellens järnbalans. Trots deras uppenbara relevans för att förhindra oxidativ stress i cyanobakterier är de bakomliggande biokemiska mekanismerna i stort okända.

I avhandlingens första kapitel presenteras och diskuteras resultat som visar att Dps-proteinerna från *Nostoc punctiforme* har specifika fysiologiska funktioner och använder skilda mekanismer för järnlagring, skydd mot ROS, samt reglering av cellens syrenivåer. För att fungera i upplagring av järn så krävs det att Dps har en globulär struktur bestående av tolv monomerer. Mina resultat försäkrade att NpDps1-NpDps5 alla var stabila multimerer under fysiologiska förhållanden och därför kunde användas för biokemiska studier. Strukturmodeller av NpDps1- NpDps3 exponerade ett för Dps proteiner typiskt ferroxidascenter (FOC), där Fe^{2+} binds och oxideras till Fe^{3+} för lagring. Spektroskopiska analyser visade att NpDps1-3 använder H_2O_2 för Fe^{2+} oxidation, vilket tyder på en funktion i ROS-tolerans.

Strukturbestämning av NpDps4 med röntgenkristallografi avslöjade ett atypiskt FOC, där konserverad aminosyror, som återfinns i typiska Dps, ersatts av andra. Sekvensjämförelser mellan Dps-proteinhomologer från cyanobakterier avslöjade en tidigare okänd FOC-klass, som jag namngett till His-typ FOC. His-typ FOC identifierades inte i Dps-proteiner från andra bakterier och kan vara en unik struktur för Dps-proteiner i cyanobakterier. Spektroskopiska analyser visade att NpDps4 använder syrgas för Fe^{2+} oxidation. Därför föreslår jag att NpDps4 har betydelse för reglering av syrgasnivåerna i heterocysten. Min slutsats är att de typiska NpDps 1 - 3 är viktiga för cellens reglering av H_2O_2, medan NpDps4 har en mer generell roll i järnlagring. Båda dessa funktioner är en del av cellens skydd mot oxidativ stress.

Den biokemiska karaktärisering visar tydligt att NpDps1 - 4 alla är intressanta kandidater i utvecklingen av en robust fotobioreaktorproduktion av vätgas.

Vi har visat att NpDps1 - 4 binder Fe^{2+} och kan lagra järn, men för att Dps proteiner ska kunna kontrollera de fria järnet i cellen så krävs även att det lagrade järnet frisätts vid behov, vilket bör ske genom att det lagrade järnet (Fe^{3+}) reduceras. Tyvärr är lite känt om denna process, och någon potentiell elektrondonator som kan interagera med Dps och främja mobiliseringen av det lagrade järnet har hittills inte identifierats. Våra resultat från protein-protein interaktionsstudier visar för första gången att elektronbärande ferredoxiner bildar komplex med Dps proteiner från cyanobakterier. Detta är intressant men ytterligare undersökningar behövs för att avgöra om denna interaktion har betydelse för frisättning av det lagrade järnet i cellerna.

Min arbetshypotes i detta arbete har varit att de specifika funktionerna i *Nostoc* skulle tydliggöras vid en biokemisk karaktärisering av de fem NpDps proteinerna. Denna biokemiska undersökning var den första där multipla Dps proteiner i en och samma organism studerats. Forskningen har varit betydelsefull för att förstå hur de individuella Dps proteinerna inom gruppen ferritinliknande proteiner i en och samma organism samarbetar för att reglera järn, syre och ROS-nivåer i cellerna. Min forskning har också bidragit till att identifiera proteiner som direkt kan ha betydelse för de processer; syrgas och

järnreglering samt skydd mot oxidativ stress, som är viktiga för vätgasproduktion i cyanobakterier.

I avhandlingens andra kapitel undersöker jag teorin att ett förbättrat H_2-utbyte kräver en omfördelning av fotosyntetisk energi från celltillväxt till H_2-produktion. För att utvärdera denna teori odlades *Nostoc* PCC 7120 ΔhupW under järnsvält i fyra veckor. Den Fe-begränsade kulturen uppvisade en ~ 5,3 gånger lägre klorofyll a-koncentration och en ~ 4,5 gånger högre kolhydratkoncentration jämfört med kontrollen. Detta resultat tyder på att energi lagras i cellerna på bekostnad av tillväxt. En annan viktig upptäckt var att den Fe-begränsade cellkulturen bestod av långa filament med en hög heterocystfrekvens på ~ 6%, och att dessa heterocyster kunde återfå sin aktivitet när Fe åter tillsattes. Den låga syrgashalten i heterocyster möjliggör effektiv H_2-produktion från O_2-intoleranta foto-fermentativa processer.

Jag förslår att järnsvält som odlingsstrategi kan nyttjas för effektiv vätgasproduktion på bekostnad av celltillväxt. För att kunna undersöka detta har jag utvecklat en prototyp-biofilmfotobioreaktor med fokus på att (i) sänka kostnaden (ii) sänka energiförbrukningen (iii) och öka cellernas kapacitet för att skörda solenergi och omvandla energin till för samhället användbara produkter.

Acknowledgements

I am happy to acknowledge to a lot of people that have been giving me the energy to write this thesis.

Thanks **Karin Stensjö**! You have given me this great opportunity to evolve as a PhD student. I will never forget the long and fruitful research discussions that we had. You have been giving me the trust I needed to develop my thoughts into ideas, into plans, into lab trials, into everything I love about science. My thoughts have been taken me on a journey that I will never forget.

Thank you **Felix M. Ho** for being my 2nd supervisor! Your expertise on basically everything has always impressed me and made me trying harder. Your comments, corrections and contributions in the paper work have been so helpful – I am very happy that you found the time and energy to do all of that! By the way, I always wondered what your 2nd name is …?!

Thanks **Stenbjörn Styring**! With your presentation during the Summer School in Green Chemistry in Göttingen in September 2011, you have sent me on a journey that has greatly changed my life. Without you, I would not have been living in Sweden and I would not have contacted Karin. Your inspiring talks on renewable energy and chemistry should be infinitely accessible to a global audience.

Thank you **Leif Hammarström**! Your great skills of chairing discussions in our CAP meetings created a fair platform of scientific communication. Your critical thoughts and your vast knowledge in chemistry contributed to everyone's vision (I think I can speak for everyone here) to become a better scientist every day.

A great thanks goes to you, Prof. Dr. **Clemens Posten**! You cordially welcomed me at the KIT in Karlsruhe being a part of your research group for 1.5 years. You have helped me to conduct the science that I wanted to do and I enjoyed this time so much!

Thanks to **Peter Lindblad** and **Pia Lindberg**! Your contributions in our weekly scientific meetings were inspiring and helpful to everyone!

Thanks **Patrícia Raleiras**! I have learned so much from you, you can't imagine. Your hard work and your critical thinking have been greatly affecting my work! Especially your presentations have always impressed me, as you tried to get everybody on-board. I have been trying to copy that and I just hope that you don't have a patent on that skills;) – otherwise I owe you lots of money…

Thank you **Adam Wegelius**! I have been appreciating all our discussions, in real life and via email! Your sense of humour and your kind soul is a combination that you should keep forever!

Thanks **Claudia Durall de la Fuente**! You are a bright shining star that has been giving a lot of energy to all our lab mates, including me. It was a pleasure to share moments of despair and others, filled with pure enthusiasm.

Thanks **Daniel Camsund**! What a man of knowledge and sympathy! I have always loved our discussions about both, research and life!

Thanks **Gustav Sandh**! You kindly introduced me to the Ångström lab for my Master thesis project in September 2012 and your critical scientific questions were always helpful to take the next research step. We definitely need more of your kind!

Thanks **Sonja Pullen**! You are a great person, and an awesome researcher, too. I am happy that you asked me to join the organisation committee for the International Solar Conference – Young! That was dream of my life that I always wanted to live, and you somehow knew about that and asked me to join!

Thanks to you, **Jessica Stålberg**, **Susanne Söderberg**, **Eva Johansson** and **Sven Johansson**! Each of you forms the supporting back bone for every PhD student that is otherwise just overwhelmed with organisation. Thanks for your actions and your great care-taking skills!

Thanks to my colleagues **Karina Persson**, **Namita Khanna**, **Bagmi Pattanaik**, **Mohammed Mirmohades**, **Rui Miao**, **Xin Li**, **Feiyan Liang**, **Elias Englund**, **Vamsi Moparthi**, **Helder Miranda**, **Isabel Moreno de Palma**, **Giovanni Barone**, **Livia Meszaros**, **Nigar Ahmadova**, **Brigitta Németh**, **Fikret Mamedov**, **Ann Magnuson**, **Jens Föhlinger**, **Sascha Ott**, **Keyhan Esfandiarfard**, **Michele Bedin**, **Gustav Berggren**, **Christer Elvingson**, **Juri Mai**, **Luca D'Amario** and **Anders Thapper** for being so kind, doing so much hard work and creating a research environment at Ångström that has been inspiring the whole time!

Thanks **Fabian Jeschull**! Our shared tea time (well…more beer than tea, I suppose), our countless bouldering sessions and moments of devouring burgers in the shady pubs of Uppsala … all that made my salary quickly disappear. .. Talking about food - I would like to join the dinner at your Nobel price party =).
Big thanks goes to all my colleagues at the KIT Karlsruhe during my guest stay: **Meike**, **Franzi**, **Kira** and **Lisa**. **Christian**, I totally can see you as a member of the first mars colonists making things work to rescue all the others from death – constantly. This might be quite stressful, so it is good that you chose to do what you do now =). A special thanks goes to **Andreas**, **Mirco** and **Inga**, who made my life joyful at the KIT in Karlsruhe! Without you I would not have survived this city. To my hard-working students **Dominik**, **Camilla** and **Daniel**, I also want to thank!

I would like to thank for the financial support from the stipend organisations **Nano Micro Facility** (KNMF) at the KIT, **Magnus Bergvalls foundation**, **Carl Tryggers Stipendiestiftelse**, **C F Liljewalch Stiftelse**, **Sven and Lilly Lawski foundation** and the **Lars Hiertas Minne Stiftelsen**.

… *sigh

Often I think about you, all the people from former Ulleråkersvägen 46 A, who lived there with me between September 2012 and December 2014. I will never forget the precious time that we spent, the love that we shared, the family that we were and the beauty of life that we created. It was a miracle, every day. Saying it with Jeff's words - You don't just move to Ulleråkersvägen. No, it calls you and you get there.

I want to especially thank my beloved friends who I got to know in this magic place Uppsala, namely, **Giovanni**, **Giuseppe**, **Linn**, **Alma**, **Emil**, **Sara**, **Yoel**, **Peter**, **Ana** and **Jeff**. Also my friends back in Germany I would like to thank, namely, **Manuel**, **Monique**, **Marius**, **Philipp**, **Falk**, **Henning**, **Kirk**, **Julia**, **Nicolas** & **Reschi**. Thanks to all my new friends in Freiburg that make this place wonderful to me. You all have given me a lot of strength to carry on.

I also would like to thank my dad making me aware of the beauty and vulnerability of nature during my early childhood.

Finally, I want to thank **my mom and Helge**, **my two sisters, and my brother** and my love **Valerie** for all the great support throughout these years. Without you, I would have just got lost. Somewhere in between… and I would not have continued to dream on.

References

1. IPCC, 2014: Climate Change 2014: Impacts, Adaptation, and Vulnerability. Part A: Global and Sectoral Aspects. Contribution of Working Group II to the Fifth Assessment Report of the Intergovernmental Panel on Climate Change [Field, C.B., V.R. Barros, D.J.
2. IPCC, 2014: Climate Change 2014: Impacts, Adaptation, and Vulnerability. Part A: Global and Sectoral Aspects. Contribution of Working Group II to the Fifth Assessment Report of the Intergovernmental Panel on Climate Change . Cambridge University Press, Ca 10.1017/CBO9781107415324.Summary
3. Scrosati, B., and Garche, J. (2010) Lithium batteries: Status, prospects and future. J. Power Sources. **195**, 2419–2430
4. Bakenne, A., Nuttall, W., and Kazantzis, N. (2016) Sankey-Diagram-based insights into the hydrogen economy of today. Int. J. Hydrogen Energy. **41**, 7744–7753
5. Mahidhara, G., Burrow, H., Sasikala, C., and Ramana, C. V. (2019) Biological hydrogen production: molecular and electrolytic perspectives. World J. Microbiol. Biotechnol. **35**, 116
6. Rodionova, M. V., Poudyal, R. S., Tiwari, I., Voloshin, R. A., Zharmukhamedov, S. K., Nam, H. G., Zayadan, B. K., Bruce, B. D., Hou, H. J. M., and Allakhverdiev, S. I. (2017) Biofuel production: Challenges and opportunities. Int. J. Hydrogen Energy. **42**, 8450–8461
7. Oey, M., Sawyer, A. L., Ross, I. L., and Hankamer, B. (2016) Challenges and opportunities for hydrogen production from microalgae. Plant Biotechnol. J. **14**, 1487–1499
8. Haikarainen, T., and Papageorgiou, A. C. (2010) Dps-like proteins: Structural and functional insights into a versatile protein family. Cell. Mol. Life Sci. **67**, 341–351
9. Khanna, N., and Lindblad, P. (2015) Cyanobacterial hydrogenases and hydrogen metabolism revisited: Recent progress and future prospects. Int. J. Mol. Sci. **16**, 10537–10561
10. Khetkorn, W., Rastogi, R. P., Incharoensakdi, A., Lindblad, P., Madamwar, D., Pandey, A., and Larroche, C. (2017) Microalgal hydrogen production – A review. Bioresour. Technol. **243**, 1194–1206
11. Prince, R. C., and Kheshgi, H. S. (2005) The photobiological production of hydrogen: Potential efficiency and effectiveness as a renewable fuel. Crit. Rev. Microbiol. **31**, 19–31
12. Avilan, L., Roumezi, B., Risoul, V., Bernard, C. S., Kpebe, A., Belhadjhassine, M., Rousset, M., Brugna, M., and Latifi, A. (2018) Phototrophic hydrogen production from a clostridial [FeFe] hydrogenase expressed in the heterocysts of the cyanobacterium Nostoc PCC 7120. Appl. Microbiol. Biotechnol. **102**, 5775–5783

13. Nyberg, M., Heidorn, T., and Lindblad, P. (2015) Hydrogen production by the engineered cyanobacterial strain Nostoc PCC 7120 ΔhupW examined in a flat panel photobioreactor system. J. Biotechnol. **215**, 35–43
14. Luan, G., Zhang, S., Wang, M., and Lu, X. (2019) Progress and perspective on cyanobacterial glycogen metabolism engineering. Biotechnol. Adv. 10.1016/j.biotechadv.2019.04.005
15. Schwarze, A., Kopczak, M. J., Rogner, M., and Lenz, O. (2010) Requirements for construction of a functional hybrid complex of photosystem I and [NiFe]-hydrogenase. Appl. Environ. Microbiol. **76**, 2641–2651
16. Nagarajan, D., Lee, D. J., Kondo, A., and Chang, J. S. (2017) Recent insights into biohydrogen production by microalgae – From biophotolysis to dark fermentation. Bioresour. Technol. **227**, 373–387
17. Fernandes, B. D., Mota, A., Teixeira, J. A., and Vicente, A. A. (2015) Continuous cultivation of photosynthetic microorganisms: Approaches, applications and future trends. Biotechnol. Adv. **33**, 1228–1245
18. Behera, S., Singh, R., Arora, R., Sharma, N. K., Shukla, M., and Kumar, S. (2015) Scope of Algae as Third Generation Biofuels. Front. Bioeng. Biotechnol. **2**, 1–13
19. Razeghifard, R. (2013) Algal biofuels. Photosynth. Res. **117**, 207–19
20. Gupta, P. L., Lee, S. M., and Choi, H. J. (2015) A mini review: photobioreactors for large scale algal cultivation. World J. Microbiol. Biotechnol. **31**, 1409–1417
21. Wang, H., Zhang, W., Chen, L., Wang, J., and Liu, T. (2013) The contamination and control of biological pollutants in mass cultivation of microalgae. Bioresour. Technol. **128**, 745–750
22. Gómez, P. I., Inostroza, I., Pizarro, M., and Pérez, J. (2013) Fromgenetic improvementtocommercial-scalemassculture of a Chilean strain of the green microalga Haematococcus pluvialis with enhanced productivity of the red ketocarotenoid astaxanthin. AoB Plants. **5**, 1–7
23. Li, J., Zhu, D., Niu, J., Shen, S., and Wang, G. (2011) An economic assessment of astaxanthin production by large scale cultivation of Haematococcus pluvialis. Biotechnol. Adv. **29**, 568–574
24. Giuliano, D., Bruno, F., Antonio A., V., and Jose A., T. (2010) Third generation biofuels from microalgae. Curr. Res. Technol. Educ. Top. Appl. Microbiol. Microb. Biotechnol.
25. Acién, F. G., Fernández, J. M., Magán, J. J., and Molina, E. (2012) Production cost of a real microalgae production plant and strategies to reduce it. Biotechnol. Adv. **30**, 1344–1353
26. Vandamme, D., Foubert, I., and Muylaert, K. (2013) Flocculation as a low-cost method for harvesting microalgae for bulk biomass production. Trends Biotechnol. **31**, 233–239
27. Trentacoste, E. M., Martinez, A. M., and Zenk, T. (2015) The place of algae in agriculture: Policies for algal biomass production. Photosynth. Res. **123**, 305–315
28. Dasgupta, C. N., Jose Gilbert, J., Lindblad, P., Heidorn, T., Borgvang, S. A., Skjanes, K., and Das, D. (2010) Recent trends on the development of photobiological processes and photobioreactors for the improvement of hydrogen production. Int. J. Hydrogen Energy. **35**, 10218–10238
29. De Vree, J. H., Bosma, R., Janssen, M., Barbosa, M. J., and Wijffels, R. H. (2015) Comparison of four outdoor pilot-scale photobioreactors. Biotechnol. Biofuels. **8**, 1–12

30. Kumar Gupta, S., Kumari, S., Reddy, K., and Bux, F. (2013) Trends in biohydrogen production: Major challenges and state-of-the-art developments. Environ. Technol. (United Kingdom). **34**, 1653–1670
31. Benstein, R. M., Çebi, Z., Podola, B., and Melkonian, M. (2014) Immobilized Growth of the Peridinin-Producing Marine Dinoflagellate Symbiodinium in a Simple Biofilm Photobioreactor. Mar. Biotechnol. **16**, 621–628
32. Li, T., Strous, M., and Melkonian, M. (2017) Biofilm-based photobioreactors: Their design and improving productivity through efficient supply of dissolved inorganic carbon. FEMS Microbiol. Lett. **364**, 1–9
33. Rubio, F. C., Fernández, F. G. A., Pérez, J. A. S., Camacho, F. G., and Grima, E. M. (1999) Prediction of dissolved oxygen and carbon dioxide concentration profiles in tubular photobioreactors for microalgal culture. Biotechnol. Bioeng. **62**, 71–86
34. Jiménez, C., Cossío, B. R., and Niell, F. X. (2003) Relationship between physicochemical variables and productivity in open ponds for the production of Spirulina: A predictive model of algal yield. Aquaculture. **221**, 331–345
35. Mendoza, J. L., Granados, M. R., de Godos, I., Acién, F. G., Molina, E., Heaven, S., and Banks, C. J. (2013) Oxygen transfer and evolution in microalgal culture in open raceways. Bioresour. Technol. **137**, 188–195
36. Bettina E Schirrmeister, Alexandre Antonelli, and Homayoun C Bagheri (2011) The origin of multicellularity in cyanobacteria. BMC Evol. Biol. **11**, 1471–2148
37. Stanier, R. Y., Deruelles, J., Rippka, R., Herdman, M., and Waterbury, J. B. (1979) Generic Assignments, Strain Histories and Properties of Pure Cultures of Cyanobacteria. Microbiology. **111**, 1–61
38. Inupakutika, M. A., Sengupta, S., Devireddy, A. R., Azad, R. K., and Mittler, R. (2016) The evolution of reactive oxygen species metabolism. J. Exp. Bot. **67**, 5933–5943
39. Latifi, A., Ruiz, M., and Zhang, C. C. (2009) Oxidative stress in cyanobacteria. FEMS Microbiol. Rev. **33**, 258–278
40. Imlay, J. A. (2003) Pathways of Oxidative Damage. Annu. Rev. Microbiol. **57**, 395–418
41. Kirilovsky, D., and Kerfeld, C. A. (2012) The orange carotenoid protein in photoprotection of photosystem II in cyanobacteria. Biochim. Biophys. Acta - Bioenerg. **1817**, 158–166
42. Bernroitner, M., Zamocky, M., Furtmüller, P. G., Peschek, G. A., and Obinger, C. (2009) Occurrence, phylogeny, structure, and function of catalases and peroxidases in cyanobacteria. J. Exp. Bot. **60**, 423–440
43. Almiron, M., Link, A. J., Furlong, D., and Kolter, R. (1992) A novel DNA-binding protein with regulatory and protective roles in starved Escherichia coli. Genes Dev. **6**, 2646–2654
44. Kranzler, C., Rudolf, M., Keren, N., and Schleiff, E. (2013) Iron in Cyanobacteria, 10.1016/B978-0-12-394313-2.00003-2
45. Honarmand Ebrahimi, K., Hagedoorn, P. L., and Hagen, W. R. (2015) Unity in the biochemistry of the iron-storage proteins ferritin and bacterioferritin. Chem. Rev. **115**, 295–326
46. Zhao, G., Ceci, P., Ilari, A., Giangiacomo, L., Laue, T. M., Chiancone, E., and Dennis Chasteen, N. (2002) Iron and hydrogen peroxide detoxification properties of DNA-binding protein from starved cells. A ferritin-like DNA-binding protein of Escherichia coli. J. Biol. Chem. **277**, 27689–27696

47. Cramer, W. A. (2019) Structure–function of the cytochrome b 6 f lipoprotein complex: a scientific odyssey and personal perspective. Photosynth. Res. **139**, 53–65
48. Rees, D. C., Tezcan, F. A., Haynes, C. A., Walton, M. Y., Andrade, S., Einsle, O., and Howard, J. B. (2005) Structural basis of biological nitrogen fixation. Philos. Trans. R. Soc. A Math. Phys. Eng. Sci. **363**, 971–984
49. Romberger, S. P., and Golbeck, J. H. (2010) The bound iron-sulfur clusters of Type-I homodimeric reaction centers. Photosynth. Res. **104**, 333–346
50. Ekman, M., Sandh, G., Nenninger, A., Oliveira, P., and Stensjö, K. (2014) Cellular and functional specificity among ferritin-like proteins in the multicellular cyanobacterium Nostoc punctiforme. Environ. Microbiol. **16**, 829–844
51. Alaleona, F., Franceschini, S., Ceci, P., Ilari, A., and Chiancone, E. (2010) Thermosynechoccus elongatus DpsA binds Zn(II) at a unique three histidine-containing ferroxidase center and utilizes O_2 as iron oxidant with very high efficiency, unlike the typical Dps proteins. FEBS J. **277**, 903–917
52. Chowdhury, R. P., Saraswathi, R., and Chatterji, D. (2010) Research communication mycobacterial stress regulation: The Dps "twin sister" defense mechanism and structure-function relationship. IUBMB Life. **62**, 67–77
53. Papinutto, E., Dundon, W. G., Pitulis, N., Battistutta, R., Montecucco, C., and Zanotti, G. (2002) Structure of two iron-binding proteins from Bacillus anthracis. J. Biol. Chem. **277**, 15093–15098
54. Stillman, T. J., Upadhyay, M., Norte, V. A., Sedelnikova, S. E., Carradus, M., Tzokov, S., Bullough, P. A., Shearman, C. A., Gasson, M. J., Williams, C. H., Artymiuk, P. J., and Green, J. (2005) The crystal structures of Lactococcus lactis MG1363 Dps proteins reveal the presence of an N-terminal helix that is required for DNA binding. Mol. Microbiol. **57**, 1101–1112
55. Turner, S., Blain, S., Watson, A. J., Follows, M., Owens, N. P. J., de Baar, H. J. W., Boyle, E. A., Coale, K. H., Schoemann, V., Levasseur, M., Pollard, R., Jickells, T., Rivkin, R. B., Takeda, S., Harvey, M., Lancelot, C., Sarmiento, J., Smetacek, V., Tsuda, A., Buesseler, K. O., Law, C. S., Cullen, J. J., and Boyd, P. W. (2007) Mesoscale Iron Enrichment Experiments 1993-2005: Synthesis and Future Directions. Science (80-.). **315**, 612–617
56. Bryant, D. A. (1995) The molecular biology of cyanobacteria, 10.1007/BF00032589
57. Narayan, Prakash, O., Kumari, N., and Rai, L. C. (2011) Iron starvation-induced proteomic changes in Anabaena (Nostoc) sp. PCC 7120: Exploring survival strategy. J. Microbiol. Biotechnol. **21**, 136–146
58. Hardie, L. P., Balkwill, D. L., and Stevens, S. E. (1983) Effects of iron starvation on the ultrastructure of the cyanobacterium Agmenellum quadruplicatum. Appl. Environ. Microbiol. **45**, 1007–1017
59. Sherman, D. M., and Sherman, L. A. (1983) Effect of iron deficiency and iron restoration on ultrastructure of Anacystis nidulans . J. Bacteriol. **156**, 393–401
60. Jacq, V., Ridame, C., L'Helguen, S., Kaczmar, F., and Saliot, A. (2014) Response of the unicellular diazotrophic cyanobacterium Crocosphaera watsonii to iron limitation. PLoS One. 10.1371/journal.pone.0086749
61. Yeung, A. C. Y., D'Agostino, P. M., Poljak, A., McDonald, J., Bligh, M. W., Waite, T. D., and Neilan, B. A. (2016) Physiological and Proteomic Responses of Continuous Cultures of Microcystis aeruginosa PCC 7806 to

Changes in Iron Bioavailability and Growth Rate. Appl. Environ. Microbiol. **82**, 5918–5929
62. van Alphen, P., Abedini Najafabadi, H., Branco dos Santos, F., and Hellingwerf, K. J. (2018) Increasing the Photoautotrophic Growth Rate of Synechocystis sp. PCC 6803 by Identifying the Limitations of Its Cultivation. Biotechnol. J. **13**, 1–8
63. Shi, T., Sun, Y., and Falkowski, P. G. (2007) Effects of iron limitation on the expression of metabolic genes in the marine cyanobacterium Trichodesmium erythraeum IMS101. Environ. Microbiol. **9**, 2945–56
64. Dougals, D., Peat, A., Whitton, B. A., and Wood, P. (1986) Influence of iron status on structure of the cyanobacterium (blue-green alga) Calothrix parietina. Cytobios. **47**, 155–166
65. Rudolf, M., Stevanovic, M., Kranzler, C., Pernil, R., Keren, N., and Schleiff, E. (2016) Multiplicity and specificity of siderophore uptake in the cyanobacterium Anabaena sp. PCC 7120. Plant Mol. Biol. **92**, 57–69
66. Rudolf, M., Kranzler, C., Lis, H., Margulis, K., Stevanovic, M., Keren, N., and Schleiff, E. (2015) Multiple modes of iron uptake by the filamentous, siderophore-producing cyanobacterium, Anabaena sp. PCC 7120. Mol. Microbiol. **97**, 577–588
67. Kranzler, C., Lis, H., Shaked, Y., and Keren, N. (2011) The role of reduction in iron uptake processes in a unicellular, planktonic cyanobacterium. Environ. Microbiol. **13**, 2990–2999
68. Qiu, G. W., Lou, W. J., Sun, C. Y., Yang, N., Li, Z. K., Li, D. L., Zang, S. S., Fu, F. X., Hutchins, D. A., Jiang, H. B., and Qiu, B. S. (2018) Outer membrane iron uptake pathways in the model cyanobacterium Synechocystis sp. strain PCC 6803. Appl. Environ. Microbiol. **84**, 1–15
69. Gledhiir, M., and Buck, K. N. (2012) The organic complexation of iron in the marine environment: A review. Front. Microbiol. **3**, 1–17
70. Nagai, T., Imai, A., Matsushige, K., Yokoi, K., and Fukushima, T. (2007) Dissolved iron and its speciation in a shallow eutrophic lake and its inflowing rivers. Water Res. **41**, 775–784
71. Chiancone, E., Ceci, P., Ilari, A., Ribacchi, F., and Stefanini, S. (2004) Iron and proteins for iron storage and detoxification. BioMetals. **17**, 197–202
72. Küberl, A., Polen, T., and Bott, M. (2016) The pupylation machinery is involved in iron homeostasis by targeting the iron storage protein ferritin. Proc. Natl. Acad. Sci. **113**, 4806–4811
73. Grossman, M. J., Hinton, S. M., Minak-Bernero, V., Slaughter, C., and Stiefel, E. I. (1992) Unification of the ferritin family of proteins. Proc. Natl. Acad. Sci. U. S. A. **89**, 2419–2423
74. Bellapadrona, G., Stefanini, S., Zamparelli, C., Theil, E. C., and Chiancone, E. (2009) Iron translocation into and out of Listeria innocua Dps and size distribution of the protein-enclosed nanomineral are modulated by the electrostatic gradient at the 3-fold "ferritin-like" pores. J. Biol. Chem. **284**, 19101–19109
75. Ceci, P., Ilari, A., Falvo, E., Giangiacomo, L., and Chiancone, E. (2005) Reassessment of protein stability, DNA binding, and protection of Mycobacterium smegmatis Dps. J. Biol. Chem. **280**, 34776–34785
76. Cellai, S., Rivetti, C., Rossi, G. L., Ceci, P., Falvo, E., and Chiancone, E. (2004) DNA condensation and self-aggregation of Escherichia coli Dps are coupled phenomena related to the properties of the N-terminus. Nucleic Acids Res. **32**, 5935–5944

77. Reon, B. J., Nguyen, K. H., Bhattacharyya, G., and Grove, A. (2012) Functional comparison of Deinococcus radiodurans Dps proteins suggests distinct in vivo roles. Biochem. J. **447**, 381–391
78. Santos, S. P., Mitchell, E. P., Franquelim, H. G., Castanho, M. A. R. B., Abreu, I. A., and Romão, C. V. (2015) Dps from Deinococcus radiodurans: Oligomeric forms of Dps1 with distinct cellular functions and Dps2 involved in metal storage. FEBS J. **282**, 4307–4327
79. Ceci, P., Mangiarotti, L., Rivetti, C., and Chiancone, E. (2007) The neutrophil-activating Dps protein of Helicobacter pylori, HP-NAP, adopts a mechanism different from Escherichia coli Dps to bind and condense DNA. Nucleic Acids Res. **35**, 2247–2256
80. Gauss, G. H., Young, M. J., Douglas, T., Lawrence, C. M., Reott, M. A., Roha, E. R., and Smith, C. J. (2012) Characterization of the Bacteroides fragilis bfr gene product identifies a bacterial DPS-like protein and suggests evolutionary links in the ferritin superfamily. J. Bacteriol. **194**, 15–27
81. Ceci, P., Ilari, A., Falvo, E., and Chiancone, E. (2003) The Dps Protein of Agrobacterium tumefaciens Does Not Bind to DNA but Protects It toward Oxidative Cleavage. J. Biol. Chem. **278**, 20319–20326
82. Huergo, L. F., Rahman, H., Ibrahimovic, A., Day, C. J., and Korolik, V. (2013) Campylobacter jejuni Dps protein binds DNA in the presence of iron or hydrogen peroxide. J. Bacteriol. **195**, 1970–1978
83. Grove, A., and Wilkinson, S. P. (2005) Differential DNA binding and protection by dimeric and dodecameric forms of the ferritin homolog Dps from Deinococcus radiodurans. J. Mol. Biol. **347**, 495–508
84. Sato, Y. T., Watanabe, S., Kenmotsu, T., Ichikawa, M., Yoshikawa, Y., Teramoto, J., Imanaka, T., Ishihama, A., and Yoshikawa, K. (2013) Structural change of DNA induced by nucleoid proteins: Growth phase-specific fis and stationary phase-specific dps. Biophys. J. **105**, 1037–1044
85. Morikawa, K., Ohniwa, R. L., Kim, J., Maruyama, A., Ohta, T., and Takeyasu, K. (2006) Bacterial nucleoid dynamics: Oxidative stress response in Staphylococcus aureus. Genes to Cells. **11**, 409–423
86. Frenkiel-Krispin, D., and Minsky, A. (2006) Nucleoid organization and the maintenance of DNA integrity in E. coli, B. subtilis and D. radiodurans. J. Struct. Biol. **156**, 311–319
87. Ren, B., Tibbelin, G., Kajino, T., Asami, O., and Ladenstein, R. (2003) The multi-layered structure of Dps with a novel di-nuclear ferroxidase center. J. Mol. Biol. **329**, 467–477
88. Andrews, S. C. (2010) The Ferritin-like superfamily: Evolution of the biological iron storeman from a rubrerythrin-like ancestor. Biochim. Biophys. Acta - Gen. Subj. **1800**, 691–705
89. Franceschini, S., Ceci, P., Alaleona, F., Chiancone, E., and Ilari, A. (2006) Antioxidant Dps protein from the thermophilic cyanobacterium Thermosynechococcus elongatus: An intrinsically stable cage-like structure endowed with enhanced stability. FEBS J. **273**, 4913–4928
90. Kauko, A., Pulliainen, A. T., Haataja, S., Meyer-Klaucke, W., Finne, J., and Papageorgiou, A. C. (2006) Iron Incorporation in Streptococcus suis Dps-like Peroxide Resistance Protein Dpr Requires Mobility in the Ferroxidase Center and Leads to the Formation of a Ferrihydrite-like Core. J. Mol. Biol. **364**, 97–109
91. Liu, X., Kim, K., Leighton, T., and Theil, E. C. (2006) Paired Bacillus anthracis Dps (mini-ferritin) have different reactivities with peroxide. J. Biol. Chem. **281**, 27827–27835

92. Schwartz, J. K., Diebold, A., Solomon, E. I., Liu, X. S., Tosha, T., and Theil, E. C. (2010) CD and MCD spectroscopic studies of the two dps miniferritin proteins from Bacillus anthracis: Role of O2 and H2O2 substrates in reactivity of the diiron catalytic centers. Biochemistry. **49**, 10516–10525
93. Romão, C. V., Mitchell, E. P., and McSweeney, S. (2006) The crystal structure of Deinococcus radiodurans Dps protein (DR2263) reveals the presence of a novel metal centre in the N terminus. J. Biol. Inorg. Chem. **11**, 891–902
94. Zanotti, G., Papinutto, E., Dundon, W. G., Battistutta, R., Seveso, M., Giudice, G. Del, Rappuoli, R., and Montecucco, C. (2002) Structure of the neutrophil-activating protein from Helicobacter pylori. J. Mol. Biol. **323**, 125–130
95. Roy, S., Saraswathi, R., Chatterji, D., and Vijayan, M. (2008) Structural Studies on the Second Mycobacterium smegmatis Dps: Invariant and Variable Features of Structure, Assembly and Function. J. Mol. Biol. **375**, 948–959
96. Miyamoto, T., Asahina, Y., Miyazaki, S., Shimizu, H., Ohto, U., Noguchi, S., and Satow, Y. (2011) Structures of the SEp22 dodecamer, a Dps-like protein from Salmonella enterica subsp. enterica serovar Enteritidis. Acta Crystallogr. Sect. F Struct. Biol. Cryst. Commun. **67**, 17–22
97. Haikarainen, T., Tsou, C. C., Wu, J. J., and Papageorgiou, A. C. (2010) Crystal structures of Streptococcus pyogenes Dpr reveal a dodecameric iron-binding protein with a ferroxidase site. J. Biol. Inorg. Chem. **15**, 183–194
98. Li, X., Pal, U., Ramamoorthi, N., Liu, X., Desrosiers, D. C., Eggers, C. H., Anderson, J. F., Radolf, J. D., and Fikrig, E. (2007) The Lyme disease agent Borrelia burgdorferi requires BB0690, a Dps homologue, to persist within ticks. Mol. Microbiol. **63**, 694–710
99. Roy, S., Gupta, S., Das, S., Sekar, K., Chatterji, D., and Vijayan, M. (2004) X-ray analysis of Mycobacterium smegmatis Dps and a comparative study involving other Dps and Dps-like molecules. J. Mol. Biol. **339**, 1103–1113
100. Zeth, K., Offermann, S., Essen, L.-O., and Oesterhelt, D. (2004) Iron-oxo clusters biomineralizing on protein surfaces: Structural analysis of Halobacterium salinarum DpsA in its low- and high-iron states. Proc. Natl. Acad. Sci. **101**, 13780–13785
101. Su, M., Cavallo, S., Stefanini, S., Chiancone, E., and Chasteen, N. D. (2005) The so-called Listeria innocua ferritin is a Dps protein. Iron incorporation, detoxification, and DNA protection properties. Biochemistry. **44**, 5572–5578
102. Pulliainen, A. T., Haataja, S., Kähkönen, S., and Finne, J. (2003) Molecular basis of H2O2 resistance mediated by streptococcal Dpr: Demonstration of the functional involvement of the putative ferroxidase center by site-directed mutagenesis in Streptococcus suis. J. Biol. Chem. **278**, 7996–8005
103. Nair, S., and Finkel, S. E. (2004) Dps protects cells against multiple stresses during stationary phase. J. Bacteriol. **186**, 4192–4198
104. Calhoun, L. N., and Kwon, Y. M. (2011) The ferritin-like protein Dps protects Salmonella enterica serotype Enteritidis from the Fenton-mediated killing mechanism of bactericidal antibiotics. Int. J. Antimicrob. Agents. **37**, 261–265
105. Meeks, J. C., Elhai, J., Thiel, T., Potts, M., Larimer, F., Lamerdin, J., Predki, P., and Atlas, R. (2001) An overview of the Genome of Nostoc punctiforme, a multicellular, symbiotic Cyanobacterium. Photosynth. Res. **70**, 85–106

106. Meeks, J. C., and Elhai, J. (2002) Regulation of Cellular Differentiation in Filamentous Cyanobacteria in Free-Living and Plant-Associated Symbiotic Growth States. Microbiol. Mol. Biol. Rev. **66**, 94–121
107. Sato, N., Moriyama, T., Toyoshima, M., Mizusawa, M., and Tajima, N. (2012) The all0458/lti46.2 gene encodes a low temperature-induced Dps protein homologue in the cyanobacteria Anabaena sp. PCC 7120 and Anabaena variabilis M3. Microbiol. (United Kingdom). **158**, 2527–2536
108. Li, X., Mustila, H., Magnuson, A., and Stensjö, K. (2018) Homologous overexpression of NpDps2 and NpDps5 increases the tolerance for oxidative stress in the multicellular cyanobacterium Nostoc punctiforme. FEMS Microbiol. Lett. **365**, 1–8
109. McWilliam, H., Li, W., Uludag, M., Squizzato, S., Park, Y. M., Buso, N., Cowley, A. P., and Lopez, R. (2013) Analysis Tool Web Services from the EMBL-EBI. Nucleic Acids Res. **41**, 597–600
110. Ow, S. Y., Nolrel, J., Cardona, T., Taton, A., Lindblad, P., Stensjö, K., and Wright, P. C. (2009) Quantitative overview of N2 fixation in Nostoc punctiforme ATCC 29133 through cellular enrichments and iTRAQ shotgun proteomics. J. Proteome Res. **8**, 187–198
111. Lee, H. M., Vásquez-Bermúdez, M. F., and De Marsac, N. T. (1999) The global nitrogen regulator NtcA regulates transcription of the signal transducer P(II) (GlnB) and influences its phosphorylation level in response to nitrogen and carbon supplies in the cyanobacterium Synechococcus sp. strain PCC 7942. J. Bacteriol. **181**, 2697–2702
112. Moparthi, V. K., Li, X., Vavitsas, K., Dzhygyr, I., Sandh, G., Magnuson, A., and Stensjö, K. (2016) The two Dps proteins, NpDps2 and NpDps5, are involved in light-induced oxidative stress tolerance in the N2-fixing cyanobacterium Nostoc punctiforme. Biochim. Biophys. Acta - Bioenerg. **1857**, 1766–1776
113. Narayan, O. P., Kumari, N., and Rai, L. C. (2010) Heterologous expression of Anabaena PCC 7120 all3940 (a Dps family gene) protects Escherichia coli from nutrient limitation and abiotic stresses. Biochem. Biophys. Res. Commun. **394**, 163–169
114. Blanken, W., Schaap, S., Theobald, S., Rinzema, A., Wijffels, R. H., and Janssen, M. (2017) Optimizing carbon dioxide utilization for microalgae biofilm cultivation. Biotechnol. Bioeng. **114**, 769–776
115. Ontiveros-Valencia, A., Zhou, C., Zhao, H. P., Krajmalnik-Brown, R., Tang, Y., and Rittmann, B. E. (2018) Managing microbial communities in membrane biofilm reactors. Appl. Microbiol. Biotechnol. **102**, 9003–9014
116. Zhang, C., Zhang, H., Zhang, Z., Jiao, Y., and Zhang, Q. (2014) Effects of mass transfer and light intensity on substrate biological degradation by immobilized photosynthetic bacteria within an annular fiber-illuminating biofilm reactor. J. Photochem. Photobiol. B Biol. **131**, 113–119
117. Wei, X., Mingjia, H., Xiufeng, L., Yang, G., and Qingyu, W. (2007) Identification and biochemical properties of Dps (starvation-induced DNA binding protein) from cyanobacterium Anabaena sp. PCC 7120. IUBMB Life. **59**, 675–681
118. Nguyen, K. H., and Grove, A. (2012) Metal binding at the Deinococcus radiodurans Dps-1 N-terminal metal site controls dodecameric assembly and DNA binding. Biochemistry. **51**, 6679–6689
119. Nguyen, K. H., Smith, L. T., Xiao, L., Bhattacharyya, G., and Grove, A. (2012) On the stoichiometry of Deinococcus radiodurans Dps-1 binding to duplex DNA. Proteins Struct. Funct. Bioinforma. **80**, 713–721

120. Fan, R., Boyle, A. L., Vee, V. C., See, L. N., and Orner, B. P. (2009) A helix swapping study of two protein cages. Biochemistry. **48**, 5623–5630
121. Swift, J., Wehbi, W. A., Kelly, B. D., Stowell, X. F., Saven, J. G., and Dmochowski, I. J. (2006) Design of functional ferritin-like proteins with hydrophobic cavities. J. Am. Chem. Soc. **128**, 6611–6619
122. Zhang, Y., Fu, J., Chee, S. Y., Ang, E. X. W., and Orner, B. P. (2011) Rational disruption of the oligomerization of the mini-ferritin E. coli DPS through protein-protein interface mutation. Protein Sci. **20**, 1907–1917
123. Chowdhury, R. P., Vijayabaskar, M. S., Vishveshwara, S., and Chatterji, D. (2008) Molecular mechanism of in vitro oligomerization of Dps from Mycobacterium smegmatis: Mutations of the residues identified by "interface cluster" analysis. Biochemistry. **47**, 11110–11117
124. Belkin, S., Mehlhorn, R. J., and Packer, L. (1987) Proton gradients in intact cyanobacteria. Plant Physiol. **84**, 25–30
125. Hinterstoisser, B., and Peschek, G. A. (1987) Fluorimetric pH measurement in whole cells of dark aerobic and anaerobic cyanobacteria. FEBS Lett. **217**, 169–173
126. Kelley, L. A., Mezulis, S., Yates, C. M., Wass, M. N., and Sternberg, M. J. E. (2015) The Phyre2 web portal for protein modeling, prediction and analysis. Nat. Protoc. **10**, 845–858
127. Ardini, M., Fiorillo, A., Fittipaldi, M., Stefanini, S., Gatteschi, D., Ilari, A., and Chiancone, E. (2013) Kineococcus radiotolerans Dps forms a heteronuclear Mn-Fe ferroxidase center that may explain the Mn-dependent protection against oxidative stress. Biochim. Biophys. Acta - Gen. Subj. **1830**, 3745–3755
128. Yang, X., Chiancone, E., Stefanini, S., Ilari, A., and Chasteen, N. D. (2000) Iron oxidation and hydrolysis reactions of a novel ferritin from Listeria innocua. Biochem. J. **349 Pt 3**, 783–6
129. Dame, R. T., and Dorman, C. J. (2018) Bacterial Chromatin, 10.1007/978-1-4939-8675-0
130. Stefanini, S., Cavallo, S., Montagnini, B., and Chiancone, E. (1999) Incorporation of iron by the unusual dodecameric ferritin from Listeria innocua. Biochem. J. **75**, 71–75
131. Havukainen, H., Haataja, S., Kauko, A., Pulliainen, A. T., Salminen, A., Haikarainen, T., Finne, J., and Papageorgiou, A. C. (2008) Structural basis of the zinc- and terbium-mediated inhibition of ferroxidase activity in Dps ferritin-like proteins. Protein Sci. **17**, 1513–1521
132. Meeks, J. C., Campbell, E. L., Summers, M. L., and Wong, F. C. (2002) Cellular differentiation in the cyanobacterium Nostoc punctiforme. Arch. Microbiol. **178**, 395–403
133. Ramsay, B., Wiedenheft, B., Allen, M., Gauss, G. H., Martin Lawrence, C., Young, M., and Douglas, T. (2006) Dps-like protein from the hyperthermophilic archaeon Pyrococcus furiosus. J. Inorg. Biochem. **100**, 1061–1068
134. Gauss, G. H., Benas, P., Wiedenheft, B., Young, M., Douglas, T., and Lawrence, C. M. (2006) Structure of the DPS-like protein from Sulfolobus solfataricus reveals a bacterioferritin-like dimetal binding site within a DPS-like dodecameric assembly. Biochemistry. **45**, 10815–10827
135. Shcolnick, S., Shaked, Y., and Keren, N. (2007) A role for mrgA, a DPS family protein, in the internal transport of Fe in the cyanobacterium Synechocystis sp. PCC6803. Biochim. Biophys. Acta - Bioenerg. **1767**, 814–819

136. Foster, J. S., Havemann, S. A., Singh, A. K., and Sherman, L. A. (2009) Role of mrgA in peroxide and light stress in the cyanobacterium Synechocystis sp. PCC 6803. FEMS Microbiol. Lett. **293**, 298–304
137. Fujisawa, T., Narikawa, R., Maeda, S. I., Watanabe, S., Kanesaki, Y., Kobayashi, K., Nomata, J., Hanaoka, M., Watanabe, M., Ehira, S., Suzuki, E., Awai, K., and Nakamura, Y. (2017) CyanoBase: A large-scale update on its 20th anniversary. Nucleic Acids Res. **45**, D551–D554
138. Park, Y., Lee, J., Buso, N., Gur, T., Madhusoodanan, N., Basutkar, P., Tivey, A. R. N., Potter, S. C., Finn, D., and Lopez, R. (2019) The EMBL-EBI search and sequence analysis toolsAPIs in 2019. Nucleic Acids Res. 10.1093/nar/gkz115
139. Lawson, T. L., Crow, A., Lewin, A., Yasmin, S., Moore, G. R., and Le Brun, N. E. (2009) Monitoring the iron status of the ferroxidase center of Escherichia coli bacterioferritin using fluorescence spectroscopy. Biochemistry. **48**, 9031–9039
140. Weeratunga, S. K., Gee, C. E., Lovell, S., Zeng, Y., Woodin, C. L., and Rivera, M. (2009) Binding of Pseudomonas aeruginosa apobacterioferritin-associated ferredoxin to bacterioferritin B promotes heme mediation of electron delivery and mobilization of core mineral iron. Biochemistry. **48**, 7420–7431
141. Thumiger, A., Polenghi, A., Papinutto, E., Battistutta, R., Montecucco, C., and Zanotti, G. (2006) Crystal structure of antigen TpF1 from Treponema pallidum. Proteins Struct. Funct. Genet. **62**, 827–830
142. Xia, X., Larios-Valencia, J., Liu, Z., Xiang, F., Kan, B., Wang, H., and Zhu, J. (2017) OxyR-Activated expression of Dps is important for Vibrio cholerae oxidative stress resistance and pathogenesis. PLoS One. **12**, 1–15
143. Reindel, S., Anemüller, S., Sawaryn, A., and Matzanke, B. F. (2002) The dpsa-homologue of the archaeon Halobacterium salinarum is a ferritin. Biochim. Biophys. Acta - Protein Struct. Mol. Enzymol. **1598**, 140–146
144. Peña, M. M. O., Burkhart, W., and Bullerjahn, G. S. (1995) Purification and characterization of a Synechococcus sp. strain PCC 7942 polypeptide structurally similar to the stress-induced Dps/PexB protein of Escherichia coli. Arch. Microbiol. **163**, 337–344
145. Peña, M. M. O., and Bullerjahn, G. S. (2002) The DpsA Protein of Synechococcus sp. Strain PCC7942 Is a DNA-binding Hemoprotein. J. Biol. Chem. **270**, 22478–22482
146. Durham, K. A., and Bullerjahn, G. S. (2002) Immunocytochemical localization of the stress-induced DpsA protein in the cyanobacterium Synechococcus sp. strain PCC 7942. J. Basic Microbiol. **42**, 367–372
147. Castruita, M., Saito, M., Schottel, P. C., Elmegreen, L. A., Myneni, S., Stiefel, E. I., and Morel, F. M. M. (2006) Overexpression and characterization of an iron storage and DNA-binding Dps protein from Trichodesmium erythraeum. Appl. Environ. Microbiol. **72**, 2918–2924
148. Castruita, M., Elmegreen, L. A., Shaked, Y., Stiefel, E. I., and Morel, F. M. M. (2007) Comparison of the kinetics of iron release from a marine (Trichodesmium erythraeum) Dps protein and mammalian ferritin in the presence and absence of ligands. J. Inorg. Biochem. **101**, 1686–1691
149. Shibata, K., Benson, A. A., and Calvin, M. (1954) The absorption spectra of suspensions of living micro-organisms. BBA - Biochim. Biophys. Acta. **15**, 461–470
150. Masukawa, H., Sakurai, H., Hausinger, R. P., and Inoue, K. (2017) Increased heterocyst frequency by patN disruption in Anabaena leads to enhanced

photobiological hydrogen production at high light intensity and high cell density. Appl. Microbiol. Biotechnol. **101**, 2177–2188
151. Salleh, S. F., Kamaruddin, A., Uzir, M. H., Karim, K. A., and Mohamed, A. R. (2016) Investigation of the links between heterocyst and biohydrogen production by diazotrophic cyanobacterium A. variabilis ATCC 29413. Arch. Microbiol. **198**, 101–113
152. Ehira, S., Takeuchi, T., and Higo, A. (2018) Spatial separation of photosynthesis and ethanol production by cell type-specific metabolic engineering of filamentous cyanobacteria. Appl. Microbiol. Biotechnol. **102**, 1523–1531
153. de los Ríos, A., Ascaso, C., Wierzchos, J., Vincent, W. F., and Quesada, A. (2015) Microstructure and cyanobacterial composition of microbial mats from the High Arctic. Biodivers. Conserv. **24**, 841–863
154. Wang, Y. J., Liao, Q., Wang, Y. Z., Zhu, X., and Li, J. (2011) Effects of flow rate and substrate concentration on the formation and H2 production of photosynthetic bacterial biofilms. Bioresour. Technol. **102**, 6902–6908
155. Guo, C. L., Cao, H. X., Guo, F. Q., Huang, C. L., Wang, H. G., and Rao, Z. H. (2015) Enhanced photo-H2 production by unsaturated flow condition in continuous culture. Biotechnol. Lett. **37**, 359–366
156. Guo, C. L., Zhu, X., Liao, Q., Wang, Y. Z., Chen, R., and Lee, D. J. (2011) Enhancement of photo-hydrogen production in a biofilm photobioreactor using optical fiber with additional rough surface. Bioresour. Technol. **102**, 8507–8513
157. Nawar, A., Khoja, A. H., Akbar, N., Ansari, A. A., Qayyum, M., and Ali, E. (2017) Physical abrasion method using submerged spike balls to remove algal biofilm from photobioreactors. BMC Res. Notes. **10**, 1–5
158. Pesek, J., Büchler, R., Albrecht, R., Boland, W., and Zeth, K. (2011) Structure and mechanism of iron translocation by a Dps protein from Microbacterium arborescens. J. Biol. Chem. **286**, 34872–34882
159. Bellapadrona, G., Chiaraluce, R., Consalvi, V., Ilari, A., Stefanini, S., and Chiancone, E. (2007) The mutations Lys 114 → Gln and Asp 126 → Asn disrupt an intersubunit salt bridge and convert Listeria innocua Dps into its natural mutant Listeria monocytogenes Dps. Effects on protein stability at low pH. Proteins Struct. Funct. Genet. **66**, 975–983
160. Wiedenheft, B., Mosolf, J., Willits, D., Yeager, M., Dryden, K. A., Young, M., and Douglas, T. (2005) From The Cover: An archaeal antioxidant: Characterization of a Dps-like protein from Sulfolobus solfataricus. Proc. Natl. Acad. Sci. **102**, 10551–10556
161. Facey, P. D., Hitchings, M. D., Saavedra-Garcia, P., Fernandez-Martinez, L., Dyson, P. J., and Del Sol, R. (2009) Streptomyces coelicolor Dps-like proteins; differential dual roles in response to stress during vegetative growth and in nucleoid condensation during reproductive cell division. Mol. Microbiol. **73**, 1186–1202

Supplementary

Table S1 Overview of the DNA-binding properties of Dps structures. N- and C-terminal sequences based on the crystal structures (http://www.rcsb.org/). Lys and Arg highlighted in blue colour. Underscored amino acids indicate the existence of α-helices structures. DNA-binding capabilities for the prokaryotic Dps sequences given for *Escherichia coli*, *E. coli* Dps (1DPS) (76); *Bacillus subtilis*, *B. subtilis* Dps (2CHP); *Mycobacterium smegmatis*, *M. smegmatis* Dps1 (1UVH) and Dps2 (2Z90) (75, 95); *Lactococcus lactis*, *L. lactis* DpsA (1ZS3) (54) and DpsB (1ZUJ) (54); *Deinococcus radiodurans*, *D. radiodurans* Dps1 (2C2U) and Dps2 (2C2J) (77, 78); *Helicobacter pylori*, *H. pylori* (1JI4) (79); *Listeria innocua*, *L. innocua* Dps (6HV1) (101); *Streptococcus pyogenes*, *S. pyogenes* Dps (2WLU) (97); *Agrobacterium tumefaciens*, *A. tumefaciens* Dps (1O9R) (81); *Thermosynechococcus elongatus* BP-1, *T. elongatus* Dps (2C41) and DpsA (2VXX) (51, 89); *Campylobacter jejuni*, *C. jejuni* Dps (3KWO) (82); *Bacteriodes fragilis*, *B. fragilis* Dps (2VZB) (80); *Mycobacterium arborescens*, *M. arborescens* Dps (2YJK) (158); *Bacillus anthracis*, *B. anthracis* Dps1 (1JI5) and Dps2 (1JIG) (53); *Streptococcus suis*, *S. suis* (2UX1) (131); *Salmonella enterica*, *S. enterica* Dps (3AK8) (96); *Listeria monocytogenes*, *L. monocytogenes* Dps (2IY4) (159); *Treponema pallidum*, *T. pallidum* (2FJC); *Kineococcus radiotolerans*, *K. radiotolerans* Dps (4A25); *Yersenia pestis*, *Y. pestis* Dps (4DYU) ; *Vibrio cholerae*, *V. cholerae* Dps (3IQ1); *Halobacter salinarum*, *H. salinarum* DpsA (100); *Staphylococcus aureus*, *S. aureus* Dps (2D5K) ; *Brucella melitensis*, *B. melitensis* Dps (3GE4); *Sulfolobus solfataricus*, *S. solfataricus* Dps (2CLB) (134, 160); *Streptomyces coelicolor*, S. DpsA (4CY9) and DpsC (4CYB) (161). Further information on protein tags for protein purification purposes found in the referred literature as only native protein sequences have been given here on the basis of KEGG protein sequence entries (https://www.genome.jp/kegg/). *N-terminal signal peptide for *D. radiodurans* Dps1 'MRHSVKTVVVVSSLLLGTALAGGAGAQSAG' not included in the displayed N-sequence.

prokaryote	*in vitro* DNA – binding	number of positive charges at N-terminus	C-terminus	N-terminal sequence	A-helix	D-helix	C-terminal sequence
E. coli	yes	4	0	MSTAKLVKSKATNLLYTRNDVS	DSEKK	WFIEC	NIE
B. subtilis	yes	1	0	MKTENA	KTNQT	LSSYL	G
M. smegmatis Dps1	yes	1	5	MTSFTIPGLSDK	KASDV	WFVRA	HLESAGGQLTHEGQSTEKGAADKARRKSA
M. smegmatis Dps2	yes	2	1	MSARRTESDIQGFHAT	PEFGG	LIRSE	NRKV
L. lactis DpsA	yes	4	1	MIELSIDEKYEAEVKKSEIDHHKPTA	GAMLS	FAGEL	GKTIGEFIEEEDED
L. lactis DpsB	yes	5	1	MITKLMIDEKYAKELDKAEIDHHKPT	AGAML	NLAGD	LGKSVADFHDEDEDNDN
D. radiodurans Dps1 *	yes	7	1	MTKKSTKSEAASKTKKSGVPETGAQGVRAGGADHADAAHLGTVNNALVNHHYLE	EKEFQ	LQAIM	DDERLD
D. radiodurans Dps2	yes	1	3	NGVPSTNVNTPAPNTGQSTAQNTNTASPLPYNRATTLPAAGT	EDLKK	WQMRA	FLQNTPTDPNTGFDINNGKPVPLRGR
H. pylori	yes	1	0	MK	TFEIL	LQAHL	A
L. innocua	no	1	1	MKTINSVD	TKEFL	FKAFL	GKAPLE
S. pyogenes	no	3	0	MTNTLVENIYASVTHNISKKEASKN	EKTKA	LQAER	GQGPAL
A. tumefaciens	no	3	1	MKTHKTKNDLP	SNAKS	WFLEA	HVQEKS
T. elongatus Dps	no	0	1	MSATTT	LKEQV	FLKEF	LAKGDGLVS
T. elongatus DpsA	no	1	1	MTTSALPRQAFGEMADTVILLE	KATTT	IGHFL	ANDSLKV
C. jejuni	no	1	0	MS	VTKQL	IGATL	QGACKM
B. fragilis	no	3	2	MAKESVKILQGKLD	VKSLI	RMKES	FLKK
M. arborescens	no	0	0	MTDTNITTPALTADP	EVAAA	LLAHL	AE
B. anthracis Dps1	no	1	0	MNKQV	IEVLN	MLRAF	LNQ
B. anthracis Dps2	no	0	1	MST	KTNVV	MLSAF	LK
S. suis	no	3	1	MMKQKYYQSPAEIASFSPRPSL	ADSKA	LQAEL	GQAPKL
S. enterica	unknown	4	0	MSTAKLVKTKASNLLYTRNDVS	ESDKK	WFIES	NIE
L. monocytogenes	unknown	1	1	MKTINS	VDTKE	FKAFL	GKAPLE
T. pallidum	unknown	2	1	MNMCTDGKKYHSTATSAAVGASAPGVPDA	RAIAA	LGATL	KA
B. brevis	unknown	0	0	MKT	SIQQL	LEAFL	E
K. radiodurans	unknown	0	4	MTTIHDVQTTGLTQDAVTGFDAS	SRLNA	WMIGS	ENRSPRRR
Y. pestis	unknown	0	1	MSTAKLVKTKPSELLYTRNDVE	EHVKV	WFIES	NIE
V. cholerae	unknown	0	1	MATNLIGLD	TTQSQ	LNAWL	K
H. salinarum	unknown	3	1	MSTQKNARATAGEVEGSDALRMD	ADRAE	IEHYL	EDDTLVTQGALE
S. aureus	unknown	0	0	MSN	QQDVV	FKSYL	S
B. melitensis	unknown	3	0	MPKKSMHATRNDLP	SNTKT	WFLEA	HVQESN
S. solfataricus	unknown	3	5	MQEKPQEPKVVGVEILEKSGLD	IKKLV	FLELL	YGRPSGHFRRSSPGNAPYSKK
S. coelicolor DpsA	unknown **	1	1	MTHDLTPKYTVPGIE	REAAG	VRAHL	ESAGGALATGSATSETEAAA RGAEVA
S. coelicolor DpsC	unknown **	6	0	MSSPKPKPPSSAEHRSDGSQPWLHQKGRTIQEFGTVKQFPVALT	MDTRL	FVAEH	LVDTPLVHA
N. punctiforme Dps1	no	1	2	MRAINIGLT	EEQRQ	RSFIE	GEALGPDGRQPAEGAKTPVGV
N. punctiforme Dps2	yes	2	0	MSSKVTVKNVNIGID	EASRA	RSLLE	E
N. punctiforme Dps3	yes	2	4	MSDNSIASRLYPTRIDIP	AKARV	AHLQI	AEIKEENGNAGTTKTQKIPAAVK
N. punctiforme Dps4	yes	1	1	MSETQTLLRNFGNVYDNPVLLD	RSVTA	SHFLA	KDSLTLGFVQAAQS
N. punctiforme Dps5	yes	0	0	MQ	ELDYK	MLRDF	S

* cleavage of the signal peptide 'MRHSVKTVVVVSSLLLGTALAGGAGAQSAG' after transportation into periplasm; underlined sequences are N-terminal helical structures

Acta Universitatis Upsaliensis

Digital Comprehensive Summaries of Uppsala Dissertations from the Faculty of Science and Technology 1837

Editor: The Dean of the Faculty of Science and Technology

A doctoral dissertation from the Faculty of Science and Technology, Uppsala University, is usually a summary of a number of papers. A few copies of the complete dissertation are kept at major Swedish research libraries, while the summary alone is distributed internationally through the series Digital Comprehensive Summaries of Uppsala Dissertations from the Faculty of Science and Technology. (Prior to January, 2005, the series was published under the title "Comprehensive Summaries of Uppsala Dissertations from the Faculty of Science and Technology".)

Distribution: publications.uu.se
urn:nbn:se:uu:diva-390471

ACTA
UNIVERSITATIS
UPSALIENSIS
UPPSALA
2019